DESIGN, DEVELOPMENT, CHARACTERIZATION, AND VALIDATION OF A PAPER-BASED MICROCHIP ELECTROPHORESIS SYSTEM

by

MUHAMMAD NOMAN HASAN

Submitted in partial fulfillment of the requirements

For the degree of Doctor of Philosophy

Dissertation Adviser: Dr. Umut A. Gurkan

Department of Mechanical and Aerospace Engineering

CASE WESTERN RESERVE UNIVERSITY

May 2020

CASE WESTERN RESERVE UNIVERSITY

SCHOOL OF GRADUATE STUDIES

We hereby approve the thesis/dissertation[1] of

MUHAMMAD NOMAN HASAN

for the degree of

Doctor of Philosophy

Dr. Umut A. Gurkan	
Committee Chair, Adviser Department of Mechanical and Aerospace Engineering	12/16/2019
Dr. Ozan Akkus	
Committee Member Department of Mechanical and Aerospace Engineering	12/16/2019
Dr. Chirag Kharangate	
Committee Member Department of Mechanical and Aerospace Engineering	12/16/2019
Dr. Chung-Chiun Liu	
Committee Member Department of Chemical Engineering,	12/16/2019

[1]We certify that written approval has been obtained for any proprietary material contained therein.

TABLE OF CONTENTS

List of Figures

List of Tables

Acknowledgments

First and foremost, I would like to acknowledge my Ph.D. advisor Dr. Umut Gurkan, who gave me the opportunity to develop invaluable skills to become an independent researcher and guided me through every step of this process. He always guided me to plan ahead, not just for my Ph.D. studies but for my long-term career plans well beyond Ph.D. He profoundly understands the necessities and requirements of a successful academic career and advised me wisely to work towards building a strong background to get ready for the road ahead. Dr. Gurkan has been an effective guide for me and promoted my career development. He has been an excellent role model as a successful researcher and a mentor for me.

I would like to acknowledge my Ph.D. committee members: Dr. Ozan Akkus, Dr. Chung-Chiun Liu, and Dr. Chirag Kharangate, for their insightful feedback. I would like to thank my committee for advising me. Without their guidance, my Ph.D. studies could not advance to this degree.

I would like to acknowledge the help and colleagueship of the previous and current lab members and collaborators from other labs: Dr. Yunus Alapan, Ryan Ung, Megan Romelfanger, Aaron Tam, Myengseop Kim, Courtney Fleming, Dr. Erdem Kuchukal, Yuncheng Man, Utku Goreke, Ran An, Arwa Fraiwan, Asya Akkus, Anowarul Islam, Bolan Lee, Mousa Yunesi, Hyungjin Jung, and Dr. Minerick. I would also like to thank Hemex Health Inc. associates who have guided and assisted my work with technical insight, expertise, and experience.

I would also like to thank all my friends and previous advisors, who helped me through, all the way to my Ph.D. education. Without their support and encouragement, I would not have been here. Last but not least, I would like to thank my dear family, who taught me far more valuable things in life and gave me the motivation and strength to embark upon this path.

Most of this study was made possible by an award from the Clinical and Translational Science Collaborative of Cleveland, UL1TR002548, from the National Center for Advancing Translational Sciences component of the National Institutes of Health (NIH) and NIH Roadmap for Medical Research. Other funding sources include Case-Coulter Translational Research Partnership Program, NIH Center for Accelerated Innovation at Cleveland Clinic funded by U54HL119810, Ohio Third Frontier Technology Validation and Start-up Fund, Consortia for Improving Medicine with Innovation & Technology, National Institutes of Health Fogarty International Center (R21TW010610), National Heart Lung and Blood Institute Small Business Innovation Research Program (R44HL140739), National Heart Lung and Blood Institute R01HL133574, and National Science Foundation CAREER Award #1552782. Scientific illustrations were made by Grace Gongaware, and videos were made by Courtney Fleming, supported by a National Science Foundation CAREER Award #1552782 and Glennan Fellowship from University Center for Innovation in Teaching and Education.

Design, Development, Characterization, and Validation of A Paper-based Microchip Electrophoresis System

Abstract

By

MUHAMMAD NOMAN HASAN

Electrophoresis techniques are analytic platforms widely used for analyzing complex analytes such as proteins, antibodies, and DNA. Often a series of analyses of these analytes is required for analytical purposes. Thus analytical systems, capable of producing accurate, reproducible results are highly desired. The advent of micro-scale total analysis system (μTAS) opened the possibility of miniaturized analytical system which can provide qualitative and/or qualitative assessment while analyzing complex analyte.

MicroChip Electrophoresis (MCE) enables fast, efficient, and reliable analysis because of the accelerated sample processing, and increased reaction rate due to the sample being analyzed is minute in volume. In addition, the ability to provide high-resolution separation of a complex mixture of analytes in a smaller length scale (compared to their traditional counterparts) enables them in high throughput applications, which demand many disciplines such as biology, chemistry, environmental testing, as well as engineering. The effort towards the miniaturization of electrophoresis techniques has yielded a plethora of materials, methods, and process development and a vast amount of these efforts have

been emphasized in greater portability, cost-reduction and large scale fabrication; thus enabling single-use rapid, reliable, high throughput analytical tools for testing in remote and/or resource-limited setting.

The potential of MCE platform prompted a surge in microfluidic implementation of miniaturization of electrophoresis, and the majority of the efforts have been concentrated on capillary electrophoresis. A great volume of analytical and experimental work has enriched the understanding of capillary electrophoresis. This ample understanding of the electrokinetic phenomena for capillary electrophoresis has curved the success of the capillary-based MCE platforms. The emergence of paper-based microfluidics in the past decade has also marked the onset of miniaturization of paper-based MCE platforms. The lower material cost (compared to capillary electrophoresis), simpler fabrication approach (such as channel fabrication, and electrode integration), ease of sample injection/transfer holds the key for a disposable, mass-producible analytical system with long self-life. These are the essential factors that govern the feasibility of the translation of lab-based proof-of-concept technology to a commercial product. The blessings of MCE technologies can only be materialized only if successful commercialization of such technologies can be made available, not only for state of the art scientific application but also for widespread application in various disciplines and different kinds of end-users. In this doctoral dissertation, I describe the design, development, fabrication, mass and thermal transport characterization, and clinical validation of the MCE platform for hemoglobin variant testing application.

Chapter 1: Electrophoresis and Its Miniaturization

1.1 Abstract

Electrophoresis, by origin, is a century-old technique. However, due to its immense potential for diverse applications in numerous disciplines, it is still one of the most widely used analytical techniques. Electrophoresis techniques of different kinds have been developed and standardized over the decades; it is an essential tool for analyzing relatively simple to a complex mixture of analytes. Large scale instrumentation of electrophoretic techniques, developed by researchers and commercialized by manufacturers, is the standard analysis tools for centralized laboratories and are used in many disciplines including but not limited to biology, medicine, and engineering. Since the arrival of miniaturized/micro total analysis systems (μTAS), the science of electrophoresis has seen new dawn, and the miniaturization of different electrophoresis techniques has flourished. Novel miniaturization, material development, fabrication and their application is still an active area of research. This chapter presents a comprehensive overview of traditional or established electrophoresis techniques, the application of traditional electrophoresis techniques, miniaturization of electrophoresis techniques, the role of microfluidics for miniaturization of electrophoresis techniques, and last, the paper-based miniaturization of electrophoresis techniques. The discussion on the paper-based microfluidic techniques has been further elaborated to cover various fabrication techniques and the challenges involving the miniaturization.

1.2 Introduction

Electrophoresis is also called as **cataphoresis**. It is the migration of dispersed particles relative to a fluid under the influence of a spatially uniform electric field. This electrokinetic phenomenon was observed for the first time in 1807 by Reuss (Moscow State University), who noticed that the application of a constant electric field caused clay particles dispersed in water to migrate. It is ultimately caused by the presence of a charged interface between the particle surface and the surrounding fluid. Electrophoresis, in a general term, is a "current-driven" or "voltage-driven" separation of charged entities, most often these entities being a complex mixture of biological and/or organic components. As this phenomenon is electricity-driven and the action is performed in a charged entity in the presence of a certain environment, the inherent factors which govern the phenomena can be categorized into three categories: (i) electrical, (ii) mechanical, and (iii) chemical. The electrical factors are the charge of the ion, the size of the ion, and the applied voltage/current/power. The mechanical factors are the electrolyte viscosity, porosity, and the friction properties of separation medium (paper/membrane/gel) and the chemical factors are the electrolyte pH and ionic strength. These are the factors that govern the migration and the separation of the analyte in an electrophoresis system. In addition to that, molecular structure, as well as the electric field characteristics and temperature, has significant influence over the migration and separation process that takes place during electrophoresis.

The electrophoretic mobility of the analyte is inversely proportional to the size, i.e., the molecular/ionic radius of the analyte since an analyte with larger molecular/ionic radius

will have to overcome higher drag (in a liquid medium) and a greater frictional resistance (in separation matrix) while migrating under the influence on an applied electric field. Thus, an analyte with a smaller molecular/ionic radius will travel faster compared to an analyte with a larger molecular/ionic radius, given that the electrophoretic condition (such as the applied field parameters, electrolyte pH, viscosity, ionic strength) remain the same for both analytes. The drag force faced by the analyte is a function of the size and shape of the analyte molecule and the viscous property if the electrolyte. The electrophoretic migration is proportional to the applied field strength resulting in increased separation rate with sharper separation, so ideally, a higher electric field is desirable for any electrophoresis technique. Nonetheless, a higher strength of the applied field will result in increased heat generation, which in addition to the high field strength can adversely affect the analyte under investigation, and can lead to other undesirable consequences, such as, change in the chemical properties of the electrolyte (pH value) and evaporation of electrolyte. The pH of an electrolyte is another driving force behind the electrophoretic mobility and separation; since it is the pH of the electrolyte that induces the net charge of the biological and organic analytes, which then responds to the applied electric field and manifest the electrophoretic mobility and separation in combination with electrophoretic condition provided for the process.

1.3 Electrophoresis Techniques

All electrophoresis techniques revolve around the basics of electrophoretic migration of charged analytes. What differs various electrophoresis techniques from each other is how the electrophoretic mobility and the separation are facilitated, enhanced, and

utilized with application-specific devices, such as the presence of support medium, the types of the support medium, uniform pH or pH distribution, the mobilized or immobilized pH distribution. Each of these criteria dictates the instrumentation and/or construction of the electrophoresis technique. For example, the support medium can provide absorption as well as molecular sieving, which significantly influences the electrophoretic separation. On the contrary, the matrix-free electrophoresis is not constituted of any support medium and can be implemented for the electrophoretic separation of not only cellular components but also for separation of complete cells, due to not having the size restriction of the sieving medium.

Arne Tiselius (Arne Wilhelm Kaurin Tiselius) is considered the pioneer of electrophoresis. Tiselius's noble prize-winning work was on free-flow electrophoresis (electrophoresis without the supporting medium). However, as the field expanded, the adverse effect of free-flow electrophoresis, such as convection current, motivated the development of other electrophoresis techniques. A concise review of different electrophoresis techniques is presented in the following section.

1.3.1 Free-Flow Electrophoresis:

Free-flow electrophoresis (FFE), or carrier-free electrophoresis, is the oldest form of electrophoresis which does not implement any supporting medium for the electrophoretic separation and analysis. By principle, the free-flow electrophoresis can be considered analogous to capillary electrophoresis. The absence of a matrix ensures the conservation of protein activity and high-resolution separation of protein complexes, protein isoforms, subcellular compartments as well as complete cells. The FFE is also

suitable for isoelectric focusing (IEF) based separation, which operates on creating a controlled pH gradient (thus controlled distribution of isoelectric points) and separation of analytes based on the differences in the isoelectric points of the components of the analyte.

The FFE is not as widely used, nowadays, as it used to be. However, FFE still plays crucial roles for specific applications such as separation of unstable proteins (at low temperature), enriching low-abundance proteins, as well as non-biological applications such as separation of metal ions, determining colloidal property (zeta potential) of particles in dispersion phase, and moving boundary electrophoresis for macromolecules [1].

1.3.2 Zone Electrophoresis:

Zone electrophoresis refers to the electrophoretic separation techniques which separate the different components present in an analyte due to differences in their electrophoretic mobility, therefore creating separate, well-defined zones and well-resolved peaks. These peaks at their designated zones, therefore, can be used for both qualitative and quantitative analysis of the analytes. Zone electrophoresis typically refers to the electrophoretic separation process involving stabilizing (or supporting) medium. The capillary zone electrophoresis (CZE) is a FFE method, which is also referred as "zone electrophoresis" since CZE techniques also separate the compounds into well-defined and well-resolved zones for detection and analysis. A brief overview of different types of zone electrophoresis is given below:

1. Paper electrophoresis
2. Cellulose acetate electrophoresis
3. Capillary electrophoresis

4. Gel electrophoresis
    4.1. Agarose gel electrophoresis
    4.2. SDS-PAGE (sodium dodecyl sulfate - polyacrylamide gel electrophoresis)
    4.3. PFGE (Pulsed field gel electrophoresis)
    4.4. 2D electrophoresis.

1.3.2.1 Paper Electrophoresis:

The paper electrophoresis is performed on a filter paper as a supporting medium (typically on a chromatography paper) due to its less absorptivity and uniform porous structure. It is particularly suitable for an analyte that is composed of small charged molecules (for example, amino acids and proteins of small size). The support medium or the filter paper is kept moist with the electrolyte, and the paper ends are kept submerged in the electrolyte where the electrodes are also submerged. The electrolyte-soaked filter paper, acting as an electrical connection between the electrodes, facilitates the electrophoretic separation, resulting in the resolved zones of analyte components. These separated components are then detected by post-processing such as chemical staining [2-4].

1.3.2.2 Cellulose Acetate Electrophoresis:

Cellulose acetate electrophoresis is a variant of paper-based electrophoresis where, a cellulose acetate membrane replaces the filter paper. Cellulose Acetate (CA) paper was first presented as a medium of separation by Jaochim Kohn in 1956 [5,6]. It was proved to be effective in immunoassays that focused on the identification of alpha 1, alpha 2, beta, and

gamma globulins along with albumin levels in the blood [7-12]. It was found that resolution so far as band separation, tailing, and the presence of proteins customarily difficult to view on filter paper was dramatically improved in cellulose acetate electrophoresis. In their immunofixation assays, Kohn et al. [5,6] commenced initial electrophoretic experimentation by using a dual agar-cellulose acetate medium but eventually moved towards the use of solely the latter due to comparable separation of minor monoclonal bands and similar resolution of cellulose acetate and agarose gel electrophoresis. The small-scale cellulose acetate electrophoresis system developed in 1958 was proven to be more economical than other options such as filter paper and agarose gel alone, due to its less serum and supply consumption. The speed of separation of bands on this electrophoretic medium was noticeably improved over time and is noticeably superior to filter paper [5,13]. A few notable advantages of cellulose acetate over filter papers are:

1. The cellulose acetate strips are chemically pure and free of lignin and hemicelluloses and generally act as barriers in free moment of large molecules.
2. Because of the low content of glucose, cellulose acetate strips are suitable for electrophoresis of polysaccharides.
3. Cellulose acetate is not hydrophilic, and this holds very little buffer, which further helps for a better resolution in a short time.

1.3.2.3 Capillary electrophoresis:

Capillary electrophoresis (CE), as the name suggests, utilizes capillarity of narrow bore tube (typically fused-silica) and separates the compounds of an analyte based on their charge to mass ratio. Capillary electrophoresis was developed between 1930 and 1960, as

an improved version of the free-flow electrophoresis. The implementation of the capillary in free-flow electrophoresis increased the surface to volume ratio, thus improving the thermal dissipation. The high filed gradient required for capillary electrophoresis is susceptible to overheating, but this capillary induced high surface to volume ratio helped improve the free-flow electrophoresis. Capillary electrophoresis widely used due to the faster separation of the components of an analyte and its high separation resolution. Capillary electrophoresis is a new class of electrophoretic separation compared to gel electrophoresis (such as agarose gel, and SDS-PAGE).

In capillary electrophoresis, the separation of the components of the analyte occurs in an electrolyte solution, which is referred as the background electrolyte. The capillary ends are connected to inlet and outlet reservoirs, containing electrolyte solution and the electrodes. The sample injection for the analysis can be performed either by hydrodynamic injection (pressure-driven) or electrokinetic injection (voltage-driven). The ends of the capillary are immersed into vials (inlet and outlet) filled with an electrolyte solution, which also contains electrodes connected to a high voltage supply. The sample solution is introduced in the capillary as a small plug by applying pressure (hydrodynamic injection) or voltage (electrokinetic injection). The high field strength causes the development of well-defined and well-resolved zones for the components of an analyte, which are detected at a designated detection window as the resolved zones of the components of analyte migrate through the capillary tube.

Capillary electrophoresis provides high-resolution separation with greater efficiency with a short analysis time while providing a low sample and electrolyte

consumption. These attributes of capillary electrophoresis established it as the most widely used electrophoresis technique in various applications in many disciplines. However, the very reason (small diameter of the capillary and the high surface to volume ratio) that established capillary electrophoresis as a superior version of free-flow electrophoresis, also introduces an increased level of diffusion (due to enhanced thermal dissipation), which can compromise the separation resolution of capillary electrophoresis.

1.3.2.4 Gel Electrophoresis:

Gel electrophoresis is a form of electrophoresis where the supporting medium is a gel type (such as agarose, polyacrylamide) and is mostly used for separation of RNA, DNA, and proteins. The differences in the molecular size play a crucial role in their electrophoretic migration and separation as the compounds of the analyte are pushed through the gel matrix (through the pores) by the influence of the applied electric field. Thus the size of the protein and the length of the DNA and their interaction with the gel matrix dictate the electrophoretic separation. Gel electrophoresis is itself a standalone analytical platform; however, it can also be used as a preprocessor for a secondary analysis such as mass spectrometry, PCR, and DNA sequencing. Gel electrophoresis is highly implemented in biotech laboratories. From an instrumentation point of view, gel electrophoresis can be vertical gel apparatus electrophoresis or horizontal gel apparatus electrophoresis.

1.3.2.4.1 Agarose Gel Electrophoresis:

The agarose gel electrophoresis is used for the electrophoresis of nucleic acids (DNA and RNA). The separation of DNA and RNA by agarose gel electrophoresis is

enacted by utilizing the negative charge of the "phosphate backbone" of these nucleic acids, as a net negative charge is evenly spread over the length of their chain [14]. The electrophoretic separation, once an electric field is applied, is dictated by the molecular size, and the components of the analyte electrophoretically migrate towards the electrode, while the agarose gel provides the necessary sieving for the size-based separation.

Agarose is a polysaccharide with a melting temperature of 90°C and a gelation temperature of 40°C, which is extracted from seaweed. The gelation of agar forms the gel matrix with varying pore sizes, typically ranging from 50 to 200 nm. The size and distribution of the pore define the overall porosity and sieving efficiency of the gelled agar matrix. The recipe of the agarose concentration (0.5 - 2.0 %) is tailored to separate nucleic acids of different molecular weights. A higher concentrations of agarose provides separation of small DNAs, and similarly, a low agarose concentration results in separation of DNA of higher molecular weight. By the principle of gel electrophoresis, the gel matrix is kept immersed in the electrolyte, and the pH of the electrolyte is assumed to remain relatively constant. The electrolyte (or buffer) used for this electrophoresis technique depends on its application. TAE (or Tris/Acetate/EDTA) buffer is an electrolyte with low buffer capacity and provides better resolution for larger DNA, while TBE (Tris/Borate/EDTA) buffer is used for smaller DNA. SB (sodium borate) buffer is another type of electrolyte used for agarose gel electrophoresis. The conductivity of these electrolytes dictates the maximum allowable voltage for the electrophoretic separation; thus, can significantly influence the time required for the electrophoretic separation process. The major advantages are the ease of the preparation of the gel matrix and the less denaturing of the analyte components. While the gel can melt during the electrophoresis

process if the voltage is not set up properly, and the melting of the gel matrix can yield unpredictable results.

1.3.2.4.2 SDS-PAGE:

The SDS-PAGE (sodium dodecyl sulfate-polyacrylamide gel electrophoresis) is a type of gel electrophoresis with a discontinuous polyacrylamide gel matrix. Unlike the charge-based separation, SDS-PAGE separates the analyte compounds by the molecular mass. The SDS is a surfactant which serves two important functions:

(1) Dissociating proteins into their individual polypeptide subunits and giving a uniform negative charge along each denatured polypeptides.
(2) Forcing the polypeptides to extend their conformation, which helps them achieve a similar charge to mass ratio.

Both of these effects combined eliminate the influence of the shape difference from the separation process, thus making the chain length (analogous to their molecular mass) the governing factor for the electrophoretic process.

For SDS-PAGE, acrylamide is the base component of the supporting medium. SDS-PAGE is a discontinuous gel system, comprised of two different gel systems - a resolving gel, and a stacking gel. Both of these gel systems are constituted from acrylamide. The concentration of the acrylamide is different for two gel systems, and the concentration of acrylamide for each gel type varies (5 - 10% for the resolving gel, and 2 - 5% for the stacking gel) depending on the application. The gel systems also use a different electrolyte

where the lower gel (the resolving gel) is maintained at a relatively lower pH compared to the upper gel (the stacking gel).

The SDS-PAGE provides a rapid separation with higher electrophoretic mobility. The sensitivity of SDS-PAGE is high and can resolve analyte components with a low mass difference. On the contrary, the higher alkaline operating pH can lead to poor band resolution, and the gel preparation is laborious and a necessity for multiple gel results at a higher cost.

1.3.2.4.3 Pulse Field Gel Electrophoresis (PFGE):

Pulsed field gel electrophoresis (PFGE) is a variant of gel electrophoresis where a periodic change in the direction of the applied electric field is employed in contrast with the constant, unidirectional electric field used for conventional gel electrophoresis. The PFGE was invented to overcome the limitation of the conventional gel electrophoresis or SDS-PAGE to separation large DNA molecules (> 15 ~ 20 kb). The periodic change in the direction of the electric field and the resultant alternating voltage gradient forces the large DNA molecules to relax and elongate, therefore improving the range of resolution for DNA fragments.

1.3.2.4.4 2D Electrophoresis:

The 2D electrophoresis is a two-stage electrophoretic separation process, where one stage separates the components of an analyte based on their charge differences, while the other stage separated the components based on their differences in molecular mass. The first stage, the change-based separation, is typically an IEF separation, and the second stage

is typically a SDS-PAGE separation process. The 2D electrophoresis is a highly sensitive electrophoretic separation technique that is widely used for purifying complex mixtures of polypeptides.

1.4 Applications of Electrophoresis Systems

The variety of electrophoresis systems exists in the first place because each category of electrophoresis system possesses its own application-specific efficiency and superiority compared to other techniques. The paper-based electrophoresis systems are widely utilized for serum analysis for diagnosis or clinical purposes. The other widely analyzed analyte for paper-based electrophoresis is myosin, albumin, casein as well as venoms of various kinds (such as insect and snake venom).

Cellulose acetate electrophoresis is highly regarded for clinical applications and is reliable for clinical investigation of human samples such as lipoprotein, glycoprotein as well as hemoglobin. Among all the electrophoretic separation techniques, the capillary electrophoresis has, by far, the most versatile application due to the immense degree of research effort dedicated to this class of electrophoresis technique. Capillary electrophoresis is used for the analysis of, for example, food products, pharmaceutical products, and environmental pollutants.

The agarose gel electrophoresis is the most preferred method for electrophoretic separation when the analyte of interest is a nucleic acid. A major application of this electrophoresis type is the analysis of the PCR products and the evaluation and assessment of the target DNA amplification. Other notable applications of gel electrophoresis include the qualitative and quantitative assessment of DNA, DNA separation, and DNA

fingerprinting. The SDS-PAGE electrophoresis has diverse applications than agarose gel electrophoresis, for example, establishing protein size, protein identification, quantifying protein, and determining sample purity.

1.5 Miniaturization of Electrophoresis System

Electrophoresis techniques, as described before, are used as an analytic platform, and the subject matters of this analysis are often not abundantly available. Micro-scale analytical systems have received considerable attention for their ability to analyze small sample volumes (a couple of microliters), increase analysis rate, and throughput via multiplexing. The reduction in sample volume required reagent volume and faster analysis results in a more economical, less hazardous, portable and more environmentally friendly system being at our disposal [15]

MCE represents a rapid and efficient separation technique for separating sample mixtures. Microchip electrophoresis techniques are able to provide good separation resolution on a smaller length scale and have proven to be useful for many disciplines such as biology, chemistry, engineering, and medicine [16].

Among any other electrophoresis techniques, capillary electrophoresis has received a significantly higher degree of focus, and effort for miniaturization, preferably because of its high separation resolution, and ease of fabrication[17]. The first reported effort for the development of MCE was in the 1990s [18]. The term microchip electrophoresis more often refers to “microchip capillary electrophoresis” [16].

The traditional and conventional capillary electrophoresis systems were comprised of fused-silica tubes embedded between two reservoirs, quite the contrary to the microfabricated capillary electrophoresis, where the microfabricated capillary utilized the advancement of microfluidics and fabricated using channels etched into planar substrates. The early microchip CE relied on quarts or glass due to their similarity with fused silica in terms of electroosmotic flow (EOF) properties [19-21]. Alternative materials such as plastics and low-temperature ceramics have been explored for the fabrication of recent microchip CE devices [22-24].

A dominating factor driving the use of planar devices for microchip CE is the ease of manufacturing of such planar systems. The fabrication techniques implemented for the fabrication of such devices are well-established and reliably used by the semiconductor industry, with the exception of handing small volume fluid flow instead of electron flow. The two major fabrication methods for the fabrication of such planar devices are photolithography and micromolding. The intended application and the choice of suitable substrate dictates the choice of fabrication method. Either fabrication method is highly capable of providing mass-producibility, as the developed pattern can be used for the repetitive fabrication of such devices [25].

The electrochemical detection is a highly suitable application for microchip CE and has recently gained much focus due to the increase in miniaturization effort for such systems. The industry standard photolithography techniques can easily be implemented for designing µm scale detection electrodes with surgical precision, high reproducibility in a cost-effective way. Such attributes ensure the high sensitivity of electrochemical detection

in microchip CE format. It is noteworthy that the miniaturization does not compromise the analytical performance. Further miniaturization of the electrical components such as power supply and potentiostat would enable a true μ-TAS [24,26].

The miniaturization of analytical separation systems provides numerous advantages. The reduced size increases the separation speed, therefore, higher sample throughput. The reduced device scale also reduces the fabrication cost, thus enabling cost-effective disposable systems. The miniaturization of analytical systems also holds the potential for parallel processing in a small working area. The parallel processing is extremely attractive for high throughput applications. High throughput analytical systems are in high demand in various emerging application fields of life science, especially in the fields of genomics and proteomics, as well as pharmaceutical field, where these analytical issues play a major role as well with regard to combinatorial chemistry and drug discovery [22].

Paper as a supporting medium, or as a substrate, offers numerous advantages, which include but not limited to - low-cost, lightweight, ease of manipulation, affordability, and biocompatibility. The first reported study of a paper-based analytical separation system was published in 1940. The early studies was focused on electrophoretic separation of amino acids, proteins and peptides. The instrumentation involved high voltage power supply and the separation processes were proceeded using a high concentration of the analytes with low resolution and long processing time [27-30].

These technical difficulties pushed the paper-based system out of scientific focus, and the analysis of biomolecules was substituted by techniques which are much

sophisticated, such as, high-performance liquid chromatography (HPLC) or gel electrophoresis and the use of paper-based system was directed toward conventional analytical techniques such as filtration and clinical applications such as pregnancy tests [31].

The microfluidic paper-based analytical devices (μPADs) was debuted in 2007 by George Whitesides's research group. They developed the μPAD as a bioanalytical platform to measure glucose and protein concentration levels [32]. μPADs bring the idea of minimum reagent waste as well as operational simplicity [33], revealing the necessity of improving the portability and reducing the cost of analysis [33-36].

The advent of μPADs has revived the significance of paper as a substrate for electrophoretic separations with an emphasis on low-cost rapid analytical systems [37]. Another crucial contributing factor behind the revival of paper as a potent substrate for electrophoretic separation is the technological advances enabling the availability of paper at various thicknesses, porous properties, and chemical modification. The concurrent development of high-voltage source and small-scale, robust detector system also paved the way for the recent uprising of μPADs. After a long pause, in 2014, another study of a paper-based separation platform for biomolecules was reported. The separation of biomolecules (lysine, serine, and aspartic acid) using an on-column wireless electrogenerated chemiluminescence detector, and the separation of fluorescent molecules and serum proteins were successfully reported by Ge et al. and Luo et al., respectively [38,39]. Though these latest studies demonstrated promising improvement for paper-based electrophoresis, some of the key aspects, such as robustness, sample injection and injection control, and separation performance, still need much attention for making μPADs suitable for everyday

use. Xu et al. developed a paper-based electrophoresis device with an electrokinetic injection to introduce sample through the floating mode. The separation of two different organic dyes was performed within 10 min and monitored using a cell phone camera, but it was also possible to accomplish the separation by naked eye [40]. After that, Wu and coworkers developed a methodology to concentrate and electrokinetically separate bovine hemoglobin and cytochrome C using a paper analytical device [36].

Electrochemical detection integrated with microchip electrophoresis is highly desirable due to high sensitivity, and low instrumental cost. The technological advancement in electrode fabrication methods, such as hand drawing with graphite pencil, sputtering, microwires, and screen printing, is making it much easier to fabricate low-cost microchip electrophoresis with electrochemical detection [41-45]. Amperometry is one of the most sensitive electrochemical detection methods, and it was already explored to monitor chromatographic separations on paper devices [43,45]. The development of a capacitively coupled contactless conductivity detector (C^4D) for electrophoresis was first reported in 1998 [46,47], which offers numerous advantages over "contact modes" and prevents problems associated with bubble generation electrode fouling and electrical interference when high voltage for electrophoresis is applied [44-46,48].

The recent and past breakthrough in miniaturization of analytical techniques, systems, and instrumentation have resulted in highly efficient μTAS and μPADs capable of accurate and reliable analysis with low reagent and sample consumption, and quicker analysis, which is ideal for the implementation of such miniaturized platforms for point-of-care testing. According to the World Health Organization (WHO), diabetes mellitus,

cardiovascular disease are two of the major causes of death. In addition, there are genetically inherited diseases as well as tropical and infectious diseases, which claim a high death toll worldwide. The miniaturized analytical platforms can reduce the death toll caused by these diseases by enabling point-of-care testing, especially in regions with limited resources.

1.6 Low-cost Microfluidic Platforms for Diagnostic Applications

The essence of the low-cost platform for diagnostics applications relies on the utilization of inexpensive substrates and other assembly materials coupled with cost-effective manufacturing processes. The combination of these two is crucial for mass production of microfluidic devices and making such technologies feasible for routine applications, especially in limited-resource settings [34]. The use of miniaturized platforms for disease detection and screening is gaining much traction in recent years [49,50]. The high demand for miniaturized systems has spurred the research efforts for microfluidic platforms in this application area. This increasing focus on miniaturized platforms has nourished the development and evaluation of new substrates, microfabrication techniques, and detection methods, resulting in portable, disposable, cost-effective point-of-care (POC) diagnostic devices especially suitable for limited resource and remote settings [51]. In such environments, POC diagnostic devices could provide an adequate solution to be used even by untrained personnel under challenging environmental conditions and limited power.

A crucial aspect of POC technology is its cost, and it is a decisive factor for the success of such technologies when intended for low-resource settings [52]. The cost-reduction can only be ensured when inexpensive material, creative, and simplified system

design is merged with a cost-effective fabrication process. The low-cost or inexpensive choice of material still needs to be able to provide the necessary biocompatibility, good analytical performance, acceptable limit of detection, detection accuracy while being easily disposable. Typically, the primary choice of materials for laboratory-based proof-of-concept microfluidic systems are PDMS and glass. These materials provide outstanding performance and easy to fabricate on a small scale. However, in terms of mass production, the scenario is quite different. The required manufacturing techniques to work with these materials, along with the associated cost, renders them less practical. To address this challenge, alternative materials such as plastic and paper are slowly but increasingly gaining attention, since they are versatile, affordable, and easily disposable [51,53-56].

Paper is affordable, biocompatible, and easily disposable. Paper-based miniaturized systems are relatively simple to fabricate, thus suitable for large-scale production with ease and low-cost. For these inherent attributes of paper, the paper-based miniaturized, or microfluidic systems are proving to be advantageous as POC systems [32].

1.7 Resurgence of Electrophoretic Separation on Paper-Based System

Point-of-care (POC) systems are designed for rapid, on-site detection of an analyte, especially for clinical and environmental testing purposes. Microfluidic paper-based analytical devices (μPADs), as described in the previous sections, is considered a frontrunner in the POC field. From an analytical point of view, “paper” is known as a substrate for well-established techniques, such as chromatography. However, paper has not been the material of choice for developing electrophoretic separation techniques, until very recently.

Separation science is a significant aspect of analytical chemistry. The established separation techniques are routinely implemented for separation, detection, and identification of both known and unknown components within an analyte. Among these established techniques, the most widely used techniques are chromatography and electrophoresis. Although, historically, capillary and gel-based electrophoresis were the centerpieces of the scientific focus for the development of electrophoretic separation techniques, one of the earliest and the most cost-effective substrate for electrophoresis has been paper [57-59].

Paper chromatography originated in the 1850s, while Friedlieb Ferdinand Runge, a German physicist, observed circular color-forming patterns on filter paper impregnated with metal solutions resulting from the difference in the complexation of different dyes with the immobilized metals [58,60]. This observation triggered a vast interest in the scientific community to invest their efforts in understanding the chromatographic separation. After years of research, in the early 1900s, Mikhail Semonovich Tswett introduced the fundamentals and principles of paper chromatography [60-62].

The paper chromatography was developed to offer a solution to the limitation of silica-gel based chromatography. The silica gel-based chromatography involves a complicated process of substrate preparation and often would suffer from detection difficulties. The introduction of paper as a substrate of chromatography, which is considered as thin-layer chromatography (TLC), eliminated the complicated process of substrate preparation, completely [63]. The paper chromatography relies on the capillary wicking of the paper substrate, where a small sample volume is placed on the

chromatography paper with the sample-end of the paper being dipped into the solvent reservoir. The capillary action dragged the components of the analyte (or sample) across the paper. The difference in the retention of the components of the analyte resulted in their separation. The visualization of the components due to the chromatographic separation was carried out by calorimetric, ultraviolet (UV), and fluorescence imaging. Among these, colorimetric detection was by far the most widely used technique.

The filter paper, as a chromatography substrate, was a preferred choice due to the fact that it could facilitate direct visualization of analyte components using the calorimetric approach. While, in contrast, the silica gel-based chromatography involved complicated post-processing, which involved substrate transfer on pre-treated papers for visualization [64]. The identification of the analyte component was based on a mobility of these mobile phases, which was the result of the interaction between the mobile phase (the analyte) and the stationary phase (the substrate) [58] and the quantitative assessment is provided by the color intensity measured by optical instruments such as, transmission densitometer, the photoelectric densitometer and the X-ray viewer [58,65-68].

In the early days of paper-based electrophoresis, it was regarded as a superior separation technique compared to the chromatography technique, as the separation time was faster due to the application of an external field. The device dimension was smaller, and the system would produce a better peak resolution. At the same time, the paper-based system was dependent on additional operational instrument, i.e., the power supply in contrast to the chromatography system [58]. The interest in paper-based electrophoretic separation started to fall short as more novel and sophisticated techniques started to

emerge, such as gel electrophoresis (agarose and polyacrylamide), capillary electrophoresis, 2D electrophoresis and isotachophoresis. These emerging techniques outperformed the paper-based electrophoresis of the early days, as they demonstrated better separation performance and efficiency in terms of separation resolution and sensitivity [30,69-71].

It would take half a century to revitalize "paper-based substrate" in analytical research. The paradigm-shifting work published by the Whitesides Research Group [32] defined a new class of electrophoretic separation platform microfluidic Paper-based Analytical Devices or µPADs, which they developed for point-of-care (POC) bioassay. The resurgence in research for the paper-based analytical system is the ability to design a passive system, which makes the platform more appealing for remote and portable applications. As a byproduct of this resurgence of µPADs, the paper-based electrophoretic research also gained traction.

1.8 Commercialization of Low-Cost Microfluidic Devices for Clinical Diagnostics

Due to the recent advancement of the paper-based analytical platforms (i.e., µPADs, paper-based electrophoresis system) and the unique advantages they provide (i.e., passive operation capability, ease of fabrication, integration, and portability), there is a huge potential land market demand for easy-to-use, reliable, robust, and cost-effective platforms for POC application for diagnostics, forensic, and contamination testing ranging from natural pollutant to hazardous contamination in industry. In a critical review published in 2012 by Chin and colleagues [52], the authors have listed the main companies

responsible for the current scenery regarded to the commercialization of POC diagnostic devices.

The paper-based miniaturized tools (i.e., µPADs, paper-based microfluidic and/or electrophoretic separation systems) have gained much attention for clinical and diagnostics applications. Both government and philanthropic organizations, including but not limited to Sentinel Bioactive Paper Network, the Bioresource Processing Research Institute of Australia (Biopria), the Program for Appropriate Technology in Health (PATH), Diagnostic for All (DFA), and the Bill & Melinda Gates Foundation have been supporting the development and commercialization of low-cost diagnostics tools, including paper-based miniaturized tools [72].

The other choice of low-cost material for miniaturized or microfluidic devices for clinical application is plastic, and the commercialization of plastic-based miniaturized systems is much easier due to the fact that the plastic processing and fabrication techniques (such as injection molding, hot embossing) are mature and well-established. These plastic processing techniques offer easier and larger-scale production of a miniaturized system with integrated components, precision sample, and reagent control, 3D device feature, excellent optical clarity. Due to these favorable features, successful commercialization of plastic made miniaturized clinical devices has been reported for analyzing whole blood, and other biofluids such as tear and urine. As plastic materials offer excellent optical transparency, optical imaging-based detection, such as fluorescence, absorbance, and calorimetric detection methods, are easy to implement, but other detection methods such as electrochemical detection are also easy to implement as techniques required for

electrode embedding in plastic is well-established. The companies who are considered as the leader for commercializing such miniaturized platforms are

Abaxis, Alere, Focus Diagnostics, Micronics (https://www.micronics.net/), Mbio Diagnostics, TearLab, and Zyomyx. Another new approach, toner-based platforms, also showed much promise for commercialization [53].

The commercialization of low-cost, miniaturized diagnostics platforms is still at its infancy, and all the above examples comprise a tiny fraction of the diagnostic industry, which is dominated by macro-scale equipment and instrumentation, suitable for centralized testing requiring hefty resources. The micro-scale or miniaturized diagnostic platforms have the potential to revolutionize the health care industry by enabling low-cost alternatives for low-resource settings. But for this scenario to be materialized, a strong and effective collaborative effort between academic and industry research is imperative. The path from the inception to proof-of-concept to the successful commercialization of such technologies is long and exhaustive. More often, a lucrative proof-of-concept technology fails to see successful commercialization due to technological difficulties, complicated operation, lack of user-friendliness, and more. The regulatory requirements for diagnostic devices are rigorous and demand extensive field trials and clinical validation. Only a strong and effective framework which combine both academic research capability with industrial resource will transform the miniaturized diagnostics platforms into the diagnostic tool of the future.

1.9 Challenges of Electrophoresis on Paper-Based Substrates

The blessings of miniaturized paper-based analytical systems have provided fast, reliable, portable, and low-cost solutions. But, the novel approach for an analytical solution does suffer from certain limitations. The increasing scientific efforts in recent times have advanced the field, while some technical challenges still need to be overcome.

The demand for rapid separation and analysis requires higher field strength, and the consequence of a higher applied electric field is an increase in in-chip heat generation [73,74]. Increased heat generation in an electrophoresis system results in increased electrolyte evaporation, which affects the electrophoretic separation process. If the heat generation is too high, it can lead to damage of the support medium, deviation of the electrophoretic condition, and denaturation of the analyte. To overcome these challenges, novel fabrication approaches have been developed and implemented [74,75].

The paper-matrix has physical and chemical properties, such as non-specific absorption of analyte components. The surface area for absorption is much higher for the porous structure of paper substrates [56,76,77] compared to others, such as capillary-based systems. Application-specific surface treatment of paper substrate can reduce these undesired effects.

As the paper-based analytical system is still at an early stage, the interaction between the paper substrate and analyte group of interest is still unexplored and not well-understood. For example, charge density is important for electrochromatography separations exploiting ion exchange interactions, but may hinder the purer electrophoretic separations. Such phenomena can greatly influence, design, and development of the paper-

based miniaturized system. Therefore, the selection of the paper substrate and its application-specific modification may be necessary for enhanced efficiency in separation to different the target components of the analyte [78-80].

Last but not least, in parallel with the paper-substrate development and modification, electrolyte modification and optimization and other aspects of the electrophoretic conditions also need to be re-assessed and optimized for balancing the demand of miniaturization, separation speed, and separation resolution [81]. Fundamental studies, such as developing an analytical framework for optimizing and correlating electrophoretic conditions and separation resolution, still need to be done to provide greater insight and understanding of the separation process in a paper-based system.

1.10 Discussion and Conclusion

Paper-based miniaturized device and its application for electrophoretic separation (microchip electrophoresis) is a novel field, and the research in this field is at an early stage compared to other contemporary technologies. The promise that paper-based microchip electrophoresis holds for diagnosis, point-of-care (POC) testing, environmental monitoring are waiting to be materialized, but it requires momentous effort from the scientific community.

The clinical application of paper-based analytical systems is not limited to countries with limited resources. They hold immense potential for in-field applications such as rapid-diagnostic tools for first responders, military troops operating in remote and challenging environments. The ultimate success of the paper-based analytical system would be to transform the healthcare industry by establishing in-house or home-based early

diagnosis/screening practices with highly accurate and reliable test results. This capability, in time, would reduce the burden of health-related costs for individuals as well as for the government.

Low cost of fabrication, simplicity of the device and the structural and application flexibility makes the paper-based analytical system an aspiration for novel exploration and low-cost solution for addressing healthcare need in developing and underdeveloped countries, where the limited resources make it impossible to address the pressing screening and diagnostics needs. The current research trend for paper-based analytical system and/or μPADs are aiming to embed: (1) multiplexing of assays, (2) sample and reagent processing capability, (3) on-chip sample separation and analysis, (4) automated analysis with embedded or external capabilities, and (5) the ability to analyze multiple samples using a single device.

The trending research on the paper-based systems would definitely result in novel design and fabrication methods. Decisive factors for evaluating the success of this technology are (1) material cost, (2) fabrication complexity and cost, (3) ease/scope of mass-production, (4) integration capability of operational accessories, (5) degree of dependency on external operational accessories, (6) user-friendliness or ability to be used by minimally trained personnel, (7) ease of result interpretation, (8) scope for automated result analysis, (9) integration capability with IoT (internet of things) for remote and personalized medicine framework, (10) limit of detection (LOD), and above all (11) reliability of the test.

It is true that the paper-based system has the capability to provide a passive operational capability, but the capability is not universal, and especially for electrophoretic separation, a passive system may not be archived by principle. Therefore, the instrumentation required for the test performance and result analysis will dictate the feasibility of remote and portable application of such paper-based systems. Systems that would rely on complicated and/or delicate instrumentation still hold promise for laboratory-based testing.

Industries or laboratories with expertise in paper development, processing, and manufacturing are expected to play a vital role in the prospect and progress of paper-based systems, especially the commercialization of paper-based diagnostics for POC testing, screening, and diagnosis. The technology and the cost of application-specific paper development and production would directly impact the market price for POC testing devices, but this is not the only driving factor for the successful commercialization of paper-based systems. The overall design, cartridge/microchip assembly, relevant accessories, complexity of the test protocol (sample collection, processing, discarding), and user-independent result interpretation would also dictate the successful commercialization of paper-based systems. That being said, the role of the supporting medium i.e. the paper, will still be the central issue for the successful development of the paper-based system. The majority of the reported studies in the literature rely on generic filter paper. Development of various grades of paper materials with controlled structure, chemical and surface properties would further expand the application and success of paper-based analytical systems.

The value of a new technique or a new product could only be embodied after it has been commercialized and accepted by the potential users. Similarly, paper-based microfluidics, as a new platform or system for liquid manipulation and sample detection, will also need time to attest its real value to society.

Chapter 2: Paper-based MicroChip Electrophoresis (MCE) System for Hemoglobin Separation

2.1 Abstract

Hemoglobin disorders are among the world's most common monogenic diseases. Hemoglobin S, C, and E are the most common and significant hemoglobin variants worldwide. Sickle cell disease, caused by hemoglobin S, is highly prevalent in sub-Saharan Africa and in tribal populations of Central India. Hemoglobin C is common in West Africa, and hemoglobin E is common in Southeast Asia. Screening for significant hemoglobin disorders is not currently feasible in many low-income countries with a high disease burden. Lack of early diagnosis leads to preventable high morbidity and mortality in children born with hemoglobin diseases in low-resource settings. In sub-Saharan African countries where SCD is highly prevalent, nearly a quarter of a million babies are born with the disease each year. An estimated 50-90% of these babies die before age 5 because they are not diagnosed or treated. The WHO estimates that more than 70% of SCD related deaths are preventable with simple, cost-efficient interventions, such as early point-of-care (POC) screening followed by treatment. Here, the first miniaturized, paper-based, microchip electrophoresis platform, for identifying the most common hemoglobin variants easily and affordably at the point-of-care in low-resource settings, has been described. HemeChip works with a drop of blood. HemeChip system guides the user step-by-step through the test procedure with animated on-screen instructions. Hemoglobin identification and quantification is automatically performed, and hemoglobin types and percentages are displayed in an easily understandable, objective way. HemeChip is a versatile, mass-

producible microchip electrophoresis platform technology that addresses a major unmet need for decentralized hemoglobin analysis in resource-limited settings.

2.2 Introduction

Screening for hemoglobin disorders is not currently feasible in many low-income countries with high disease burden [82]. Hemoglobin S is highly prevalent in sub-Saharan Africa [83] and in tribal populations of Central India [84]. Hemoglobin C is common in West Africa [85], and hemoglobin E is common in Southeast Asia [86]. With increasing migration and inter-racial marriages, combinations of these hemoglobin variants are expected to be encountered more all around the world [87,88]. In sub-Saharan African countries [83], and in tribal populations of central India [84], where hemoglobinopathies have the highest prevalence [82], hundreds of thousands of undiagnosed afflicted babies are born each year [89-91]. For example, in Nigeria, where the occurrence of sickle cell disease (SCD), the most common hemoglobin disorder, is the highest in the world. The prevalence of the disease is up to 20-30 per 1000 births, or at least 150,000 children born with the disease every year [92]. An estimated 50-90% of these babies die before age 5, in part because they are not diagnosed and hence not treated [89,93-96]. It is projected that by 2050, about 400,000 babies will be born with SCD annually worldwide [82,97].

Hemoglobinopathy screening after birth is mandated by all 50 states in the United States and in the District of Columbia, as well as in many other developed states, including The United Kingdom and France [96,98-101]. Newborn screening programs in the United States and other developed countries typically involve the collection and shipping of blood samples to centralized laboratories [98,102,103]. While decentralized blood sample collection and

centralized testing work in developed countries, this approach is not practical in resource-limited regions due to the logistical and infrastructural challenges. Hemoglobinopathy screening studies conducted in low-resource settings, using centralized laboratories, have reported up to 50% lost to follow-up [104-106].

In resource-rich countries, standard clinical laboratory tests (high-performance liquid chromatography (HPLC) and hemoglobin electrophoresis) are typically used in the diagnosis of hemoglobin disorders [107]. Additionally, genetic testing, usually polymerase chain reaction-based, can be used to precisely identify globin gene mutations [108]. However, these advanced laboratory techniques require trained personnel and state-of-the-art facilities, which are lacking or in short supply in countries where the prevalence of hemoglobin disorders is the highest [82]. Furthermore, these tests are costly in terms of time, labor, and resources [95,109]. For example, it may take days to weeks to receive the test results from centralized clinical laboratories [109], and when screening is conducted in remote areas, locating those who test positive may be difficult or impossible [94,95,109]. Therefore, there is a need for affordable, portable, easy-to-use, accurate point-of-care tests to facilitate decentralized Hb testing in resource-constrained countries [82,110]. The realities of resource-limited environments demand a fundamentally different approach to diagnosis: one that is affordable, portable, and easily administered by entry-level healthcare workers in local health service settings or in rural areas at the point-of-need [94,95,109]. Importantly, test results must be available while the patient is still present so that the test result can be given to the patient or legal guardian(s) immediately, and the treatment and education can begin without losing the patient to follow-up.

In this chapter, the design, development, manufacturing, and testing of a novel point-of-care hemoglobin test, HemeChip has been described. HemeChip is a paper-based, microchip electrophoresis technology that helps with the diagnosis of hemoglobin disorders in resource-limited settings. HemeChip is single-use and cartridge-based, which can be mass-produced at low-cost. HemeChip separates, images, and tracks hemoglobin variants in real-time during electrophoresis. The fundamental principle behind the HemeChip technology is Hb electrophoresis, in which different variants can be separated based on charge differences, when subject to an electric field in the presence of a carrier substrate [111,112]. The HemeChip test works with a standard finger-prick or a heel-prick blood sample. HemeChip test is completed within ten minutes and can be run at the point-of-care; hence, the results would be available during a patient's visit. Furthermore, the compact design of the HemeChip allows portability for decentralized testing and use at the point-of-need, which eliminates blood sample transfer to central laboratories.

2.3 Methods

2.3.1 Fully Integrated Mass-Produced Paper-Based Microchip Electrophoresis Cartridge

The HemeChip cellulose acetate paper-based microchip electrophoresis system (**Figure 2.1**) facilities, for the first time, real-time tracking and quantitative analysis of hemoglobin electrophoresis process (**Figure 2.2**). The HemeChip cartridge is composed of two injection-molded plastic parts made of Optix® CA-41 Polymethyl Methacrylate Acrylic. This single-use, the cartridge-based design was transformed from a proof-of-

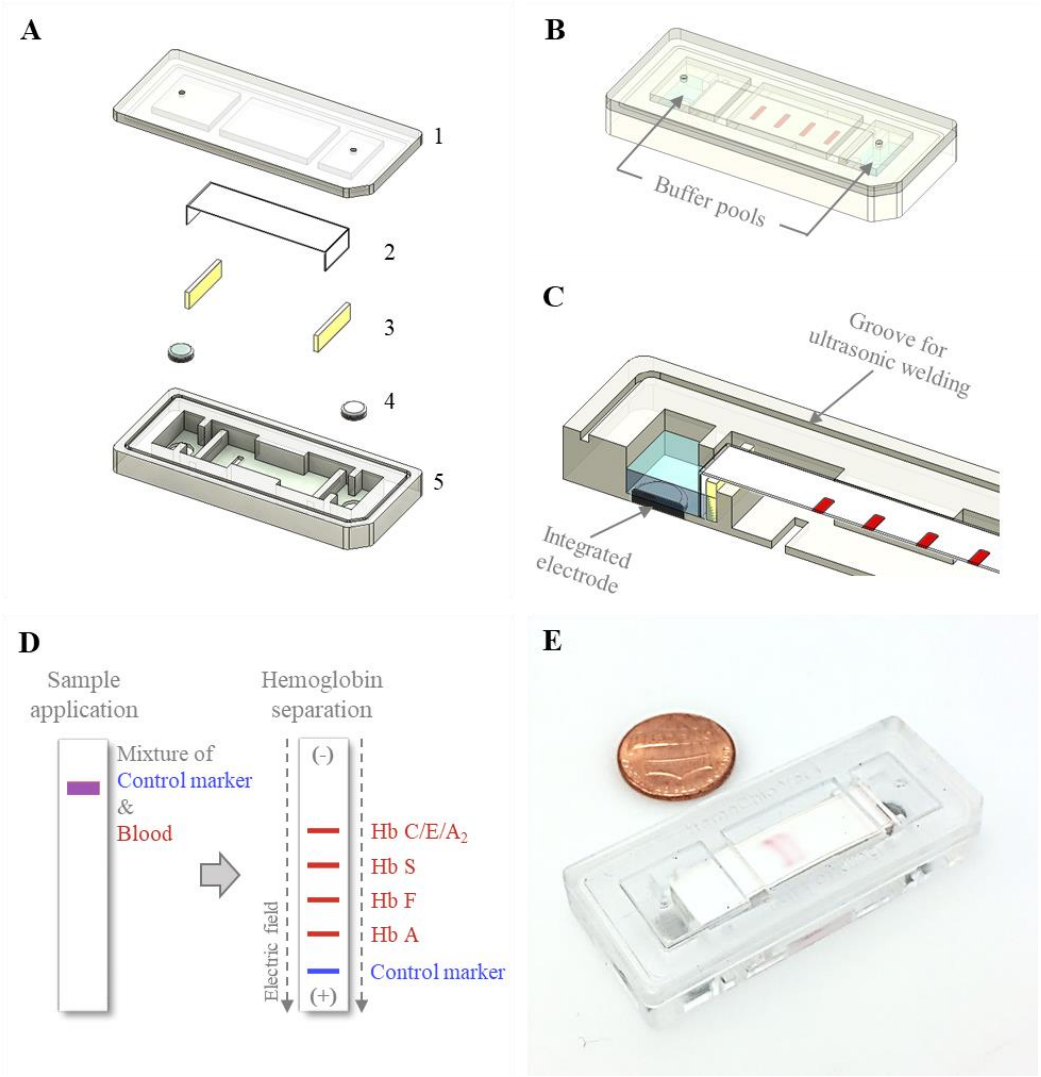

Figure 2.1. HemeChip: paper-based microchip electrophoresis for hemoglobin testing. HemeChip is a miniaturized, fully integrated cartridge-based microchip electrophoresis system that can be mass-produced. **(A)** Top (1) and bottom (5) plastic parts are manufactured via injection molding. The cartridge contains a single strip of cellulose acetate paper (2), a pair of blotting pads (3), and integrated stainless-steel electrodes (4). **(B)** HemeChip cartridge design is compact, fully integrated, and self-contained, including liquid compartments (buffer pools). One corner of the HemeChip cartridge is chamfered to restrict orientation and facilitate correct placement during use. **(C)** A partial section view of the internal components of HemeChip, showing the cross-section of an electrode and the cellulose acetate paper. **(D)** A schematic representation of the separation of hemoglobin variants in HemeChip: normal hemoglobin (Hb A), fetal hemoglobin (Hb F), sickle hemoglobin (Hb S), and hemoglobins C/E/A_2 that co-migrate. A blue control marker (xylene cyanol) is pre-mixed with blood before sample application into the cartridge. **(E)** A fully assembled injection molded HemeChip is shown after a completed test with hemoglobin S and C bands that are visible.

concept laboratory prototype to a version that supports low-cost mass-production via injecting molding (**Figure 3.1**), as described in **Chapter 3**. The top and bottom parts (**Figure 3.2**) were manufactured with a 1+1 injection mold. Cartridge design embodies specific geometrical features and a precisely designed energy director (**Figure 3.2**) for rapid ultrasonic welding after assembly. Cellulose acetate paper was chosen because of its

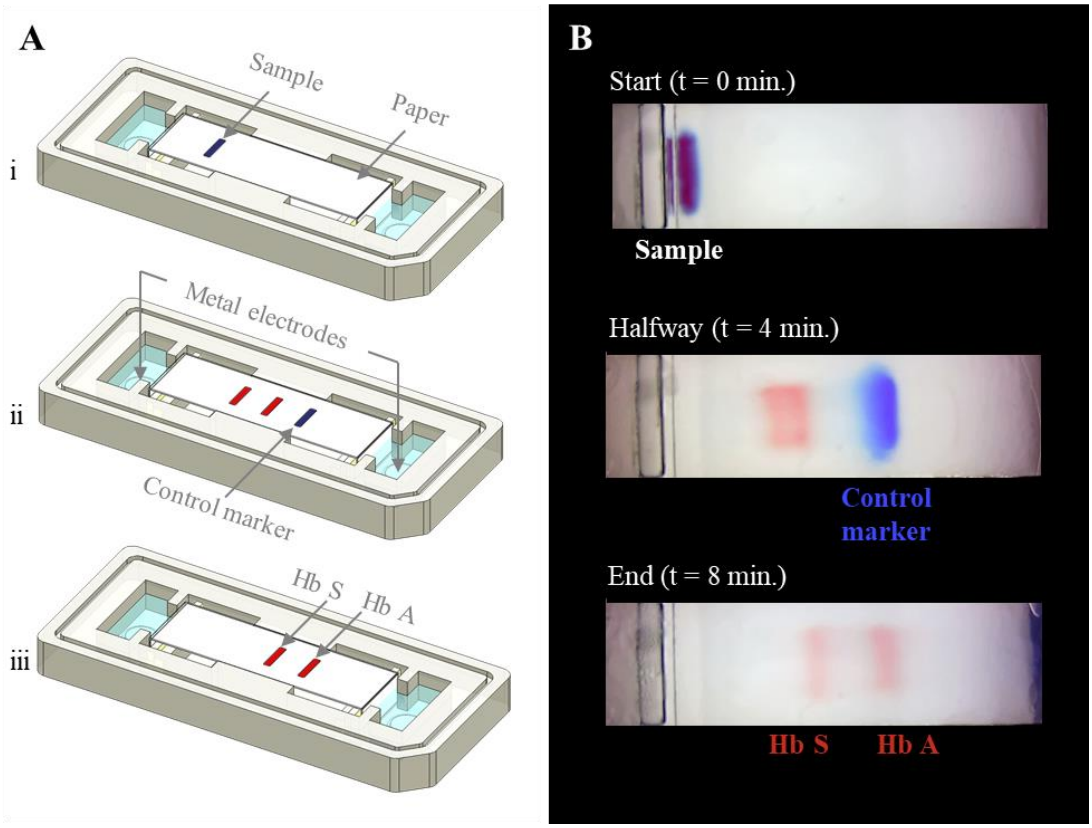

Figure 2.2. Overview of HemeChip operation and hemoglobin variant separation with a control marker. (A) Schematic illustration of hemoglobin separation and the blue control marker (xylene cyanol) migration in HemeChip. **(i)** The beginning of the test is shown with a blood sample and marker mixture applied. **(ii)** Hemoglobin bands and the control marker start migrating. The migration of the blue control marker is used image processing algorithm to confirm that the test is running as expected. **(iii)** Fully separated hemoglobin bands appear at the end of the test. The control marker migrates all the way to the end and leaves the field of view, at which time, hemoglobin bands are imaged and analyzed in their final positions. **(B)** Time-lapse images captured during a HemeChip test demonstrate the separation of hemoglobin A and S bands and the migration of the control marker.

stability over environmental conditions [113]. Cartridge layout, plastic material selection, and injection molding process were engineered to achieve structural integrity, uniform optical clarity, and high light transmission (up to 80%) in the visible spectrum (**Figure 3.3**). The injection-molded HemeChip cartridge embodies a pair of round corrosion-resistant [114], biomedical grade stainless steel 316 electrodes [115]. HemeChip electrodes provide oxidative resistance, stability against electrochemical reactions during operation, and reliability

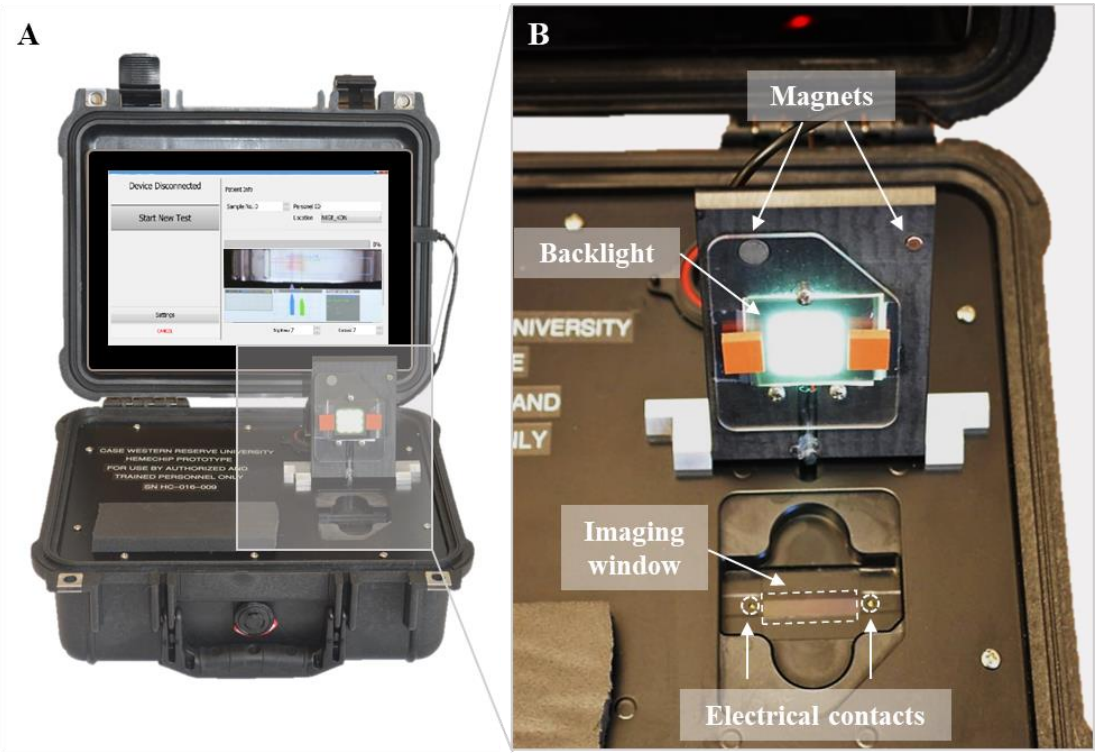

Figure 2.3. Portable reader for HemeChip. (A) The portable HemeChip prototype readers were built for research use only in a robust Pelican Protector Case for clinical studies worldwide. The reader includes a rechargeable battery, a touch-screen tablet computer, and an integrated imaging system. The reader guides the user through the test procedure via on-screen instructions, allows real-time imaging, automated data analysis, result storage, and wireless transmission of test results. **(B)** The cartridge chamber in the reader houses electrical contacts, an imaging window, and a backlight for imaging in transmission mode. The chamber door is equipped with magnetic contacts as a safety feature for sensing the door status as open or closed,

of electrical connection with the power source (**Figure 2.1A**). The combination of high stability cellulose acetate paper [113], injection-molded Polymethyl Methacrylate Acrylic plastic, and corrosion-resistant biomedical grade stainless-steel electrodes [114,115] results in shelf life of at least two years. The cartridge also houses a pair of buffer pools that are in direct contact with the electrode top surface and the cellulose acetate paper strip (**Figure 2.1B&C**). One corner of the HemeChip cartridge is chamfered to facilitate correct orientation during use (**Figure 2.1A&B**).

2.3.2 HemeChip Portable Reader Design

One advantage of point-of-care technologies is that they can be used in remote locations where the use of existing technologies is not feasible [116-118]. HemeChip has been designed as a battery-powered, portable test platform to enable hemoglobin testing in remote locations (**Figure 2.3**). HemeChip reader consists of a rechargeable battery power supply, a data acquisition system, and an imaging and image analysis unit (**Figure 3.4**). The portable HemeChip Reader, once fully charged, allows a minimum of ten hours of testing, which corresponds to at least 48 tests per charge. The reader is equipped with a rechargeable 12V lithium-ion battery with a capacity of 11,000 mAh, yielding 132-Watt hours. Each test consumes about 2-Watt hours. The reader enables automated interpretation of test results, local and remote test data storage, and includes geolocation (Global Positioning System). The user is guided through the test process, and the test result is shown on the reader's display and the reader stores the results. The reader can link via Bluetooth or Wi-Fi to a cell phone or PC to transfer the information for review or retention. The data acquisition system is a national instruments data acquisition board (USB-6001)

controlled by a custom-built LabVIEW program that records the voltage and current values for the duration of the test. The imaging system consists of an ELP video camera (ELP-USB500W02M) that captures real-time video and the run-time images (**Figure 3.4**). The

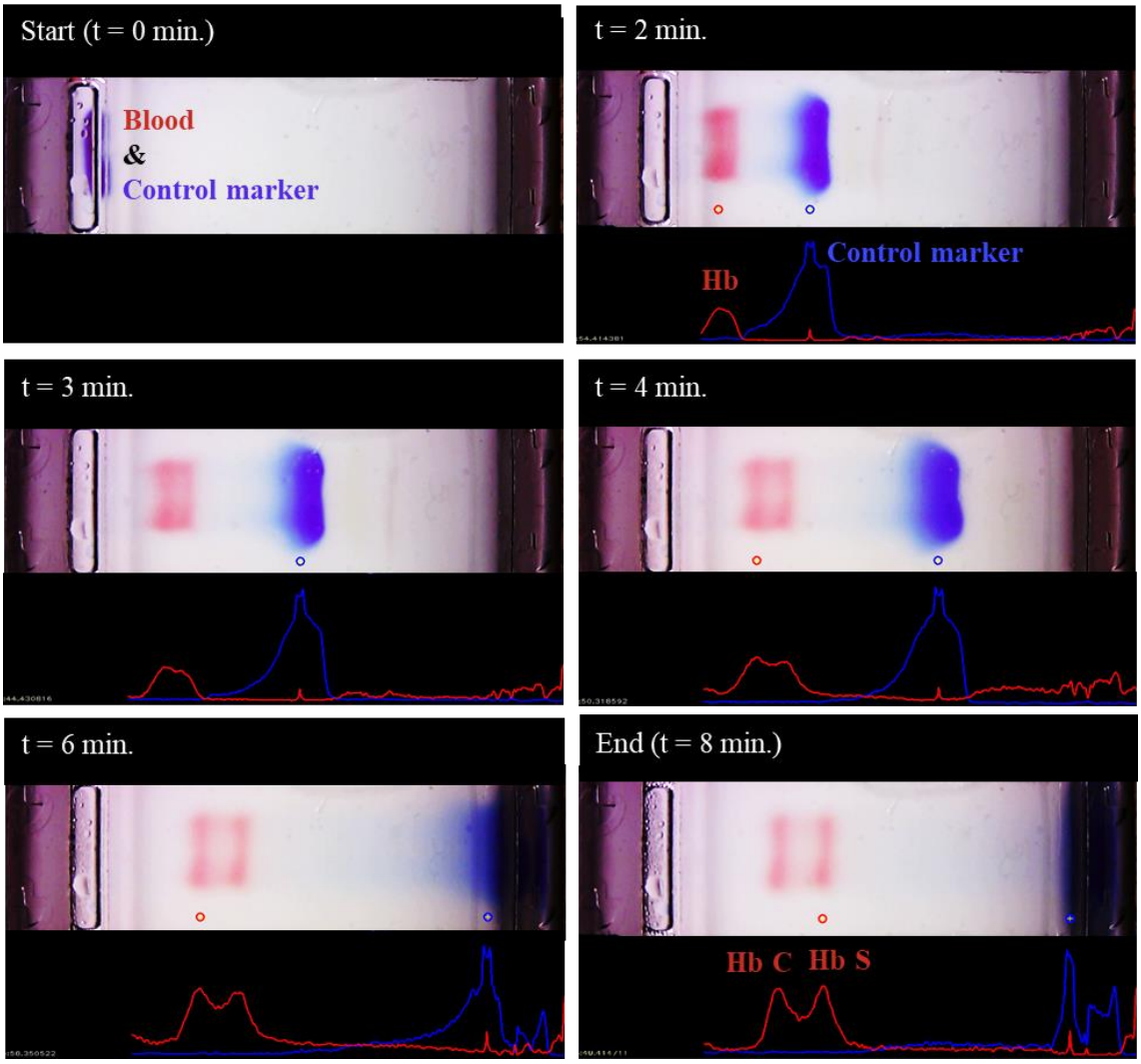

Figure 2.4. Real-time imaging, image analysis, and tracking of control marker and hemoglobin bands in HemeChip. The time-lapse images show the real-time tracking of the blue control marker and hemoglobin bands. Hemoglobin bands and the control marker are imaged, automatically recognized, and identified. The movement of the control marker is tracked and used to confirm that the test is running as expected. In this example, hemoglobin types S and C were identified by the algorithm.

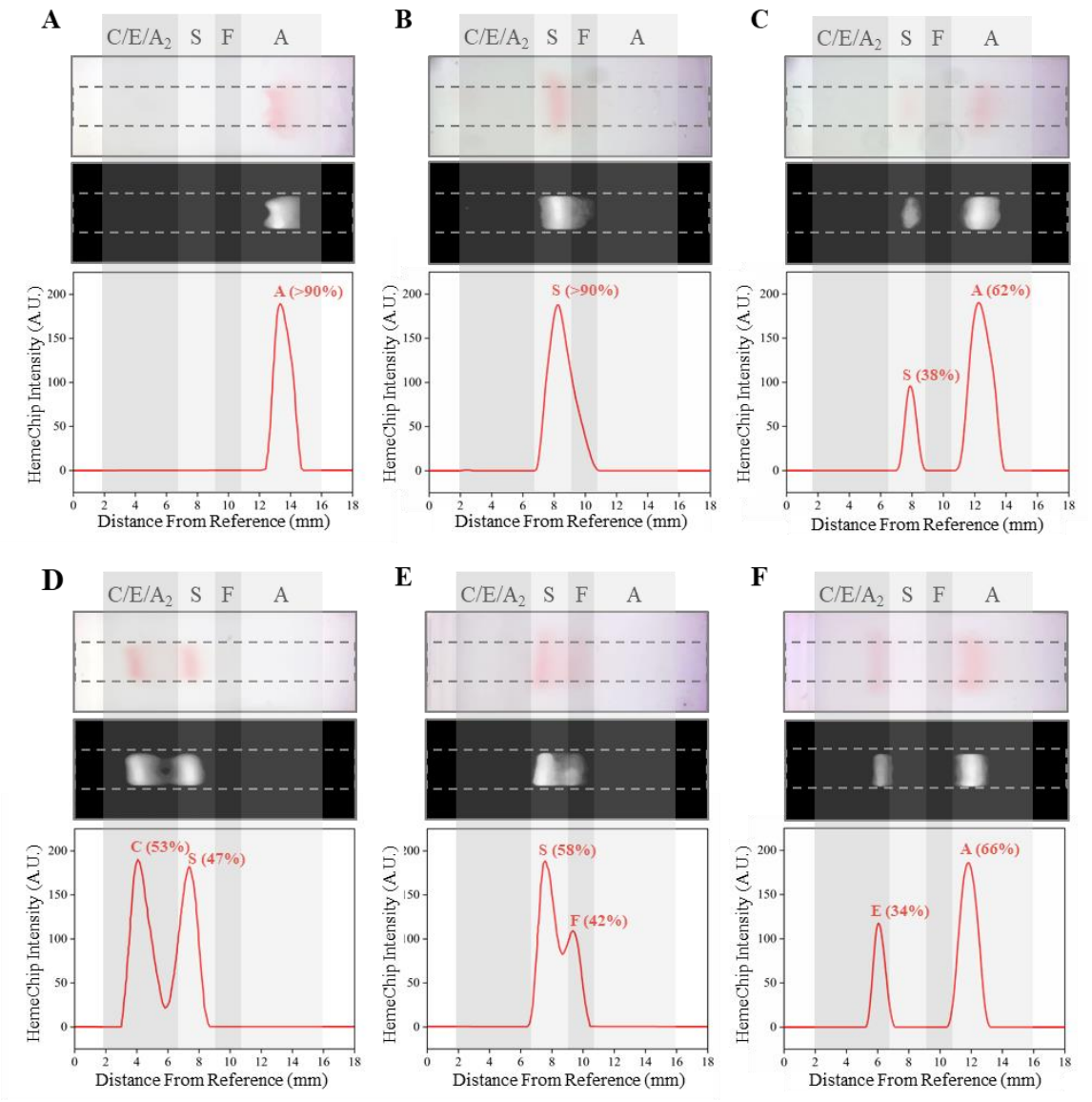

Figure 2.5. Identification of hemoglobin types and quantification of hemoglobin percentages by HemeChip. Typical HemeChip results are presented for the main hemoglobin variants tested. For each subset, the top image represents the raw image captured by the HemeChip reader at the end of the test. The middle black and white image are generated by the image analysis software algorithm to produce the HemeChip intensity curves (bottom image) for peak identification and Hb % quantification. Hb % values displayed were determined by HemeChip, which showed agreement with the reference standard method (HPLC). Gray regions indicate the approximate zones in which A, F, S, and C/E/A_2 bands appear at the end of the test. **(A)** Normal (no abnormal Hb) with Hb AA (>90%). **(B)** SCD-SS with Hb SS (>90%). **(C)** SCD Trait with Hb AS (A: 62%, S: 38%). **(D)** SCD-SC with Hb SC (S: 47%, C: 53%). **(E)** SCD-SS with Hb SF (S: 58%, F: 42%). **(F)** Hb E Trait with Hb AE (A: 66%, E: 34%).

imaging system includes 85º wide-angle 5 megapixel HD USB camera, and the camera optics are modified with a 3.6 mm, F1.3 megapixel, CCTV Board Lens. The imaging system and the developed software are calibrated to correct for the fish-eye effect (due to the wide-angle lens) and to normalize the nonlinear pixels-to-distance relation. The power supply, imaging system and data acquisition system are assembled inside a rugged Pelican 1400 case (**Figure 2.3A**). An embedded tablet computer runs the custom-built software to control the Reader as well as to acquire, process, and analyze the run-time data. The chamber door houses the backlight used in the imaging system and a magnetic door sensor to ensure that the high voltage supply turns on only when the door is closed (**Figure 2.3B**). An array of white light LEDs is used as the light source for the imaging system. The HemeChip cartridges are imaged using a transmissive light mode.

2.3.3 User Interface and Automated Image Analysis

A user-friendly user interface (UI) has been developed to guide the user through the test, perform quality checks, and analyze the results. This UI has the following functionalities (**Figure 3.5**): **(i)** perform hemoglobin separation with HemeChip by controlling the Reader electronic circuit, **(ii)** collect runtime data for quality checks, **(iii)** guide the user through the test procedure using step-by-step instructions (**Figure 3.6**), and **(iii)** analyze post-run data analysis from the collected real-time data and images. The UI performs the test control and run-time data collection simultaneously and automatically without any interference or assistance from the user. The UI is designed to generate the data files with a specific file name and format based on the information provided before the test, which contains the patient, sample and test identifier. HemeChip tests are

monitored in real-time with a custom developed application. The real-time tracking of hemoglobin bands (**Figure 2.4**) and automated image analysis provide necessary information for the identification and quantification of the test results. The application is configured to automatically detect the sample application point and the separated hemoglobin bands. Relative pixel intensities along the paper are used to identify the peaks corresponding to each type of hemoglobin band. The area under each peak is calculated to obtain the relative hemoglobin percentages. The area under each peak is outlined using the valley-to-valley method commonly used in gas chromatography [119]. The HemeChip image analysis algorithm was developed to find the position and intensity of the single hemoglobin band (for homogeneous hemoglobin types) or multiple hemoglobin bands (for heterogeneous hemoglobin types) that appear on the cellulose acetate paper strip inside the HemeChip after a test has been performed. The captured RGB image is analyzed to determine how far the hemoglobin band(s) propagated and the relative percentage of each band based on pixel intensity data.

2.3.4 Blood Sample Acquisition and Testing

Blood samples used in this study were collected as part of the standard clinical care, and only surplus de-identified blood samples were utilized for testing. The whole blood samples were tested with both HemeChip and the reference standard HPLC (VARIANT™ II, Bio-Rad Laboratories, Inc., Hercules, California) in Cleveland, Ohio. The HemeChip reader guides the user step-by-step through the test procedure (**Figure 3.6**) with animated on-screen instructions to minimize user errors. Users were trained to use a custom-designed micro-applicator (**Figure 3.7**), which is included in a kit (**Figure 3.8**) with graphical

instructions for use (**Figure 3.9**). Hemoglobin identification and quantification is automatically performed with custom software on the reader and results are reported to the user in a clear and objective way.

2.4 Results

2.4.1 HemeChip Separates, Images, and Tracks Hemoglobin Variants Real-Time During Electrophoresis

The fundamental principle behind the HemeChip technology is hemoglobin electrophoresis, in which different hemoglobin variants can be separated based on electric charge differences when subjected to an electric field in the presence of a carrier substrate [30, 31]. The HemeChip test works with a standard finger-prick or a heel-prick blood sample that is collected according to the World Health Organization (WHO) guidelines for drawing blood [46], which typically yields about 25 µL per drop [47]. For ease of handling, 20 µL of blood is collected and diluted with 40 µL of lysing solution. Next, less than 1 µL (0.56 µL ± 0.17 µL, N=5) of lysed blood sample is transferred into the cartridge for electrophoresis (**Figure 2.1D**). The actual blood volume utilized per test is approximately 0.2 µL. The HemeChip separates hemoglobins A, F, S, and C/E/A_2 on cellulose acetate paper, which is subjected to an electric field (**Figure 2.1D**). Tris/Borate/EDTA (TBE) buffer is used to provide the necessary ions for electrical conductivity at a pH of 8.4 in the cellulose acetate paper [30, 31]. The pH-induced net negative charges of the hemoglobins to cause them to travel from the negative to the positive electrode when placed in an electric field (**Figure 2.1D**). Differences in hemoglobin mobilities due to their negative electrical charge allow hemoglobin separation to occur (**Figure 2.1D&2.2**) with visible results at the

end of a HemeChip test (**Figure 2.1E**). Among the four major hemoglobin types, which were tested, hemoglobin C/E/A_2 co-migrate and they are the slowest. Hemoglobin A is the fastest moving hemoglobin in an alkaline solution. A unique feature of HemeChip is that it utilizes a blue control marker (xylene cyanol) that is pre-mixed with the blood sample before application into the cartridge (**Figure 2.1D&2.2A**). Towards the end of the test, the blue control marker reaches the end of the cellulose acetate paper strip (**Figure 2.2A&B**) and disappears into the buffer pool, leaving behind the separated hemoglobin variants (**Figure 2.2B**). At this point, the hemoglobin bands are automatically identified by a custom software, running in the HemeChip Reader (**Figure 2.3**) based on their respective locations on the cellulose acetate paper strip relative to the sample application point (**Figure 2.4**). Hemoglobin in the blood sample form visible bands at the end of the test due to the natural bright red color of the protein **(Figure 2.1E&2.2B**). This feature of naturally red, visible hemoglobin, combined with optically clear HemeChip cartridge (**Figure 3.3**) in transmission imaging mode (**Figure 2.2B**) within the reader's imaging chamber (**Figure 2.3A&B**), negates the need for picrosirius red staining, which is typically utilized in benchtop cellulose acetate hemoglobin electrophoresis [30, 31].

2.4.2 HemeChip Automatically Identifies Hemoglobin Variants and Determines Their Relative Percentages

The blue control marker mobility on the cellulose acetate paper strip is tracked in real-time by the image processing and decision algorithm (**Figure 3.5**). The mobility of the control marker is then used to confirm that the test is running as expected (**Figure 2.4**). Briefly, the algorithm searches and finds the sample application mark (**Figure 2.4, t=0**

min.), and the intensity curve is generated for the red hemoglobin bands and the blue control marker. The intensity curve is evaluated to detect and track the movement of the peaks throughout the process (**Figure 2.4**). The peaks are identified based on their final locations at the end of the test (**Figure 2.4, t=8 min.**). The distance between each peak and the application point and the relative percentage of the areas under the peaks are evaluated to determine whether they fit into the categories pre-defined in the software for hemoglobin C/E/A_2, hemoglobin S, hemoglobin F, and hemoglobin A. The amount of hemoglobin is presented as a percentage that is relative to that of the other hemoglobin bands in the sample. In the case of a single hemoglobin variant is detected, such as Hb AA (**Figure 2.5A**) or Hb SS (**Figure 2.5B**), the HemeChip software reports a percentage value greater of >90%, which agrees with the results reported by the reference standard method (HPLC). If there is more than one peak identified, then the areas under each of the peaks are calculated and the relative percentages are reported, for example in the cases of Hb AS (**Figure 2.5C**), Hb SC (**Figure 2.5D**), Hb SS blood containing fetal hemoglobin (Hb F) (**Figure 2.5E**), and Hb AE (**Figure 2.5F**). Hemoglobin A and hemoglobin S separation is significantly greater ($p<0.001$) than hemoglobin F and hemoglobin S separation (**Figure 5.3**), which can be used to distinguish between Hb SF and Hb AS.

2.5 Discussion and Conclusion

HemeChip combines the benefits of standard hemoglobin electrophoresis with the benefits of a point-of-care test. HemeChip technology has a number of fundamental differences and unique features when compared to standard hemoglobin electrophoresis techniques. For example, HemeChip replaces the benchtop laboratory setup [111,112] with a

portable reader and replaces the hemoglobin controls [111,112] with a blue control marker (**Figure 2.4**). HemeChip provides hemoglobin type identification and quantitative results of relative hemoglobin percentages (**Figure 2.5**). The overall simplicity of the HemeChip enables any user to quickly and accurately screen for SCD and other hemoglobin disorders. The user is guided through the step-by-step process (**Figure 3.5**) with on-screen animated instructions, which minimizes errors (**Figure 3.6**). HemeChip does not require a dedicated lab environment and battery operation allows use in remote places lacking electrical power. These critical features distinguish HemeChip from currently available laboratory methods (**Table 3.1**) and other emerging point-of-care technologies for hemoglobin testing (**Table 3.2**).

Deploying a robust, portable, battery-operated platform as part of a point-of-care test has several advantages over alternatives (**Table 3.2**). For example, the reader includes a touchscreen display that guides and helps the user with the test procedure, reduces the training time and minimizes user errors. The portable reader also allows digital data entry, including patient demographics. The reader also enables secure, encrypted data storage and wireless transmission to the cloud, which would enable tracking and follow-up of patients using electronic records and mobile networks [82]. The reader displays results on the screen in a clear and objective way, removing user interpretation errors. In comparison, point-of-care lateral-flow assays lack a portable reader for objective analysis or electronic record keeping (**Table 3.2**). Therefore, these methods rely on the user to visually interpret the results and manually record the clinical data, which is prone to errors. In fact, in clinical research databases, user misinterpretation and data entry errors have been reported to range between 2.3% to 26.9% [120].

Electrophoresis techniques share a common limitation. Some hemoglobin types appear in the same electrophoretic window, as they exhibit the same or similar electrophoretic mobility in a given condition. For example, in capillary zone electrophoresis, it can be challenging to quantify hemoglobin A_2 in the presence of hemoglobin C, due to partial overlap between the two zones for these two hemoglobin types [121,122], which may be improved using curve fitting methods. Hemoglobin G and hemoglobin D are difficult to separate because they have identical migration in gel electrophoresis, in capillary electrophoresis, and they have overlapping elution times in HPLC. This sharing of detection window or peak overlapping is also a challenge for the reference standard method, HPLC, as well as its alternatives [121,123,124]. For example, in HPLC, hemoglobin S elutes in the S window with 28 other hemoglobin variants, including 10 other β-chain variants [125]. A similar issue occurs in the A_2 window for HPLC, where hemoglobin E and 18 other hemoglobin variants elude in the same window, and 13 of these 18 variants are β-chain variants [125]. hemoglobins C, E, and A_2, co-migrate in paper-based hemoglobin electrophoresis [111,112]. Hemoglobins C, A_2, and E are all detectable, but it is not possible to differentiate them [111,112]. Therefore, instead of reporting Hb C or E or A_2 individually, HemeChip reports hemoglobin C/E/A_2.

In summary, HemeChip enables, for the first time, cost-effective identification of hemoglobin variants at the point-of-need. The HemeChip reader guides the user step-by-step through the test procedure with animated on-screen instructions to minimize user errors. Hb identification and quantification is automatically performed, and Hb types and percentages are displayed in an easily understandable, objective, and quantitative way. HemeChip is a versatile, mass-producible microchip electrophoresis platform technology

that may address unmet needs in biology and medicine when rapid, decentralized hemoglobin or protein analysis is needed.

Chapter 3: System and Process Development for Paper-based MicroChip Electrophoresis (MCE) System

3.1 Abstract

The journey from the inception of a miniaturized system to the proof-of-concept prototyping and its transformation to a mass-producible version of the concept is an excruciating and difficult process. The vast majority of the reported literature in the field of miniaturized analytical systems are focused on the design and development of the proof-of-concept prototype and their performance evaluation, while the transformation of the proof-of-concept prototype to a fully functional mass-producible commercial prototype is close to non-existence in the literature. The successful transformation of the proof-of-concept prototype into a mass-producible commercial platform demands not only the transformation of the miniaturized device, but also the development and optimization of operational accessories, and user-friendly test protocol. In this chapter, the transformation of the proposed paper-based microchip electrophoresis system into a mass-producible system is presented. The scope of this chapter includes the necessary hardware and process development for the successful implementation of the system in the field for clinical validation of the developed point-of-care (POC) system.

3.2 Materials

HemeChip was originally designed and developed using a lamination approach, with Poly (methyl methacrylate) (PMMA) sheets from McMaster-Carr (Elmhurst, IL), and ePlastics (San Diego, CA) that were later laser-cut (VersaLASER VLS2.30) and laminated with 3M optically clear double-sided adhesive (DSA) purchased from iTapeStore (Scotch Plains, NJ). The injection-molded HemeChip was developed in collaboration with Thogus Products (Avon Lake, OH). The Poly (methyl methacrylate) (PMMA) resin (Optix CA-41 FDA) for injection molding was procured from Plaskolite Inc. (Columbus, OH). The blotter pads were purchased from Helena Laboratories, Inc. (Beaumont, Texas). 1x Tris/Borate/EDTA (TBE) buffer solution (pH 8.3) was made from 10x TBE Buffer solution (Invitrogen™, Carlsbad, CA), diluted with deionized (DI) water (MilliQ Academic, Billerica, MA). Ultrapure DNase/RNase-free water was purchased from Thermofisher Scientific (Waltham, MA). Ultrapure grade Xylene Cyanol and the plastic-backed cellulose acetate sheets were purchased from VWR International LLC (Radnor, PA). Individually wrapped, sterile, stainless steel, disposable lancets were purchased from Med-Tex (Philadelphia, PA). The USB camera (ELP-USB500W02M) was purchased from eplcctv (Guangdong, China). The HemeChip Reader was developed in collaboration with Hemex Health (Portland, OR). The 3D CAD designs of the components developed for HemeChip were created using SolidWorks 3D CAD (Waltham, MA). Designs for the laser-machined component were created using CorelDRAW Suite X6 (Corel Corporation, Ottawa, Ontario).

3.3 Design Transformation of HemeChip from Laboratory Prototype to Mass-Producible Cartridge

The HemeChip cartridge was previously fabricated by a lamination approach composed of five distinct plastic layers and did not incorporate integrated electrodes (**Figure 3.1A&B**). In the injected molded design, the number of plastic parts was reduced to two, a top part, and a bottom part, which can be ultrasonically welded to encompass the internal components and integrated stainless-steel electrodes (**Figure 3.1C&D**). This reduction in the number of injection-molded parts reduced the final assembly time and effort. The current design employs integrated stainless-steel electrodes (**Figure 3.1C&D**). The choice for electrode material was constrained by the cost and the corrosion resistance of the electrode material. The use of noble metals and/or their alloys, which are the preferred materials for specialized applications [126-129], would have increased the cost of the chips significantly. In addition, noble metals can corrode when subjected to electrochemical processes [129-132]. The 316 stainless steel, which was employed, is known for its high corrosion resistance [115]. It is inexpensive and is available in a variety of stock shapes that are easily machined or processed into the required dimensions. Although the design is complicated in view of all the delicate interior features, this adaptation provided more control over the design of the complex interior features, which were unattainable with the lamination-based fabrication approach (**Figure 3.1A**). These interior features include custom-designed buffer pools, buffer basin ribs, metal electrode enclosures, alignment and positioning features for the cellulose acetate paper strips, sample and buffer ports, fiducial markers, and product artwork (**Figure 2.2A&B**). Another improvement to the HemeChip design was the inclusion of the in-chip blotting mechanism (**Figure 3.1C**). The blotting

mechanism is designed to handle any excess TBE buffer that may be applied to the cellulose acetate paper. A notable addition to the transformed design is the energy director and ultrasonic welding groove for the purpose of ultrasonic welding to fully seal the HemeChip cartridge top and bottom pieces (**Figure 3.2A&B**).

3.4 Mass-Production of HemeChip Cartridges via Injection Molding

3.4.1 Injection Mold Design

The HemeChip prototype design (**Figure 3.1A&B**) has been transformed into a moldable injection design (**Figure 3.1C&D**) with a plastic bottom and a top part (**Figure 3.2A&B)** using a 1+1 mold. A 1+1 mold design is economical as it reduces the production cost due to less machine run time with reduced labor cost to produce each part. This is a very crucial aspect for mass-producing a point-of-care (POC) single-use cartridge as the cost per unit needs to be as low as possible. Optix® CA-41 Polymethyl Methacrylate Acrylic (PMMA) material was used in injection molding. The visual clarity of the Optix CA-41 is excellent. However, this visual clarity may be greatly impaired after the injection molding process due to the surface finish of the mold (**Figure 3.3A-C**). The visual clarity of the HemeChip is crucial since the detection method is based on image acquisition and analysis, and any impairment of visual clarity will significantly impact the performance of the detection system. Visual clarity and light transmission of the injection molded parts significantly improved after the mold underwent aluminum oxide polishing, which improved the visual clarity of the finished HemeChip part to its desired level (**Figure 3.3B-D**). Optical transmission for HemeChip components with both standard machine finishing and aluminum oxide finishing were tested and compared (**Figure 3.3B**). The optical

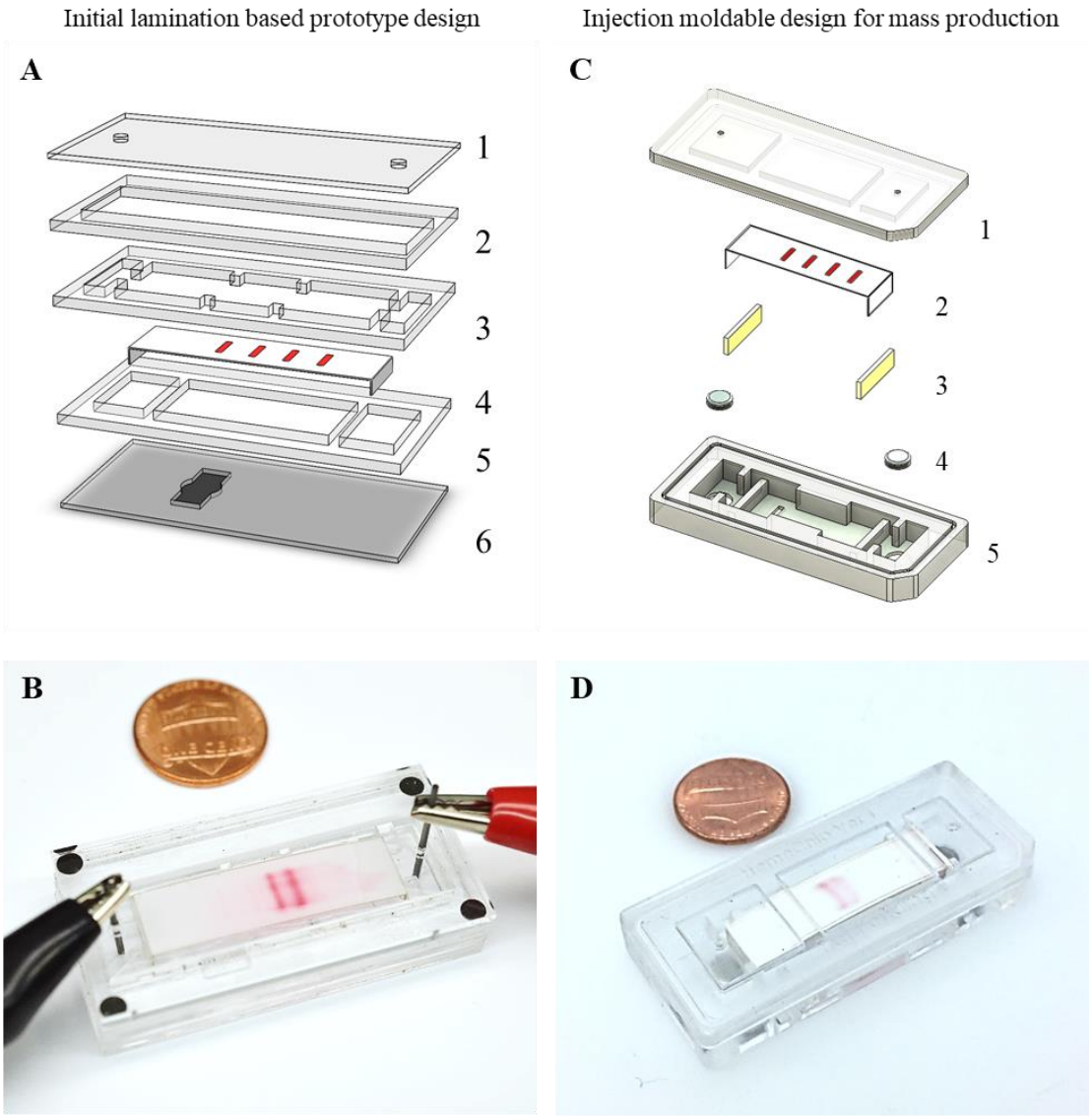

Figure 3.1. Transforming HemeChip design for injection molded mass production. **(A)** The first proof-of-concept design of the HemeChip utilized a lamination-based fabrication approach without integrated electrodes. This proof-of-concept prototype was made by laser micromachining and stacking five layers of PMMA sheets (1-3, 5&6) encompassing the cellulose acetate paper (4). **(B)** This lamination-based design helped us establish the proof-of-concept using manually inserted graphite electrodes (pencil leads) and an external power source. Separated hemoglobin bands are visible at the end of a proof-of-concept experiment. **(C)** Transformed mass-producible design of HemeChip includes a top (1) and bottom (5) injection molded Optix® CA-41 Polymethyl Methacrylate Acrylic (PMMA) parts, encompassing the cellulose acetate paper (2), blotting pads (3), and integrated stainless steel 316 electrodes (4). **(D)** An injection-molded, assembled, and ultrasonic welded HemeChip cartridge at the end of a test run with visible hemoglobin bands.

transmission for the HemeChip component was tested using the VASE Ellipsometer (J.A. Woollam Co., Inc., Lincoln, NE). The optical transmission was measured at an angle of 0° for wavelengths ranging from 300 ~ 1000 nm. The results showed that the HemeChip components produced in the aluminum oxide polished mold have a much higher optical transmission (up to 80%) compared to the standard machine polished mold. Optical clarity and light transmission significantly improved after the mold underwent aluminum oxide polishing (**Figure 3.3B-D**).

3.4.2 Injection Molding Process Parameters and Quality Control

HemeChip parts were manufactured using a Vertical Injection Molding Machine (VIMM). For the HemeChip injection molding, the Optix CA-41 was dried with a desiccant dryer at 93 °C (200 °F). The top and the bottom parts of the HemeChip were processed following different process parameters since the thickness and the design complexity differ for these two parts of the HemeChip cartridges. The top part of HemeChip was processed at a melt temperature of 241 °C (465 °F), keeping the rate of injection at 3 grams per

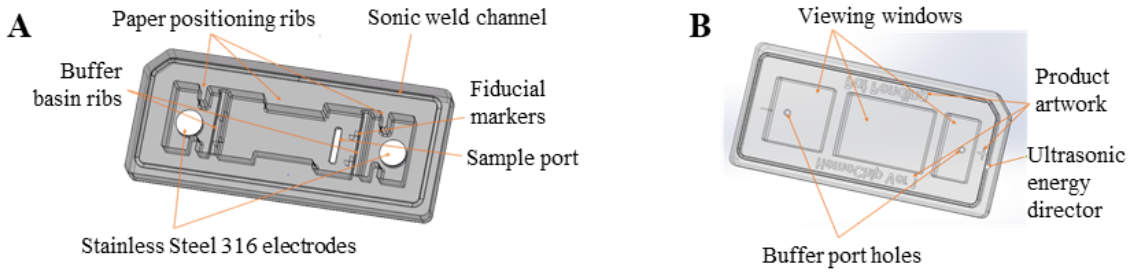

Figure 3.2. Injection moldable HemeChip design with bottom and top plastic parts. **(A)** 3D computer-aided design (CAD) illustration of the bottom part. Design embeds the metal electrodes as well as the internal features necessary for buffer reserve, cellulose acetate paper positioning and aligning ultrasonic weld groove, and a port for the blood sample application. **(B)** 3D CAD design of the top part that contains the product artwork, ultrasonic energy director, viewing windows, and buffer loading ports.

second. The mold surface temperature was kept at 82 °C (180 °F). Packing pressure was established at 71361 kN (10,350 psi) for 8 seconds. The processes then allow the mold to cool down for 15 seconds. The total process requires 45 seconds to complete. The bottom parts of the HemeChip were processed at a melt temperature of 244 °C (470° F) while maintaining an injection rate of 4.5 grams per second. The mold surface temperature was

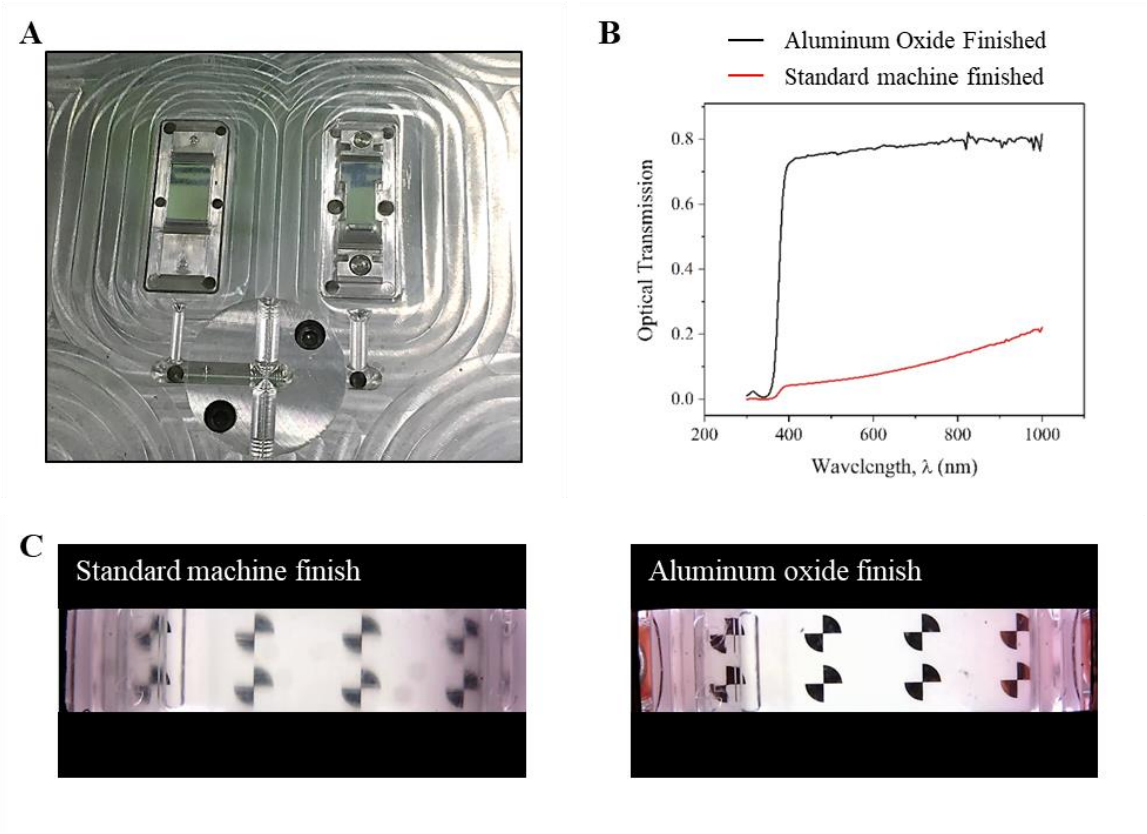

Figure 3.3. Injection molding of HemeChip and effect of the mold finish on optical quality. (A) HemeChip is fabricated using injection molding of general-purpose commercial grade PMMA. The figure shows HemeChip body parts just after the injection molding process. The metal electrodes are embedded in the bottom part of the HemeChip during the injection molding process. **(B)** Optical transmission comparison between HemeChip parts made from the standard machine-finished mold (red line) and aluminum (oxide) finished mold (black line). **(C)** The optical clarity of the HemeChip with two different surfaces finished implemented into the mold. The left image shows the visual clarity for HemeChip, where the mold was just machine finished. The right image shows the improved visual optical clarity after the mold has undergone through aluminum oxide polishing.

controlled at the same temperature as the top parts of HemeChip. Packing pressure was established at 75843 kN (11,000 psi) for 10 seconds. This process was given a cooling time of 20 seconds, with the overall cycle time at 70 seconds. The injection-molded HemeChip cartridges are sealed via ultrasonic welding. As Optix CA-41 is a thermoplastic material, the use of ultrasonic welding was well suited. Ultrasonic welding is one of the most preferred welding methods in the industry for joining plastic or polymer components.

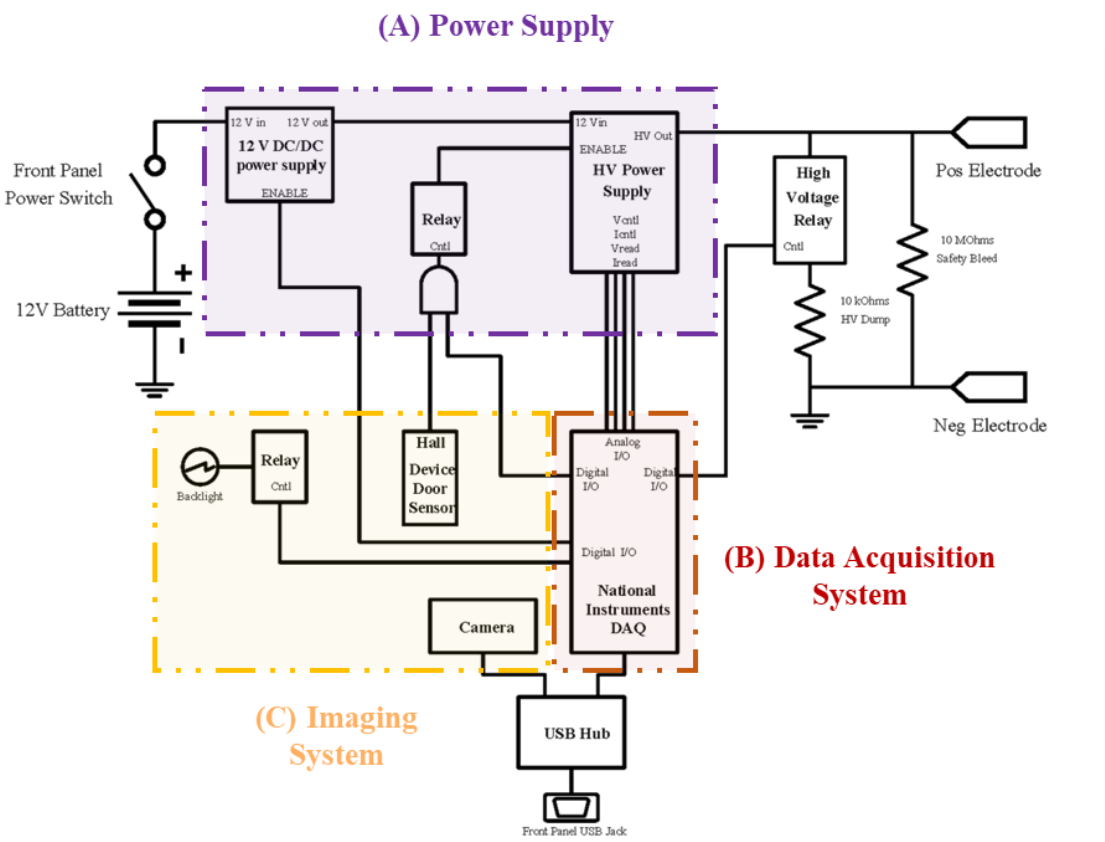

Figure 3.4. The electronic circuit design of the HemeChip Reader. HemeChip Reader consists of three major parts: : **(A)** a rechargeable power supply, **(B)** a data acquisition system that collects current and voltage data for the duration of the test, and **(C)** an imaging system that records video and images for the duration of the test, which are transferred into an image processing software for analysis.

Implementation of ultrasonic welding requires certain design considerations for the parts to be welded or joined. The parts to be ultrasonically welded require three main components in their design (**Figure 3.2A&B**): **(i)** an energy director, usually closest to

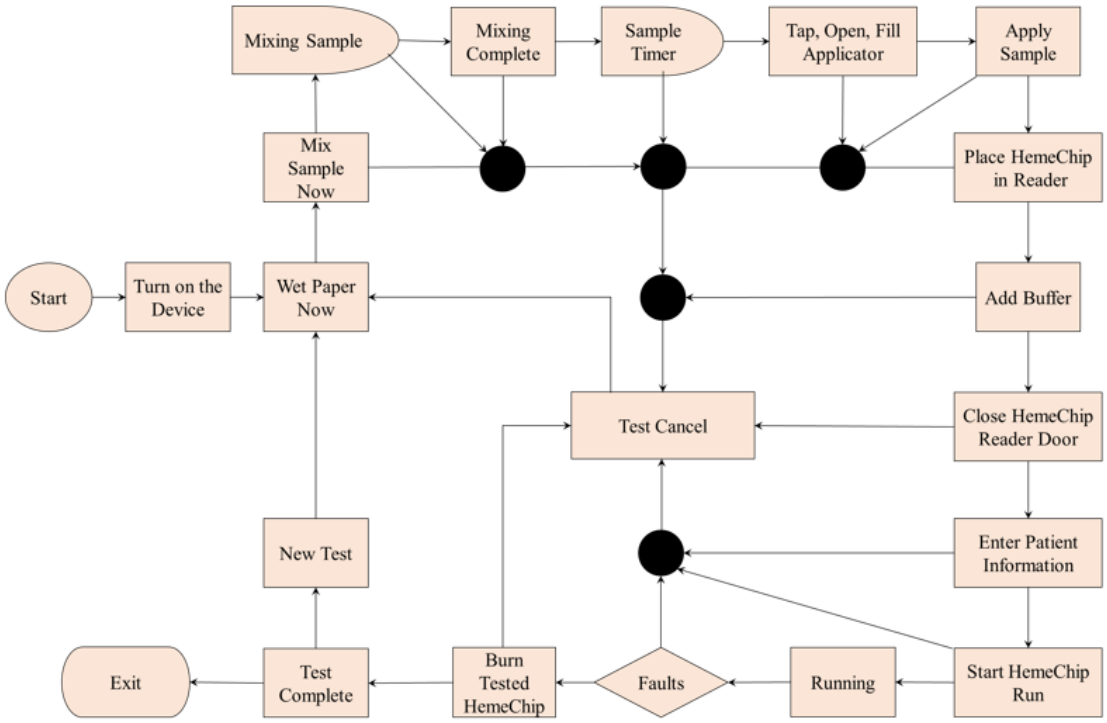

Figure 3.5. Software algorithm for the HemeChip Reader user interface. The software algorithm guides the step-by-step walkthrough of the test procedure, which is integrated, into the designed user interface.

ultrasonic horn that focuses the ultrasonic energy and melts, **(ii)** a gap or groove that accommodate the additional material of the energy director after the energy director melts during the welding process, and **(iii)** a positive stop feature on the parts to be welded. The HemeChip cartridges were welded at an ultrasonic frequency of 32 kHz for a time of 0.6 seconds, keeping the downward horn pressure at 55psi. The total machine cycle time to seal a fully assembled single HemeChip cartridge with the above-mentioned process

parameters was 12 seconds. The total volume of PMMA material that was melted during ultrasonic welding was calculated as 0.0061 ccs.

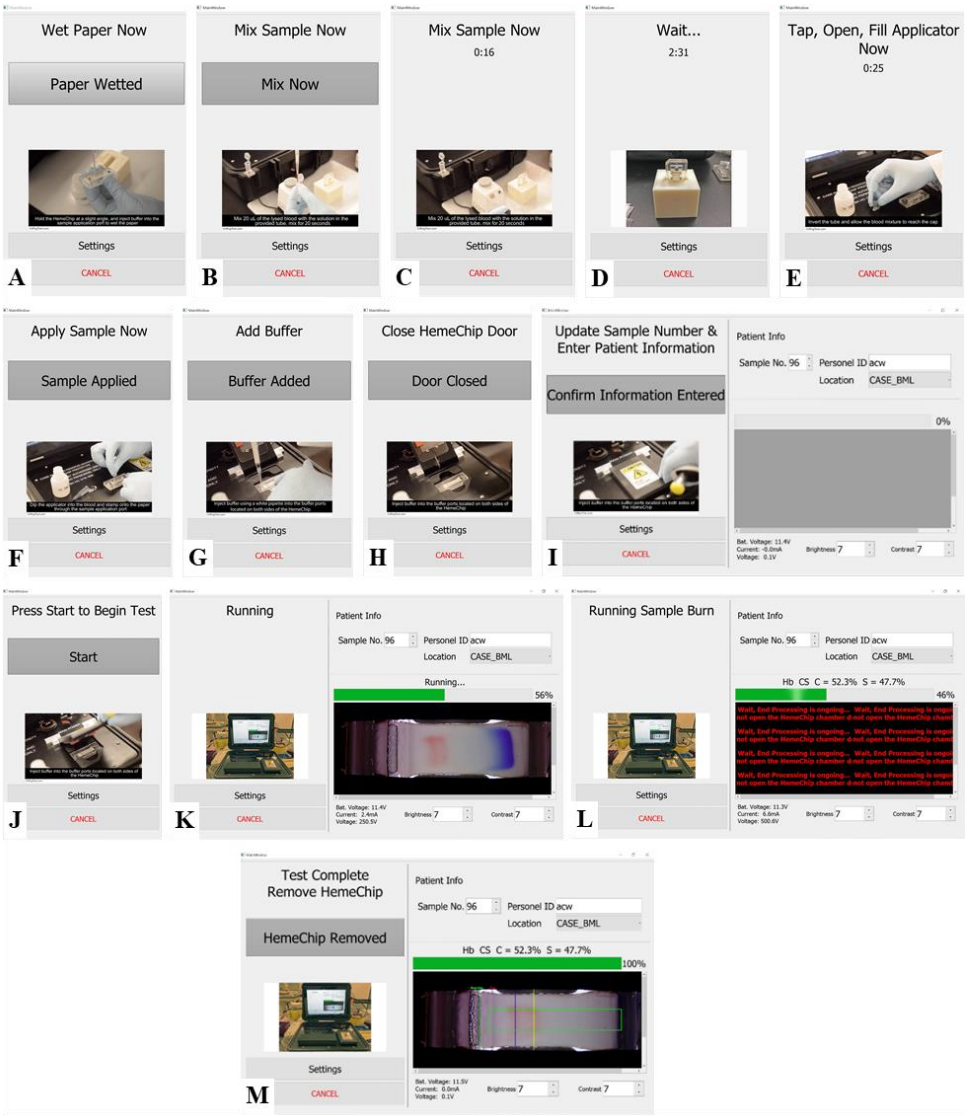

Figure 3.6. Screen views of the step-by-step instructions provided by the HemeChip user interface. The protocol integrated user interface guides the user through the test with visual, animated instructions. This step-by-step guidance facilitates rigorous control of the test steps and reduces human error. **(A–D)** The steps of HemeChip cartridge and sample preparation are demonstrated. **(E–H)** The steps for sample application and HemeChip test initiation are demonstrated. **(I–J)** The steps for logging sample information and starting the test. **(K)** A HemeChip test is started. The blue marker and the separating Hb types are visible in the frame. **(L)** The HemeChip test ends. **(M)** At the end of the test, the detected Hb type(s), their relative percentages are displayed on the result screen.

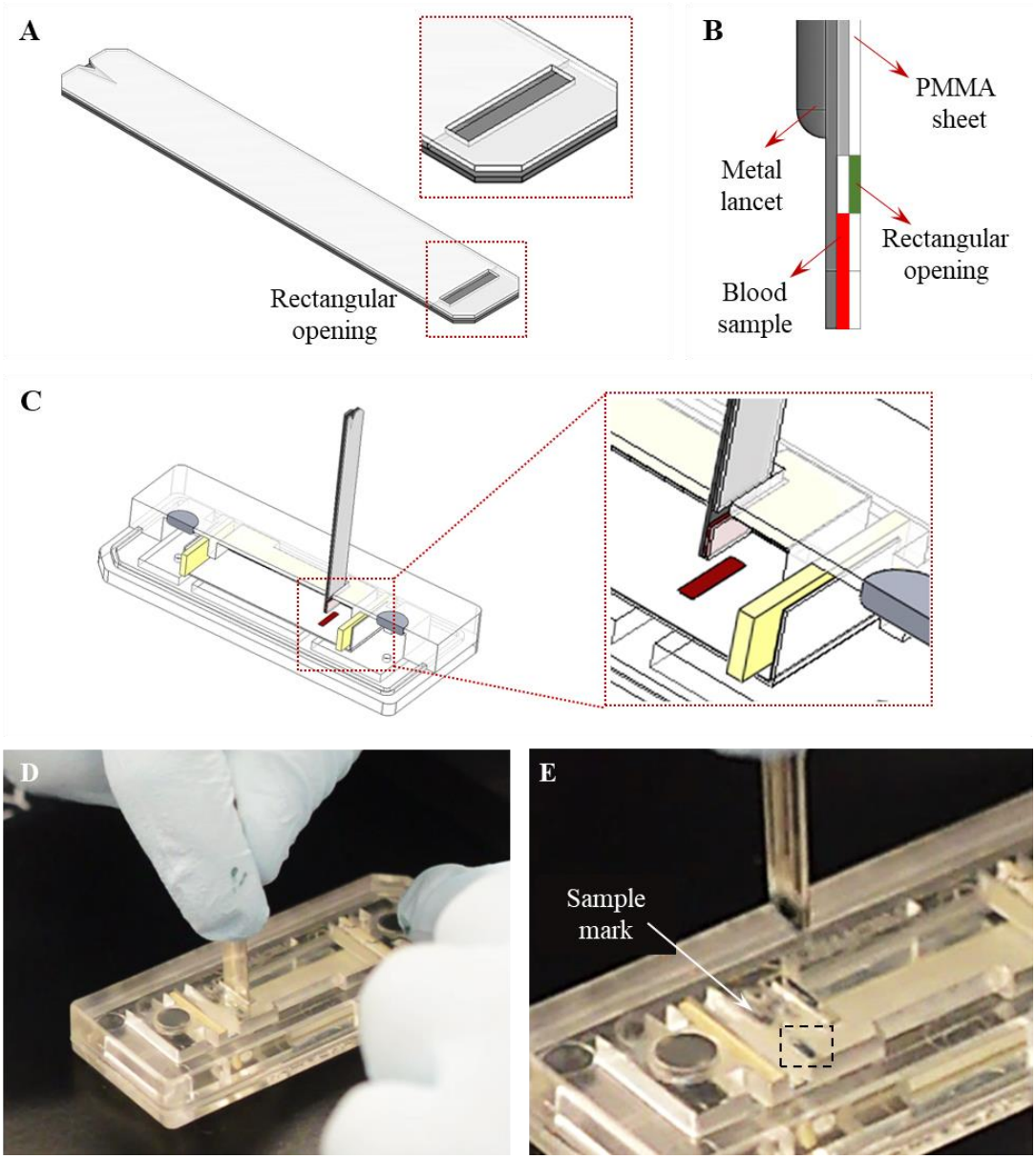

Figure 3.7. Micro-applicator design and precise application of blood samples into HemeChip. (A) 3D CAD design of the custom-developed capillary micro-applicator. A zoomed-in view of the application end is shown in the inset. **(B)** An illustration showing the application end of the micro-applicator. **(C)** A 3D CAD representation of the blood sample application process. The sample loaded micro-applicator in inserted into the HemeChip through the sample loading port, located at the bottom of the HemeChip. A close-up view shows the application mark after the micro-applicator has applied a blood sample on the cellulose acetate strip. **(D)** The user is shown applying a blood sample into HemeChip cartridge. **(E)** The sample application mark is visible on the cellulose acetate paper strip.

3.5 Micro-Applicator Design and Operation

A capillary-based micro-applicator to apply blood samples into HemeChip cartridge (**Figure 3.7**) were developed for sample transfer. This simple, easy-to-use component ensures a controlled and repeatable application of whole blood sample and facilitates repeatable and reliable test results. The micro-applicator consists of a metal lancet and a PMMA sheet attached using a double-sided adhesive (DSA) (**Figure 3.7A**). The spacing between the metal and the PMMA sheet is 150 µm. When the micro-applicator is dipped into the blood sample, it loads and retains a specific amount of the sample (**Figure 3.7B**). A rectangular opening micro-machined onto the PMMA part of the micro-applicator (**Figure 3.7B**) ensures this controlled amount of sample loading. The sample loading ports, located at the bottom of the HemeChip (**Figure 3.7C**), are designed to provide just enough space to insert the micro-applicator (**Figure 3.7D**), thus ensuring vertical alignment of the micro-applicator during the sample application process. This design improves the accuracy and consistency of the application of blood samples at the same spot (**Figure 3.7E**).

3.6 HemeChip Test Procedure

3.6.1 HemeChip Test Kit

The consumables and accessories needed for the sample preparation are as follows (**Figure 3.8**):

1. A 20 µL capillary blood collection tube, this tube is used to collect exactly 20 µL of blood needed for the test, from either a heel or finger prick.

2. A 1.5 mL tube containing 40 µL of the lysing solution is premixed with the blue marker (Xylene Cyanol). The resulting lysing solution to the blood ratio is 2:1.

3. A custom made applicator, which is dipped in the lysed blood mixture and applied to the surface of the cellulose acetate strip inside the HemeChip.

4. 50 µL and 200 µL fixed volume pipettes are provided to minimize user error. The 50 µL pipette is used to wet the cellulose acetate strip in the first step of the HemeChip preparation, and the 200 µL is used to load the buffer into the buffer ports just prior to starting the test.

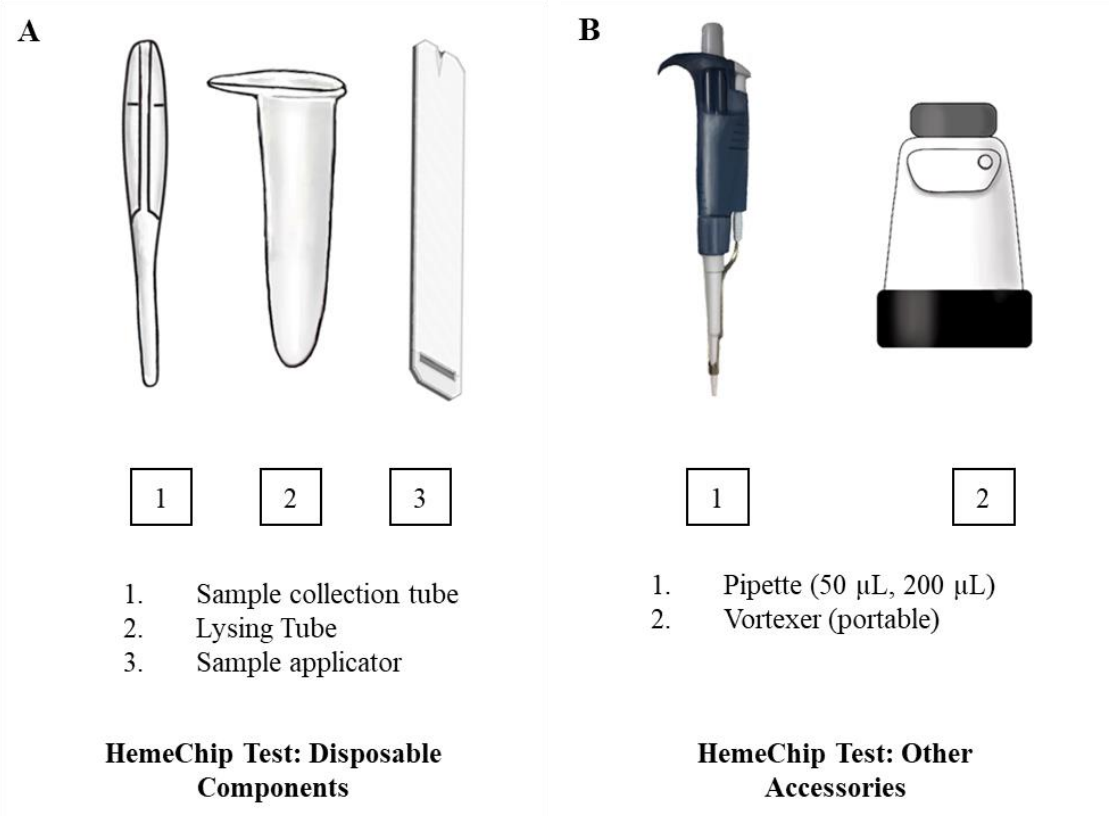

Figure 3.8. HemeChip test kit components. (A) Disposable components of the test kit are the sample collection tube, blood lysing tube, and the sample applicator, which come into contact with the blood sample. **(B)** A Pipette and a portable vortexer assist the HemeChip test procedure.

5. A battery-operated mini vortexer that is lightweight and portable, and is powered by four AA batteries.

3.6.2 Blood Collection and HemeChip Test Protocol

1. Pipette 50 µL of the buffer solution onto the paper through the sample loading port, located at the bottom of the HemeChip cartridge. Then allow the paper to soak (**Figure 3.9A**).
2. After administering a finger/ heel prick, touch the drop of blood with the capillary sample collection tube at a slight angle. Allow the tube to fill the black line (**Figure 3.9B**).
3. Squeeze the top part of the tube to empty the blood into the tube containing the lysing solution (**Figure 3.9C**).
4. Place the tube on top of the vortexer to mix the blood and lysing solution for 20 seconds (**Figure 3.9D**).
5. Invert the tube containing the blood mixture. Tap the tube on a solid surface to allow the mixture to reach the cap. Next, keep the tube inverted and open the cap. Dip the tip of the applicator into the blood mixture in the cap (**Figure 3.9E**).
6. Stamp the blood mixture in the applicator onto the paper through the sample loading port by gently touching the paper surface with the applicator, while making sure not to puncture the paper with the applicator (**Figure 3.9F**).

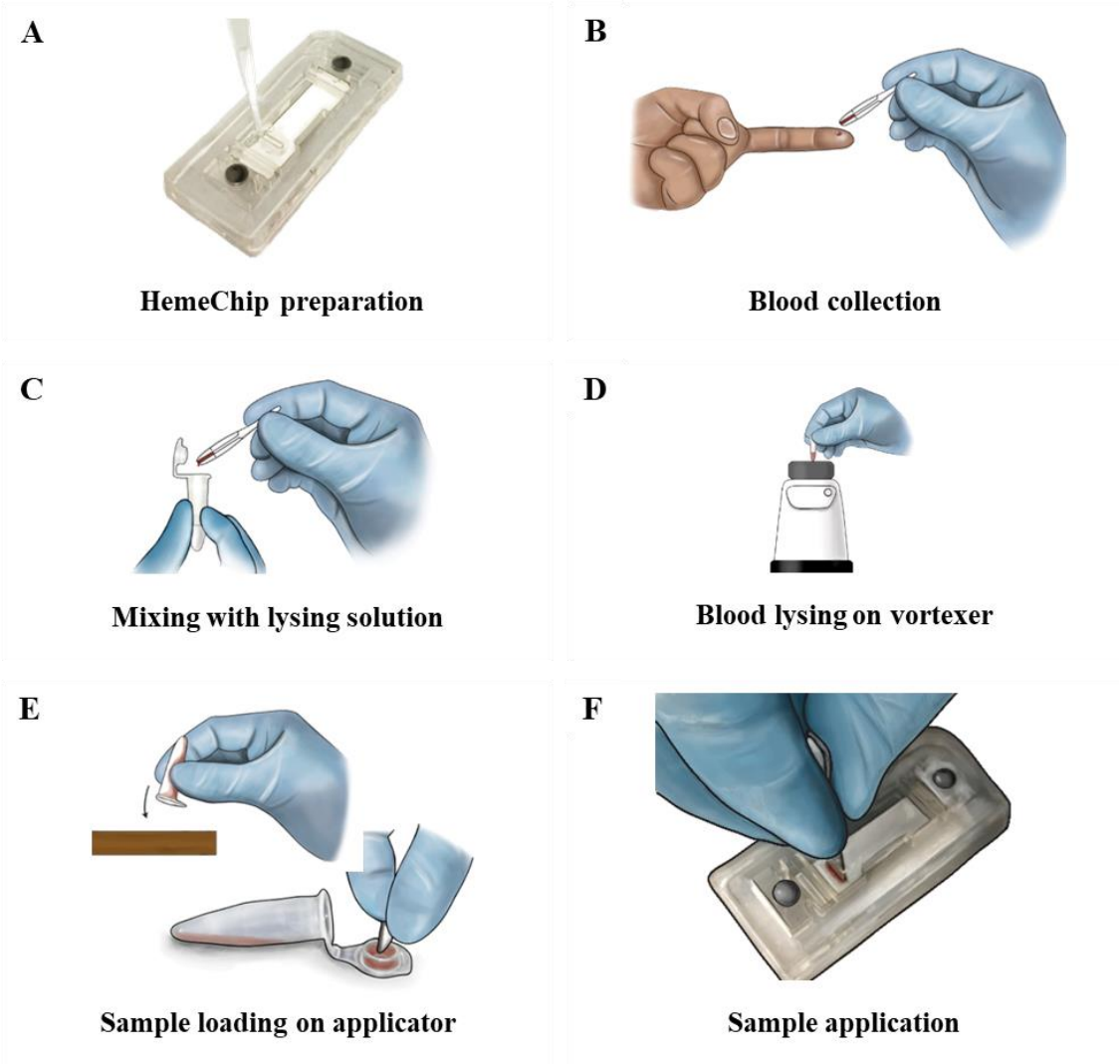

Figure 3.9. Blood collection and HemeChip test protocol steps. (A) As a preparation for the HemeChip test, the HemeChip cellulose acetate paper in the cartridge is wetted with 50 µL of 1x TBE buffer. **(B)** In this step, the blood sample is collected from a person via a finger or heel prick. Then the blood sample collection tube is used to collect the blood sample (~ 20 µL). **(C)** The collected blood sample is then poured into the lysing tube. The lysing tube contains the lysing solution with the Xylene Cyanol solution (the blue marker). **(D)** The blood is mixed with the lysing solution using a portable battery-powered vortexer for effective lysing. **(E)** Before the sample application into the cartridge, the blood lysing tube is flipped upside down and tapped against the workbench, which results in the accumulation of lysed blood samples in the tube cap. Then, the tube is opened, keeping the tube in the up-side-down position and the lysed blood sample is loaded into the micro-applicator. **(F)** The processed blood sample loaded micro-applicator is inserted into the HemeChip and the sample is loaded onto the cellulose acetate strip inside the HemeChip. Next, the cartridge is placed into the Reader chamber and the test is started. Then the Reader takes over, completes the test run and automatically analyzes the results.

Table 3.1. Comparison of HemeChip with standard laboratory methods for hemoglobin testing

	HemeChip (Microchip Electrophoresis)	Electrophoresis (IEF)	HPLC	Microscopy-based tests	Sickledex –Turbidity Test
Differentiates between trait and disease	**Yes**	Yes	Yes	No	No
Quantification	**Yes**	No	Yes	No	No
Operator skill required	**Low**	High	Medium	High	Medium / Low
Cost per test	**$2.00**	$5-10	$10-15	$3-$5	$0.50
Initial equipment cost	**<$500**	>$10,000	$30-80K	$2500	None
Time to result	**< 10 minutes**	24+ hours	24+ hours	24+ hours	6-10 min
Sensitivity	**High**	High	High	Poor sensitivity; Only detects SCD, not a trait or other hemoglobinopathies	Can't be used on infants under 6 months, can't differentiate trait/disease. Confounders such as severe anemia; Only detects Hb S
Specificity	**High**	High	High		
Reference	**This article**	[111,112]	[111,112]	[133,134]	[135]

Table 3.2. Comparison of HemeChip with standard laboratory methods for hemoglobin testing

	HemeChip (Microchip Electrophoresis)	Paper-based hemoglobin solubility	Density-based red cell separation	SickleSCAN (Lateral flow immunoassay)	HemoTypeSC (Lateral flow immunoassay)
Hemoglobin types identified	**A, F, S, C/E/A_2**	A, S	A, S	A, S, C	A, S, C
Hb% quantification	**Yes**	No	No	No	No
SCD-SC identification	**Yes**	No	No	Yes	Yes
Sβ-thal identification	**Yes (as SCD-SS)**	Yes (as SCD-SS)	No (as SCD trait)	Yes (as SCD-SS)	No (as SCD trait)
Differentiates between Trait and Disease	**Yes**	No	No	Yes	Yes
Newborn/infant testing	**Yes (best > 6 weeks)**	> 6 months only	> 6 months only	Yes	Yes
Hb F identification and quantification	**Yes**	No	No	No	No
Automated interpretation of results	**Yes**	No	No	No	No
Digital test result storage	**Yes**	No	No	No	No

	HemeChip (Microchip Electrophoresis)	Paper-based hemoglobin solubility	Density-based red cell separation	SickleSCAN (Lateral flow immunoassay)	HemoTypeSC (Lateral flow immunoassay)
Wireless connectivity for data transfer	**Yes**	No	No	No	No
Works without uninterrupted power	**Yes**	Yes	No	Yes	Yes
Biological reagents	**No**	No	No	Yes (polyclonal antibodies)	Yes (monoclonal antibodies)
Temperature range	**5-45°C**	15-25°C	4-8°C	2-30°C	15-40°C
Required blood volume	**<1 µL**	20 µL	5 µL	5-10 µL	1.5 µL
Total test time: finger stick to results reported	**<10 minutes**	<35 minutes	<12 minutes	5-10 minutes	10 minutes (plus sample preparation time)
Cost per test	**$2.00**	$0.70	$0.50	$4.20	$2.00
References	**This dissertation**	[136-138]	[139]	[109,140-144]	[109,145-148]

Chapter 4: Characterization of the Paper-based MicroChip Electrophoresis (MCE) System

4.1 Abstract

MCE has the potential and the capability of bringing a laboratory test to the point-of-care setting, which would provide a quick, reliable, and accurate analysis needed for time-sensitive applications. In this chapter, a novel image-based measurement of dynamic change in pH and temperature within a paper-based microchip electrophoresis system is presented. The paper-based system under investigation is a single-use, mass-produced, commercialized platform for detecting hemoglobin variants from whole blood, using an alkaline buffer (pH 8.4 - 8.6) based electrophoretic separation. The dynamic measurement of pH is based on the calorimetric manifestation of a pH indicator. The electrophoretic separation medium is 9.5 mm wide and 30 mm long (end to end). The pH gradient is tracked for 22 mm in the middle of the separation medium, which is the length designated for electrophoretic separation. The dynamic measurement of the runtime pH change has been performed for a range of 50 - 250 volts. A higher pH gradient at the cathode-end of the separation medium was observed compared to the anode-end. A treatment process of the separation medium, to reduce the runtime pH change, has also been presented. The runtime temperature distribution was measured using infrared image analysis, which revealed the temperature increase could be as high as 40°C during a test. The assessment of runtime temperature distribution also showed an asymmetric temperature distribution, where the location of the maximum temperature (or hot spot) tends to shift toward the anode during the test. The presented pre-treatment of the separation medium has also been

proved to impact the temperature and its distribution over the separation medium of the paper-based microchip electrophoresis system.

4.2 Introduction

Miniaturized total analysis system, later acronym as "μ-TAS" was first introduced in 1990 [18], as a chemical sensor, which opened up a field of miniaturized devices, especially planar devices, for rapid, highly efficient, and reliable analysis of chemical and/or biological samples. The most compelling attribute to miniaturized systems that they require a tiny fraction of the sample volume compared to their traditional counterparts, yet are able to produce accurate and reliable results. For chemical and clinical application miniaturization of electrophoretic separation techniques have received much attention due to its immense potential for rapid detection and diagnosis capability.

MCE provides a compact, rapid, and streamlined means for complete diagnostic workflow for disease detection, which is the essence of any point-of-care (POC) technology [149]. The significant advantages electrophoresis or electrochemical detection possess over other analytical detection techniques (for example, fluorescence, mass-spectroscopy) are ease of fabrication and potential of miniaturization along with high sensitivity. Capillary electrophoresis (CE) based microchips have been widely implemented for various analytical applications, namely for the detection and analysis of amino acids, peptides, carbohydrates. The reason for capillary electrophoresis (CE) being preferred for MCE is because the high field strength voltages required for achieving electrophoretic separation can be used as an advantage for microfluidic flow control (electroosmotic flow, EOF) [150].

Paper-based microfluidics or microfluidic paper-based analytical device (μPADs) was first reported in 2007. Paper-based microfluidics is a growing research field with great potential, especially for life science, food industry, and environmental monitoring. Moreover, paper-based microfluidic devices are cheaper, chemically compatible, and passive [55]. The device material for paper-based microfluidics is usually cellulose-based. It provides an excellent platform for immobilizing chemical or analytical compounds for chemical [151,152], biomedical [153], forensic [154], and life science [32,57,155] applications. Paper-based microfluidics is highly suitable for designing passive devices, with proper design, the capillary force can act as an effective driving force [156,157].

Paper-based microfluidics (μPADs) were first introduced as an electrophoretic separation platform in 2014 [38,39]. These techniques relied on chemiluminescence and fluorescence detectors. Although these reported techniques implemented simple device fabrication, there were some major challenges, such as sample integration, device robustness and separation performance [158]. Efforts have been made to develop simple paper-based electrophoretic separation devices with improved sample injection and relatively simple detection and analysis process using smartphones [40]. The paper-based microfluidics reported above are still at a development stage and possess great potential as rapid, portable analytical detection devices.

In previous chapters, a mass-producible, paper-based microchip electrophoresis (HemeChip) system, which can detect hemoglobin variant from whole blood, has been presented[9,159,160]. HemeChip is a point-of-care technology that uses a strip of cellulose acetate (CA) as the separation medium for the electrophoretic separation process. It

performs electrophoretic separation of hemoglobin variants in whole blood; and can detect, identify, and quantify the hemoglobin variants present in a blood sample.

Monitoring pH is an essential task for a large spectrum of applications, especially for the food industry, environmental testing (ground, and marine) as well as pharmaceuticals and life sciences [161]. In traditional microchip systems (mainly CE based), extensive studies have been performed on system electrochemical behaviors such as ion migration, electrochemical reaction and pH change [24,162,163]. Optical methods for dynamic measurement of pH for microfluidics have been reported for traditional microchannel based microfluidic systems [164-166]. However, this information is missing for paper-based microchip systems since they are mostly based on passive capillary flow or pressure-driven flow instead of electric or electrochemical driving forces. This knowledge discrepancy may affect diagnosis accuracy and precision for a paper-based microchip electrophoresis system. Because hemoglobin separation in CA electrophoresis takes place based on charge to mass ratio, which can be affected by the pH due to the fact that the charge induced in hemoglobin molecules is dependent on the pH of the environment.

Electrophoretic separation techniques rely on an applied electric field to mobilize the mixture of analytes and separate the analytes based on the differences in their electrophoretic mobility. Heat generation in the electrophoresis system can greatly influence electrophoretic mobility of analytes as well as the performance of the separation. Although an elevated temperature would yield faster electrophoretic mobility and quicker separation [167-170], increased temperature also introduces undesired consequences, such as high-performance variability [167], Joule-heating-induced zone/sample dispersion [171-173],

increased electromigration dispersion [174-176]. In addition to these effects, the paper-based electrophoresis system also faces high electrolyte evaporation as the temperature increases. Moreover, increased temperature also alters the electrolyte pH and electrophoretic mobility of analytes [167]. Most of the available literature on the undesired effect of temperature increase is focused on capillary electrophoresis. The majority of these studies provide an analytical framework for the dispersive behavior of capillary electrophoresis. These above-mentioned nonlinearities (high variation and dispersive behavior) may also present in a paper-based electrophoresis system but, not much work is available in the form of analytical and experimental work.

In this chapter, a method to investigate dynamic pH variation and an assessment of dynamic temperature distribution within the paper-based microchip electrophoresis system is presented. A robust image-based dynamic measurement of pH gradient on the separation medium of the paper-based microchip electrophoresis system is demonstrated. In addition to these, a treatment method for reducing the runtime pH gradient is presented. The thermal response of the paper-based microchip electrophoresis system has been measured using the infrared image-based dynamic thermal assessment system.

4.3 Methods

4.3.1 Buffer Preparation

Image-based tracking of dynamics pH change is based on a calorimetric manifestation of change in pH in electrophoretic separation medium and the conversion and quantification of calorimetric changes into pH values (color-to-pH conversion). The electrophoretic running buffers are purchased in a concentrated form (at 10x concentration)

from the vendors and then diluted (using ultrapure water) to the required concentration (typically to 1x concentration). These diluted running buffers are then used

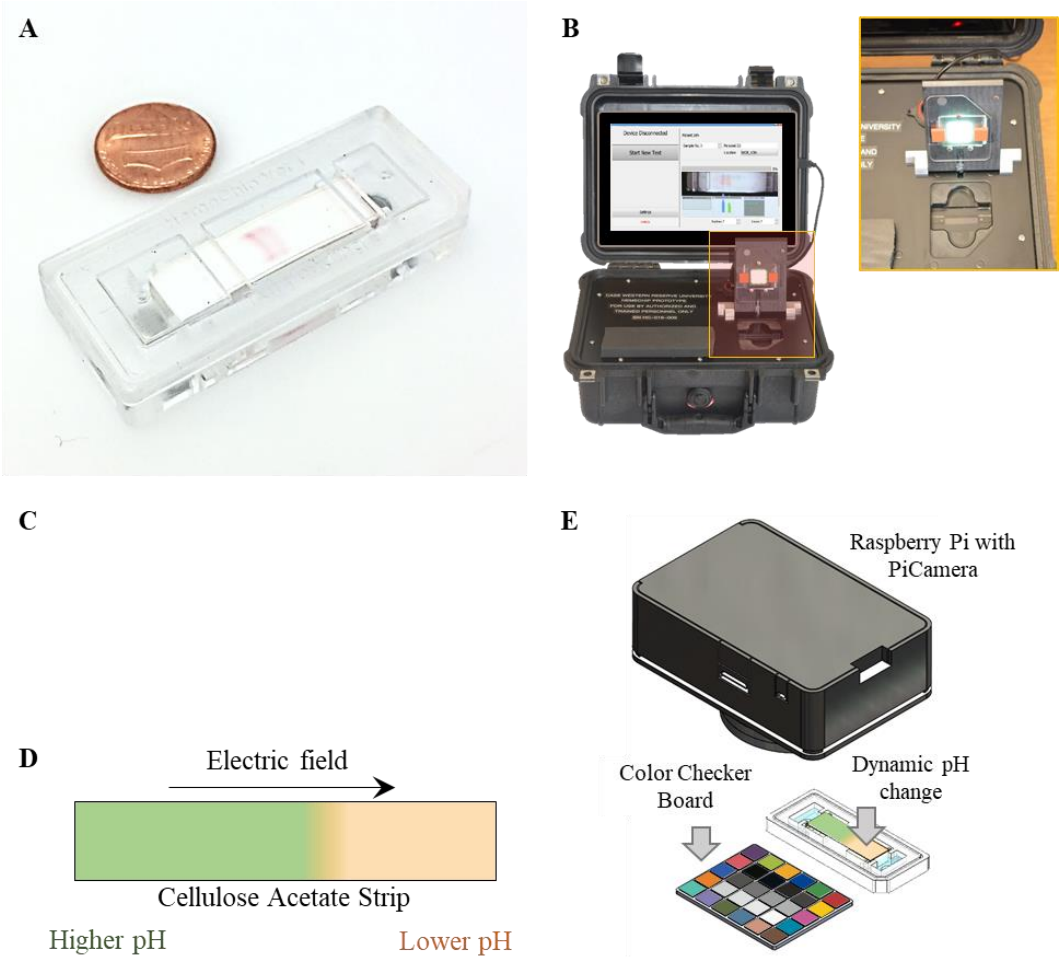

Figure 4.1. HemeChip technology and dynamic tracking of the run-time pH change in the HemeChip cartridge. (A) an injection-molded mass-produced HemeChip cartridge. **(B)** The HemeChip reader contains the hardware, software and a user interface to guide the user through the test and display test results at the end of the test. **(C)** Illustration of run-time pH change on a cellulose acetate (CA) paper. **(D)** Illustration of longitudinal pH gradient along the direction of the applied electric field. **(E)** The imaging system for the dynamic tracking of the run-time pH change contains an off-the-shelf camera (raspberry pi) for image acquisition and a standard micro color checkerboard for color calibration.

for the electrophoretic separation of different components of the analyte (**Figure 4.1A**). For the tracking of dynamic pH change and the spatial pH distribution in the paper-based MCE, the dilution procedure of the concentrated running buffers was modified to prepare a modified running buffer (MRB). The UPI solution was added to the ultrapure water for

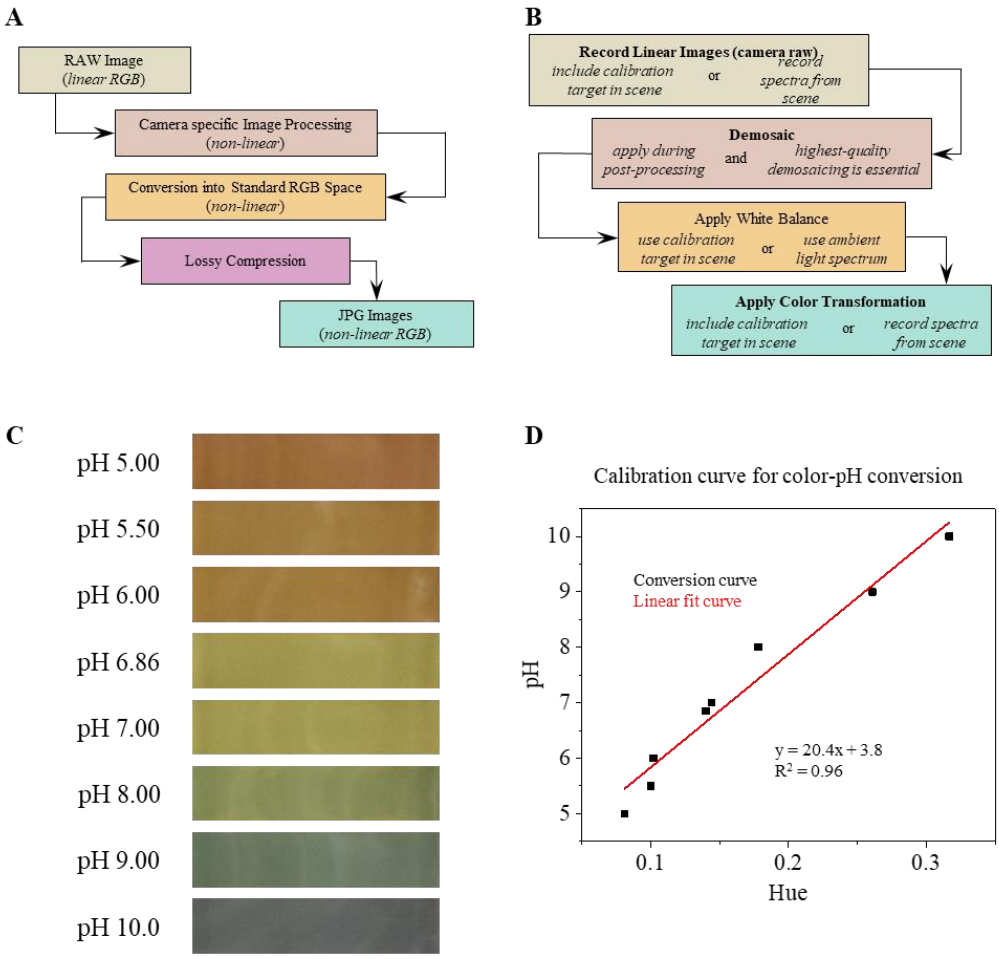

Figure 4.2. Comparison between lossy and lossless image compression and calorimetric pH calibration curve. (A) Image processing algorithm for with lossy compression. **(C)** Image processing algorithm for loss-less processing. **(C)** CA paper images soaked with standard buffer and universal pH indicator solution. Standard pH solution of different values (range: 5 ~ 10) was used, and these images were used to general the pH calibration curve, **(D)** A calibration curve was developed from and image library developed in (C). The calibration curve was used for the conversion of the run-time color change in the HemeChip into the corresponding pH value.

the dilution of the concentrated electrophoresis running buffers. The addition of the UPI was maintained in such a way so that the volume of the added UPI and the volume of the final diluted MRB has a ratio of 1:2. For generating the calibration curve for color-to-pH conversion, a set of buffer was prepared using the UPI and asset of pH standard solutions (pH range: 5 - 10). The pH standard solution and the UPI were mixed in a 1:1 volume ratio so that the volume ratio of the UPI and the prepared solution is 1:2 (same as the MRB).

4.3.2 Imaging System

The run-time pH imaging system implemented to tracking the dynamic pH change consists of a HemeChip reader (**Figure 4.1B**), a RPi, and a standard color checkerboard (SCCB) (**Figure 4.1E**). The HemeChip reader controls the test parameters and executes the test, while the pH imaging system is set to acquire image data avoiding a lossy compression (**Figure 4.2A**) rather in an uncompressed raw and linear image data format (YUV420) (**Figure 4.2B**) for the pH tracking analysis. A calibration curve to convert the calorimetric change on the separation medium into pH change was developed (**Figure 4.2C&D**) using a set of modified buffer (discussed later) using a set of pH standard solutions (ranging from pH 5 - 10). The presence of the SCCB in the acquired image data ensures the correct white balance and color transformation for the color to pH conversion during the post-processing stage (**Figure 4.3**).

4.3.3 Experiment Preparation and Procedure

The test preparation for the image-based tracking of the dynamic pH change and the spatial pH distribution is similar to the process described in the above section, except the wetting of the CA paper. The CA paper strip is carefully and gradually submerged in

the MBR to avoid any uneven wetting and trapping of air in the CA paper strip. The paper was kept in the modified running buffer solution for 4 minutes. The MBR soaked CA paper is then carefully retrieved and carefully wiped-off/blotted to remove the excess amount of MBR. The MBR soaked CA paper is then placed inside a HemeChip cartridge. After the test cartridge was assembled with the MRB soaked CA paper, the buffer reservoirs of the cartridge were filled with MRB. The cartridge loaded with prepared CA paper and the MRB was then placed in the cartridge chamber of the HemeChip reader and a test was run (**Figure 4.3**).

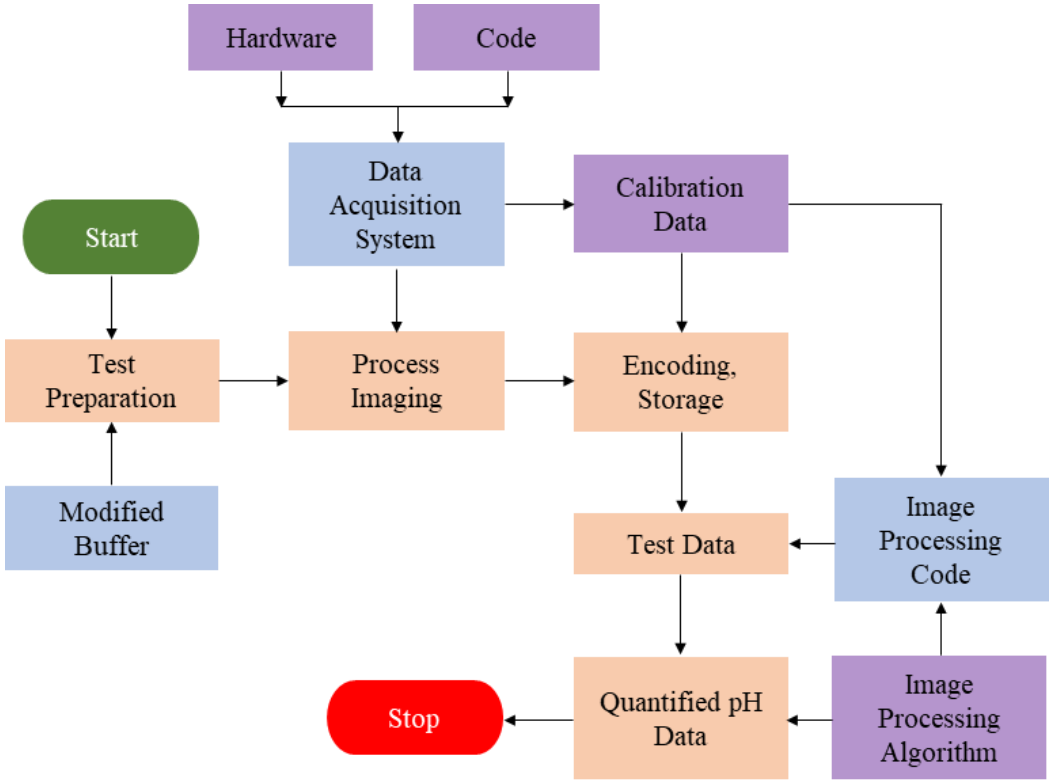

Figure 4.3. Process flow-chart for the dynamic mapping of the runtime pH shift over the CA paper during a HemeChip test. The test starts with the cartridge being prepared using the modified TBE buffer. The test begins after the test preparation, and the pH imaging system acquires image data (raw, YUV420 format) at a regular interval. The acquired image data was later post-processed and the color change due to the run-time pH change is converted into the corresponding pH using the calibration curve.

4.3.4 pH Image Acquisition and Analysis

The accuracy of the conversion and quantification of calorimetric changes into pH values (color-to-pH conversion) is dependent on the image acquisition and compression by the image acquisition hardware. A commercial off-the-shelf (COTS) digital camera were used as a part of the image acquisition system for the proposed image-based tracking of the dynamic pH change. The capability of COTS to produce reliable and high-quality images required for research application has been demonstrated in the literature [38, 39]. However, it is imperative to understand that these COTS digital cameras are more often not optimized for research application but to produce images which are eye-catching and attractive to the users [38, 40, 41]. Thus, the careless use of COTS digital cameras for the research application can result in unreliable and inconsistent data due to a lack of data accuracy and repeatability. The following criteria must be met by an image acquisition system to provide accurate, repeatable and device-independent data - (i) unbiased image acquisition (linear, or known non-linear relation of images to the scene radiance), and (ii) ability to capture data in a lossless (linear) format. Readers can read the referred article [38] to know more about the desired and/or required qualities of the image acquisition system needed for scientific application. The developed image acquisition system and the analysis method was implemented for the assessment of the run-time pH change during the HemeChip test (**Figure 4.4&4.5**).

4.3.5 Thermal Imaging System and Calibration

The imaging system consists of a handheld dual-camera (visible and infrared) infrared camera (FLiR One) which can be connected with a smartphone and perform

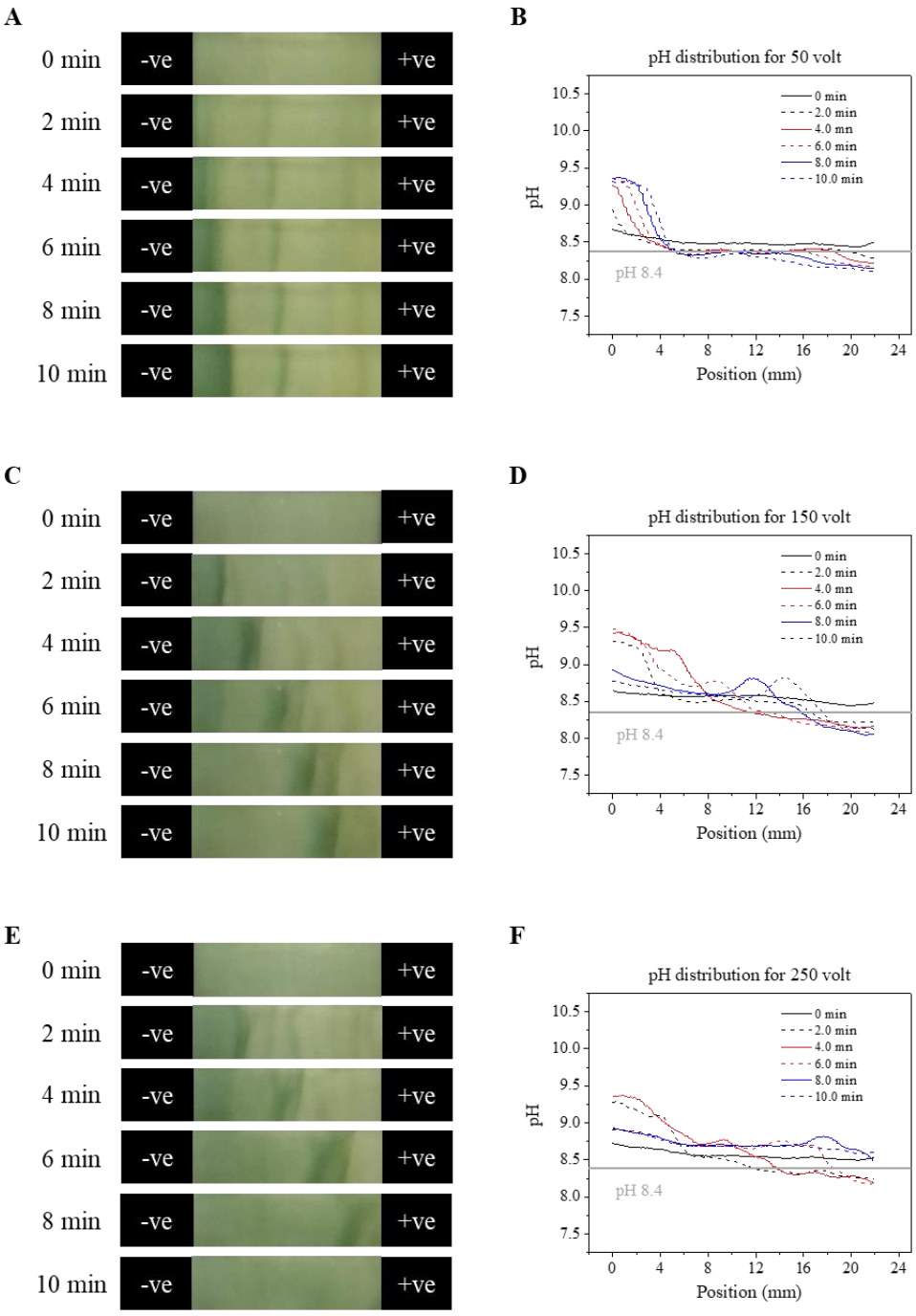

Figure 4.4. Run-time longitudinal pH gradient at 0, 2, 4, 6, 8, 10 minutes for HemeChip test. (A) time-lapse of a HemeChip test run at 50 volt, **(B)** pH distribution of a HemeChip test run at 50 volt, **(C)** time-lapse of a HemeChip test run at 150 volt, **(D)** pH distribution of a HemeChip test run at 150 volt, **(E)** time-lapse of a HemeChip test run at 250 volt, and **(F)** pH distribution of a HemeChip test run at 250 volt.

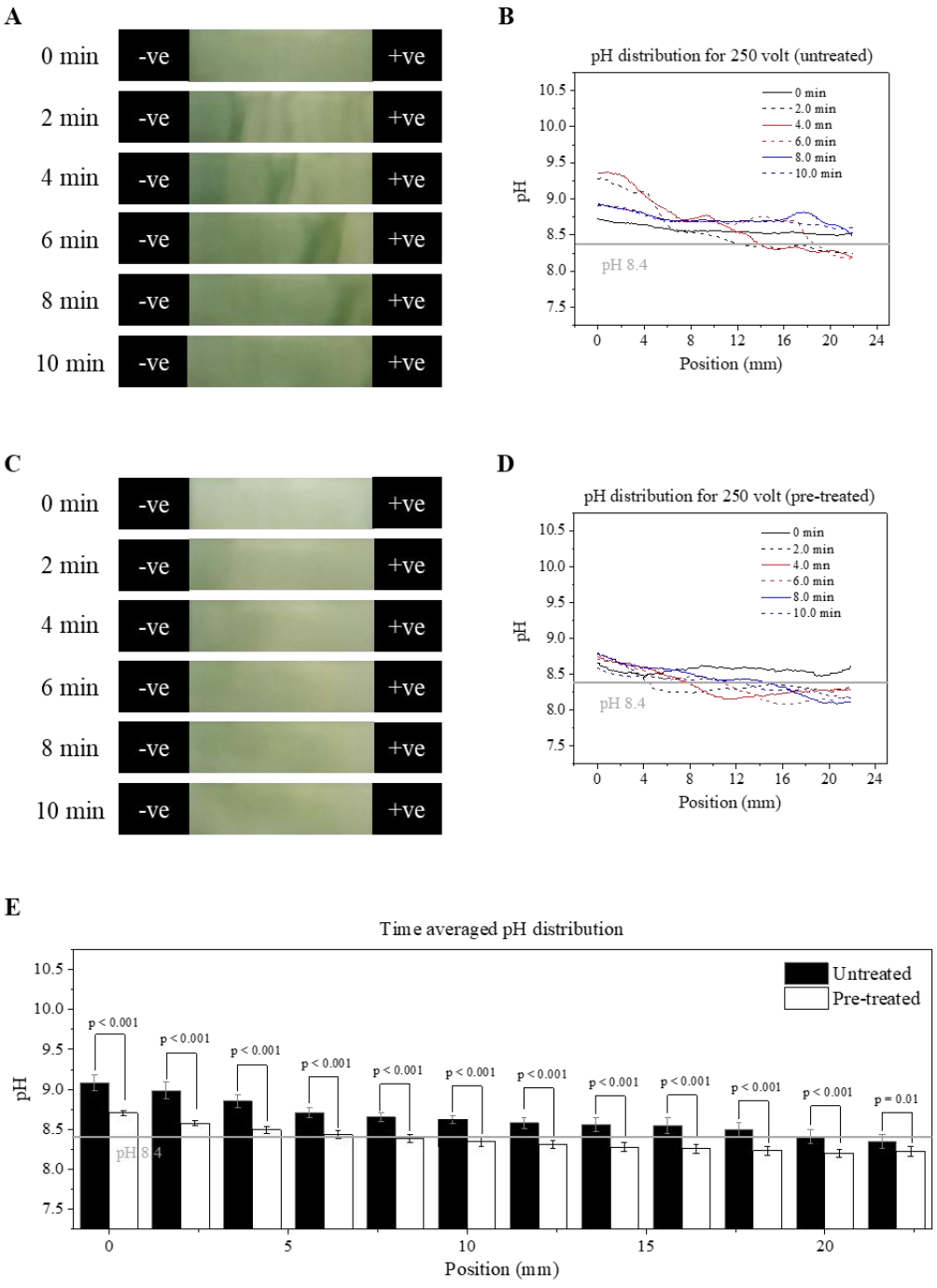

Figure 4.5. Pre-Treatment of the CA paper to reduce the run-time pH shift. (A) time-lapse of a HemeChip test run at 250 volt with an untreated CA paper, **(B)** pH distribution of a HemeChip test run at 250 volt with an untreated CA paper, **(C)** time-lapse of a HemeChip test run at 250 volt with a pre-treated CA paper, **(D)** pH distribution of a HemeChip test run at 250 volt with a pre-treated CA paper and **(E)** time-averaged pH distribution for a untreated and a pre-treated CA paper test (at 250 volt).

thermal imaging. For reliable interpretation of the infrared images, the analyzed infrared image has been calibrated with a calibration curve (**Figure 4.6**).

4.3.6 Cellulose Acetate Pre-treatment

The purchased CA papers were placed in a container. A diluted hydrochloric acid, HCl (pH 4.0) were slowly poured into the container. The diluted HCl solution was added until the CA sheets are completely submerged into the solution. The CA papers were kept into the diluted HCl solution for 30 minutes. After 30 minutes, the CA papers were removed from the solution and let dry for overnight. The dry CA paper was then laser-cut into the required dimension and used for running the HemeChip test.

4.4 Results

4.4.1 System Calibration

To develop the calibration curve for color-to-pH conversion, the separation medium (the CA paper) was slowly dripped into the prepared solution (of pH standard solution and UPI) and kept in the solution for 4 minutes. After this soaking period, the CA paper is retrieved carefully, to avoid any damage to the wet CA paper. The retrieve CA paper is then gently tapped by placing it between two blotter pads. The prepared CA paper is then placed in the imaging area in the presence of the SCCB and imaged (**Figure 4.2C**). This process was repeated for all the solutions prepared with pH standard solution and the UPI. This process generated an image library of the CA paper manifesting a specific color for a specific pH. The image library was later processed using a MATLAB code to correlate

the color manifested on the CA paper and the corresponding pH value and plotted (**Figure 4.2D**) to develop the calibration curve.

The analysis provided by the infrared imaging software relies on the surface emissivity of the object being infrared imaged and the relative humidity of the air. To eliminate the contribution of an infrared image calibration setup (**Figure 4.6A**) and an infrared image calibration curve (**Figure 4.6B**) was developed. In the calibration setup, the CA paper was attached on top of a plate heater. The plate heater was used to heat up the CA paper at different temperatures within the range of 35-90°C. A K-type thermocouple

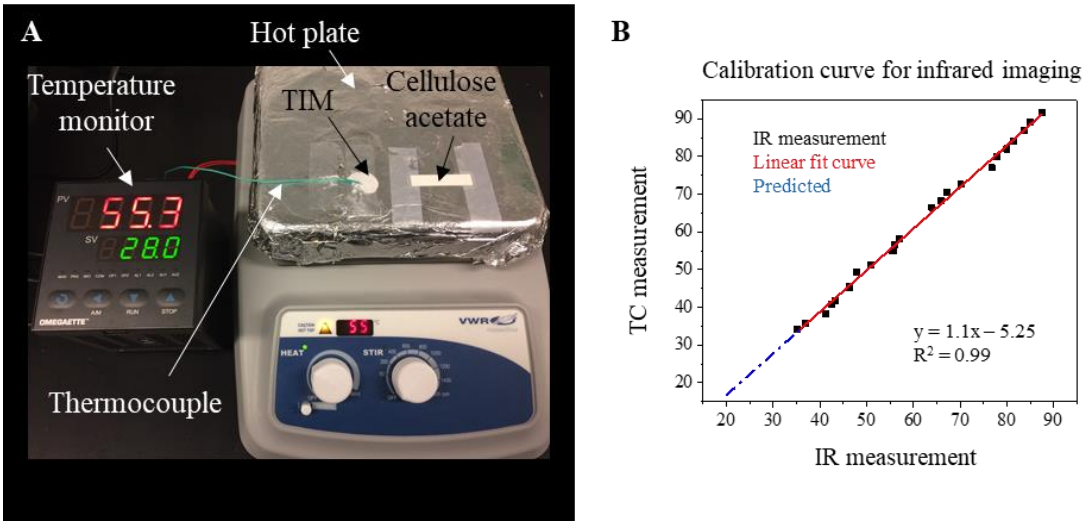

Figure 4.6. Experiment setup for calibration of the infrared (thermal) imaging. (A) Cellulose acetate (CA) paper was heated on a hot plate at different temperatures. A thermocouple (k-type) was mounted on the hot plate to collect the thermocouple (TC) measurement. A thermal interface material (TIM) was implemented between the hot plate surface and the thermocouple probe end. A PID temperature controller unit was used as a monitor for thermocouple reading. An infrared camera was used to image the heated CA paper. **(B)** The infrared images were analyzed using FLiR Studio software and the analyzed infrared (IR). The measurement data was potted against the thermocouple data to generate the calibration curve. The black line represents the thermocouple reading; the red line represents the linear fit for the thermocouple measurement. The blue dash-dot line represents an extrapolated range of data based on the linear fit.

was attached on the plate heater with TIM placed between the heated surface and the thermocouple probe. The reading end of the thermocouple was connected to a PID temperature controller feedback port. The PID temperature controller unit functioned as the thermocouple reading monitor. The heating surface of the plate heated was gradually heated at small steps. At each step of the temperature increment, the temperature reading the PID temperature controller was monitored. Once the temperature of the heated surface becomes steady, the heated CA paper was thermally imaged and the thermocouple reading displayed on the PID temperature controller was recorded. The acquired thermal images were later analyzed using FLiR Studio (FLiR systems). The temperature data obtained from the thermal imaging calibration setup (**Figure 4.6A**) was correlated with the temperature data recorded using the thermocouple to develop the calibration curve for infrared imaging (**Figure 4.6B**). For calibration of thermal image data below the range of 35-90°C, the calibration fit line (**Figure 4.6B**, red line) was extrapolated down to 20°C (**Figure 4.6B**, blue line). The thermal image data acquired during the experiment are calibrated using the calibration curve (**Figure 4.7**).

4.4.2 pH Change in Separation Medium

Electrophoresis is the process of inducing migration and separation of charged entities and this process is set forth by the presence of an external electric field. The electric field is applied via two electrodes and the field is established by an electrically conductive medium, an electrolyte or buffer. The electrophoretic separation is the result of the difference of electrophoretic mobility, the mobility obtained by a charged entity under the influence of an electric field. This mobility is a function of the charge, size and shape of

the charged entity. The electrophoretic mobility is a property of the charged entity which is considered to remain constant as long as the electrophoretic conditions remain stable and unaltered. The electrophoretic condition of a system is defined by its electrical, chemical, and mechanical properties [177]. The pH of the buffer is one of the crucial defining factors for electrophoretic mobility especially for protein separation whose net induced charge depends on the pH of the buffer. Protein, such as hemoglobin, is charge-neutral in a neutral pH environment. In the event of the presence of an acidic or alkaline environment, the net charge of the protein is no longer zero. This pH-induced charge and the degree of variation in the induction of pH-induced charge for protein variations is the mechanism behind electrophoresis.

Figure 4.4 shows the runtime change in buffer pH for a paper-based microchip electrophoresis system (HemeChip). **Figure 4.4** shows the pH change for a test run at three different applied electric fields: 50 volts (**Figure 4.4A&B**), 150 volts (**Figure 4.4C&D**), and 250 volts (**Figure 4.4E&F**). The tests were run for 10 minutes and were imaged in real-time and the recorded data was post-processed using a custom image analysis algorithm. For each applied voltage, the time-lapse of the runtime pH change, as well as the quantified pH distribution over the CA paper, has been presented.

Anode (oxidation)	: $2H_2O(l) \rightarrow O_2(g) + 4H^+(aq) + 4e^-$	$E^o = +1.23V$	(1)
Cathode (reduction)	: $2H^+(aq) + 2e^- \rightarrow H_2(g)$	$E^o = 0V$	(2)
	: $O_2 + 2H_2O + +4e^- \rightarrow 4OH^-$		(3)
Water equilibrium	: $H^+ + OH^- = H_2O$	$K_w = 10^{-14}$	(4)

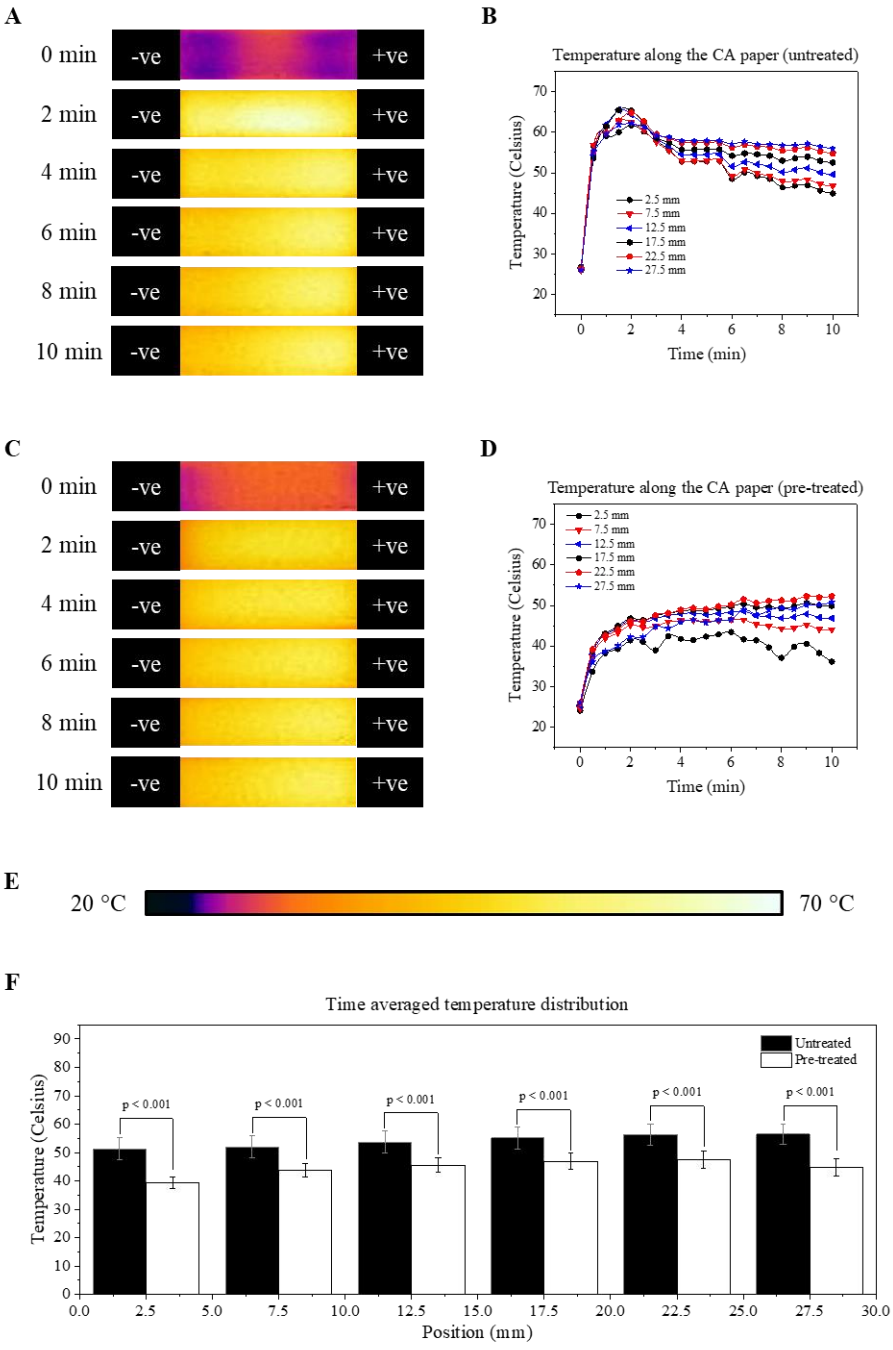

Figure 4.7. Thermal mapping of the CA paper. (A) time-lapse of a HemeChip test run at 250 volt with an untreated CA paper, **(B)** Temperature distribution of a HemeChip test run at 250 volt with an untreated CA paper, **(C)** time-lapse of a HemeChip test run at 250 volt with a pre-treated CA paper, **(D)** temperature distribution of a HemeChip test run at 250 volt with a pre-treated CA paper, **(E)** the colormap for the thermal images (range: 20 ~ 70 °C), and **(F)** time-averaged temperature distribution for an untreated and a pre-treated CA paper test (at 250 volts).

The onset of electrochemical reaction (water hydrolysis) at the electrode surface causes the pH to change in the HemeChip buffer stored at the cartridge reservoir (Eqn (1)-(3)). The H^+ generation at the anode, balanced out by the water equilibrium (Eqn (4)), leads to a reduction of OH^-. Meanwhile, the reduction reaction at cathode reduces the proton concentration by converting H^+ into H_2 (Eqn (2)) and a coupled reaction (Eqn (3)) causes the increase in pH thus resulting in a pH shift toward a more alkaline direction. The localized pH change at the close vicinity of the cartridge electrode is consequently followed by the ionic migration (due to the electro-neutrality), which becomes apparent by the change in MRB color across the CA paper.

4.4.3 Measurement of Runtime pH Change

The pH change across the CA paper for different applied voltage has been presented in **Figure 4.4**. The length of the CA paper, reported in the pH gradient plots, excludes the ends of the paper (4 mm at each side). The mid-section of the CA paper is the region where the pH electrophoresis separation occurs, and the runtime pH change has been reported for this section only. The length of this window of the separation medium has been relabeled from 0 - 22 mm. The presented pH values along the length of the CA paper is averaged along the lateral direction. **Figure 4.4A** shows an example of a HemeChip test run at 50V. The rate of electrochemical reaction at the electrode surface is proportional to the applied field strength so as the electro-migration of ions. At the beginning of the test, the pH distribution over the CA paper is uniform (**Figure 4.A**, 0 min). As the test progresses, the electrochemical reaction introduces the opposite pH shift in anode and cathode. The electro-migration of ions makes the cathode-end of the CA paper greener indicating a

higher pH at that end compared to the initial pH of the CA paper at the beginning of the test. Similarly, the anode-end of the paper changes its color toward a more yellowish hue indicating a lower pH at that end compared to the initial pH over the CA paper (**Figure 4.4A**, 2-10 min). **Figure 4.4B** is a quantitative representation of the phenomena described above. The quantitative results in **Figure 4.4B** show the pH change at the cathode-end of the paper is significantly higher than the pH change at the anode-end of the CA paper. The initial measured pH on the CA paper is approximately 8.5 at the beginning of the test (**Figure 4.4B**, 0 min). After 2 minutes, the pH at the cathode-end pH increases to 9 and an average pH gradient of 0.11/mm extending for ~5 mm appears. As the test progresses, the cathode-end pH rises to 9.26 - 9.36, while the location of the pH gradient shifts from 0.43 - 2.34 mm with a pH gradient of 0.18 - 0.23.At the anode-end of the CA paper between 2 - 10 minutes, the pH drops from 8.28 - 8.11 and the pH gradient shifts from 22 - 17 mm. The pH gradient increases from 0.03/mm - 0.07/mm and then drops to 0.05/mm.

The runtime pH change over the CA paper for 150 volt tests has been illustrated in **Figure 4.4C&D**. The pH shift and the pH gradient changes much faster at 150 volts compared to a 50 volt test. After 2 minutes of runtime at the cathode-end, the pH is 9.31 and the pH gradient shifts at 1.2 mm with an average gradient of 0.17/mm extending over 4.78 mm. While at the anode-end, the pH drops at 8.22. The pH gradient shifts to 18.1 mm with an average gradient of 0.08/mm extending over 3.12 mm. After 4 minutes of runtime, the pH at the cathode-end and the anode-end of the CA paper is 9.43 and 8.17, respectively. The pH gradient shift at the cathode-end and the anode-end of the CA paper are 2.17 mm and 20.23 mm, respectively. However, the nonlinear pH gradient from both ends of the CA paper merges at the mid-section of the CA paper. At 6 minutes, a continuous pH gradient

with a pH inflection appears on the CA paper with a maximum pH of 9.47 (cathode-end) and a minimum pH of 8.07. The pH inflection appears as a peak of pH and it is located at 6.67 - 12.13 mm. As the test progresses further, the pH drop at the anode-end remains somewhat stable. On the other hand, the pH at the cathode-end drops significantly at 8 and 10 minutes (compared to 6 minutes), but the pH inflection shifts to 8.57 - 15.07 mm for 8 minutes and to 11.26 - 18.97 mm for 10 minutes.

For the applied electric field of 250 volts (**Figure 4.4E&F**), the pH rises reach 9.28 and 8.25 at the cathode and anode-end, respectively. A small pH inflection point appears between 3.24 - 6.92 mm. By 6 minutes, the pH at the cathode-end of the CA paper drops at 8.9, while the pH at the anode-end of the CA paper remains the same. The pH gradient is milder at the cathode-end at this point and the pH inflection zone extends between 11.75 - 21 mm. Moving from 6 to 8 minutes, the pH distribution over nearly half of the CA paper (cathode-side) remains the same, but the pH at the anode-end rises to close to 8.5. The pH inflection zone shifts very close to the anode-end (15.16 - 19.90 mm) of the CA paper. At the end of 10 minutes runtime, the only observed change in pH distribution that the increase in pH of the anode-end to 8.61 and the pH inflection zone is no longer visible.

4.4.4 Effect of Pre-Treatment

The treatment process described before (section 2.5) affects the electro-migration across the CA paper significantly. **Figure 4.5** shows a comparison of the pH distribution over the CA paper between a pre-treated and an untreated CA paper. **Figure 4.5A&B** shows the pH distribution over an untreated CA paper, whereas, **Figure 4.5C&D** shows the pH distribution over a pre-treated CA paper. Test for both cases were run at 250V. The

results show that the pH at the cathode-end of the CA paper remains somewhat constant over the period of the time. The anode-end of the CA paper shows the usual drop in pH, as it was observed for the untreated paper (**Figure 4.5C**). The quantitative results (**Figure 4.5B&D**) reflects this contrast of pH distribution between a pre-treated and untreated CA paper (**Figure 4.5E**).

At the initial stage of the test, the observed change in pH distribution for a pre-treated CA paper was a pH increase at the cathode-end (pH 8.8) and a smooth pH gradient of 0.10/mm extending over a region of 5 mm. The remaining of the CA paper has an average pH of 8.3. After 4 minutes runtime, the pH at both ends (cathode and anode) remains the same. However, there is a pH gradient of 0.05/mm extends from the cathode-end to the mid-section (11.3 mm) of the CA paper, which is followed by a gradual pH increase of 0.01/mm extending up to the anode-end of the CA paper. For the remaining of the test, the pH at the cathode end of the CA paper remains stable. The pH at the anode-end of the CA paper slightly drops from 8.2 to 8.1 (from 6 to 8 minutes) and rises back to 8.2 at 10 minutes of runtime. The pH gradient over the CA paper during 6 to 10 minutes shows a somewhat smooth pH gradient.

4.4.5 Runtime Thermal Assessment

Electrophoresis being an electrochemical process, the runtime heat generation comes as an inherent challenge for any electrophoretic system. The role of temperature increase can be positive and negative at the same time. For electrophoretic separation, increased temperature causes an increase in the electrophoretic mobility of the charged entities, resulting in a faster separation. On the other hand, when the charged entities are

biological samples, the effect of temperature increase can be detrimental due to degradation, denaturation of the sample. The electrophoretic mobility of such degraded and denatured samples differ from the non-degraded samples, and in addition to the altered mobility, the increased temperature also causes distortion of the separated bands. The degree of these undesired effects depends on the degree of temperature increase. **Figure 4.7** shows the runtime temperature change and the thermal distribution over the CA paper during a test. **Figure 4.7A** shows the time-lapse of temperature distribution over the CA paper for a test (run at 250V). The temperature distribution data, acquired by the thermal camera (FLiR One) at an interval of 30 seconds and analyzed by the thermal image analysis software (FLiR Studio), was then calibrated using the calibration plot (**Figure 4.6B**) described in the previous section. The analyzed thermal data was plotted for a set of equally spaced points (at 2.5, 7.5, 12.5, 17.5, 22.5, and 27.5 mm along with the CA paper) along the midline (longitudinal) of the CA paper (**Figure 4.7B**). The analysis of the thermal imaging data revealed there is an initial phase (phase I) during the test when the temperature is rising, which is followed by another phase (phase II) where the temperature increase reaches its peak and then undergoes a small drop (**Figure 4.7B**). Following the later phase, there is the final phase (phase III) where the temperature of the CA paper shows a slowly decaying pattern, and the rate of decay depends on the location of the points. At the beginning of the test, the average temperature over the CA paper is 26.3°C. After 30 minutes, the temperature over the CA paper rises to an average of 54.6°C (maximum: 75.3°C, and minimum: 48.2°C) (**Figure 4.7B**). The phase II, where the temperature reaches a peak and drops then slightly drops, extends between 1.5 - 2.5 minutes of the runtime. The maximum temperature reached during this phase is 65.3°C and the minimum

temperature is 54.7°C. The location of the maximum temperature or the "hot spot" is located at the midsection of the CA paper (**Figure 4.7A**, 2 min). During the final phase, the location the hot spot moves closer to the anode-end of the CA paper (**Figure 4.7A**, 6-10 min) and the temperature of the hot spot drops from 59.8 to 55.9°C (**Figure 4.7B**).

The runtime thermal assessment for the test, where pre-treated CA paper was used, depicts a slightly different picture (**Figure 4.7C&D**). The degree of temperature increase and the trend of the thermal profile is much smoother for the case of pre-treated CA paper (**Figure 4.7D**). For pre-treated CA paper, the initial phase (phase I) of temperature increase is present, but the temperature (average: 36.2°C) is less than what has been observed for a test performed with untreated CA paper (56.4°C). The phase where a distinct peak of temperature rise was observed (phase II for untreated CA paper) is not present for in case pre-treated CA paper. The initial phase of temperature increase is followed by a phase where the temperature over the CA paper shows a location-dependent trend were - (i) a slowly rising temperature, (ii) steady temperature, and (iii) steady drop of temperature was observed from the anode-end to the cathode-end of the CA paper. The presence of a shifting hot spot is observed for the CA paper for pre-treated CA paper as well. But the temperature magnitude of the hot spot is lower for pre-treated CA paper compared to the untreated CA paper (**Figure 4.7F**). There a drop in the hot spot temperature for the pre-treated CA paper test and the drop in temperature at 2, 3, 4, 5, 6, 7, 8, 9, and 10 minutes are 18.5°C, 12.2°C, 9.0°C, 8.9 °C, 6.8°C, 6.5°C, 5.3°C, 4.8°C, and 3.0°C, respectively.

4.5 Discussion and Conclusion

A method for image-based dynamic tracking of runtime pH change and another method for assessment of runtime temperature distribution on the separation medium for a paper-based microchip electrophoresis system has been presented. The presented method for dynamic tracking of runtime pH change showed a distinct shifting pH gradient over the paper with time. The dynamic tracking of runtime pH shows a greater pH shift toward a higher alkaline pH at the cathode-end of the paper compared to the decrease in pH value at the anode end of the paper. The source of this dynamic pH shift is the change in the concentration of H^+ and the OH^- ions, caused by the electrochemical reaction at the electrode surface. The electrode used in the HemeChip cartridge design is large and no treatment or preventive measures are embedded in the cartridge design. Thus the large exposed electrode surface can significantly change the H^+ and the OH^- ion concentration. The effect of the change in the H^+ and the OH^- ion concentration on the separation medium i.e. the cellulose acetate paper is manifested due to their ionic migration. The ionic migration of these species is also dependent on the applied field strength and the longer the process continues, the interaction of the ionic migration of these two species tends to alleviate. This is why, after 10 minutes of run-time at 250 volts, the pH distribution over the extent of the cellulose acetate paper becomes more uniform. A similar trend is visible for the lower voltages (150 and 50 volt); however, it would require longer runtime to achieve this state. The runtime pH assessment also validated the effectiveness of a pre-treatment process, developed for cellulose acetate paper. The pre-treatment of the cellulose acetate paper seems to reduce the increase in pH at the cathode-end but, the trend in pH

change at the anode-end deemed to be unaltered by the pre-treatment. But the overall change in pH across the CA paper decreases due to the pre-treatment of the paper.

The dynamic assessment of the runtime thermal distribution over the cellulose acetate paper also reveals a characteristic trend on the thermal state of the process. The temperature variation, mapped across the cellulose acetate paper, demonstrated three distinct phases. The initial phase is defined by a sharp rise in temperature, which can go up to 50 ~ 50°C (at 250 volts). The following phase represents a stabilization of the temperature increase, where the temperature increase reaches its peak and then starts to drop. The temperature variation at this phase is 15°C, approximately. During the last and third phase, a spatial dependence in the drop of temperature is apparent. The cathode end of the cellulose acetate paper experiences a grated drop in temperature (~10°C, at 250 volts), while the anode-end of the paper barely experiences any drop in temperature. The dynamic mapping thus reveals the generation of the anode-biased hot spot on the cellulose acetate paper. The pre-treatment of the cellulose acetate paper also shows different characteristics in the run-time thermal state across the cellulose acetate paper. In contrast to the untreated cellulose acetate paper, the thermal distribution across the pre-treated cellulose acetate paper shows two distinct phases, instead of three - the initial rise and the spatially dependent temperature variation, or the generation of the anode-biased hot spot. The pre-treatment of the cellulose acetate paper also reduces the degree of the initial rise in temperature (~15°C, at 250 volts).

The general conclusion of the presented study is the runtime pH change across the paper, and its spatial distribution is dependent on the field strength. The pre-treatment of

the cellulose acetate paper reduces the shift in pH toward a more alkaline range. The runtime thermal assessment demonstrates a characteristic thermal distribution and variation (both spatial and temporal), and the pre-treatment noticeably alters the thermal distribution and variation across the cellulose acetate paper.

Chapter 5: International Multi-Site Testing and Clinical Validation of the Paper-Based MicroChip Electrophoresis (MCE) System

5.1 Abstract

Nearly 7% of the world's population lives with a hemoglobin variant. Hemoglobins S, C, and E are the most common and significant hemoglobin variants worldwide. The most prevalent variant, hemoglobin S, when inherited from both parents, results in sickle cell disease, chronic hemolytic anemia with significant morbidity and mortality. For example, in sub-Saharan Africa, where hemoglobin S is highly prevalent, nearly a quarter of a million babies are born with sickle cell disease each year. Less than half of these babies survive beyond five years of age due to delays in diagnosis and timely treatment. In this chapter, the validation of HemeChip, the first paper-based, microchip electrophoresis platform for identifying and quantifying hemoglobin variants easily and affordably at the point-of-care, has been described. HemeChip works with a drop of blood, automatically analyzes and displays the results, stores the test results, and wirelessly transmits them to an electronic database. The feasibility and high accuracy of HemeChip have been shown via testing 768 subjects by clinical sites in the United States, Central India, sub-Saharan Africa, and Southeast Asia. Validation studies include hemoglobin E testing in Bangkok, Thailand, and hemoglobin S testing in Chhattisgarh, India, and in Kano, Nigeria, where the sickle cell disease burden is the highest in the world. In this chapter, HemeChip has been presented as a versatile, mass-producible, microchip electrophoresis platform that enables rapid, affordable, quantitative, accurate, decentralized hemoglobin testing.

5.2 Introduction

Globin gene disorders are among the world's most common inherited diseases. It is estimated that more than 7% of the world's population carries globin gene variants, with the most prevalent being the β-globin gene mutations, β^S or S, β^C or C, and β^E or E, taken together [178-180]. Hemoglobin S is highly prevalent in sub-Saharan Africa [83] and in tribal populations of Central India [84]. Hemoglobin C is common in West Africa [85], and hemoglobin E is common in Southeast Asia [86]. β^S, β^C, and β^E all arise from a single point mutation in the β-globin gene [181-183].

Homozygous sickle cell disease (Hb SS) causes the highest morbidity and mortality among hemoglobin disorders [184]. Variant SCD arises when these mutations are inherited in a heterozygous manner, such as with another β-globin gene mutation, such as Hb SC or Hb $S\beta^{thal+/0}$. Approximately 70% of individuals with SCD have homozygous Hb SS, and over 25% have compound heterozygous Hb SC or Hb $S\beta^{thal+/0}$ [181].

In SCD, abnormal polymerization of deoxygenated hemoglobin S makes red blood cells (RBCs) stiff, changes membrane properties, alters the shape, and triggers deleterious activation of inflammatory and endothelial cells [185-187]. Sickled RBCs are non-deformable and adhesive in the microcirculation [95,110,188-191], particularly in parts of the body where the oxygen tension is relatively low, such as the kidney or spleen [186,189,192,193]. Abnormally shaped RBCs result in microvascular occlusion and a vicious cycle of enhanced sickling, hemoglobin desaturation, and further vascular occlusion [194-196]. In childhood, recurrent splenic infarction from sickled RBCs increases the risk for life-threatening infections [82,183,197-199]. In addition, young children with SCD are at risk of life-threatening cerebral

vasculopathy [82]. Afflicted patients who survive to adulthood can suffer both acute and chronic painful crises as well as cumulative organ damage and early mortality [82,200]. Infections, stroke, and numerous other SCD-related complications can be mitigated by newborn/neonatal screening and comprehensive medical care [82,201,202].

Individuals who inherit one copy of hemoglobin S and one copy of the normal hemoglobin A (Hb AS) have sickle cell trait. Individuals who carry one copy of hemoglobin S, C, or hemoglobin $\beta^{thal+/0}$ may have offspring with a hemoglobin disorder, depending upon the Hb composition of their partner [107].

Hemoglobin E decreases expression of the β-globin gene and results in an increased sensitivity to oxidative stress [86,203]. Individuals with hemoglobin E trait (Hb AE or Hb E Trait) are asymptomatic, and homozygous hemoglobin E (Hb EE or Hb E Disease) causes mild microcytic anemia. However, hemoglobin E in combination with β^{thal} (Hb E$\beta^{thal+/0}$) causes thalassemia of varying severity [87]. Hemoglobin SE disease is clinically similar to Hb Sβ^{thal}, but rarely seen due to the geographical separation of these variant globin genes [87,88]. However, with increasing migration, these unusual combinations of these globin variants are expected to be encountered more frequently [87,88].

Regardless of their geographic origin, all of these common hemoglobin variants need to be screened for, so that individuals with the disease can be diagnosed early and managed in a timely manner. Newborn/neonatal screening, currently available in resource-rich countries, is needed for optimal management of hemoglobinopathies worldwide [204-206]. For example, in high-income countries, which have less than 1% of the global disease burden, over 90% of babies born with SCD survive into adulthood due to established

national screening programs and comprehensive care [82]. In contrast, in low-income countries, due to lack of nationwide screening and comprehensive care programs, up to 80% of babies born with SCD are undiagnosed and less than half of them survive beyond 5 years of age [82].

In resource-rich countries, standard clinical laboratory tests (high-performance liquid chromatography (HPLC) and hemoglobin electrophoresis) are typically used to establish and confirm the diagnosis of hemoglobin disorders [107]. Additionally, genetic testing can be used to precisely identify these globin gene mutations. Most of the genetic tests are based on polymerase chain reaction assays [108]. These advanced laboratory techniques require trained personnel and state-of-the-art facilities, which are lacking or in short supply in resource-limited countries, where the prevalence of hemoglobin disorders is the highest [82]. Furthermore, these tests are costly in terms of time, labor, and resources [95,109]. For example, it may take days to weeks to receive the hemoglobin test results from centralized clinical laboratories in resource-limited countries [109]. Further, when screening is conducted in remote areas, locating those who test positive may be challenging to impossible [94,95,109]. Therefore, there is a need for affordable, portable, easy-to-use, accurate point-of-care tests to facilitate decentralized hemoglobin testing in resource-constrained countries [82,110].

In this chapter, the clinical validate HemeChip, for common hemoglobinopathies, has been presented and benchmarked against the reference standards in 768 subjects in the United States, sub-Saharan Africa, Central India, and Southeast Asia. Tests were performed by local users, including healthcare workers and clinical laboratory personnel.

Clinical validation studies include hemoglobin E testing in Bangkok, Thailand; and hemoglobin S testing in Jagdalpur, Chhattisgarh, India, and in Kano, Nigeria, where the SCD burden is the highest in the world [92,207,208]. In clinical validation studies, HemeChip correctly identified all subjects with SCD-SS, SCD-SC, SCD Trait, hemoglobin E Disease, and hemoglobin E Trait with 100% sensitivity. HemeChip displayed an overall diagnostic accuracy of 98.4% in comparison to reference standard methods for all hemoglobin variants tested.

5.3 Methods

5.3.1 Clinical Study Design and Participants

Clinical study design, study participants, sample size calculation (**Table 5.1**), and details on test methods are described according to the Standards for Reporting Diagnostic Accuracy (STARD) 2015 guidelines [209]. Institutional Review Board (IRB) approved study protocols included the following common objectives: to validate HemeChip technology as a point-of-care platform for hemoglobin testing, to compare the screening results obtained from HemeChip with that obtained from laboratory electrophoresis and/or HPLC as the standard reference methods, to determine the diagnostic accuracy of the test including sensitivity and the specificity, and to determine the feasibility of using HemeChip as a point-of-care testing platform in low and middle-income countries (results presented in **Table 5.2-5.4**). Approvals were obtained from Institutional Review Boards at University Hospitals Cleveland Medical Center (UHCMC IRB# 04-17-15), University of Nebraska Medical Center (UNMC IRB# 754-17-CB), Amino Kano Teaching Hospital in Kano, Nigeria (AKTH/MAC/SUB/12A/P-3/VI/2102), the Kano State Ministry of Health in

Nigeria. (MOH/Off/797/T.I/377). The study was registered in the United States Library of Medicine's ClinicalTrials.gov (Identifier: NCT03948516). The study protocol in India was

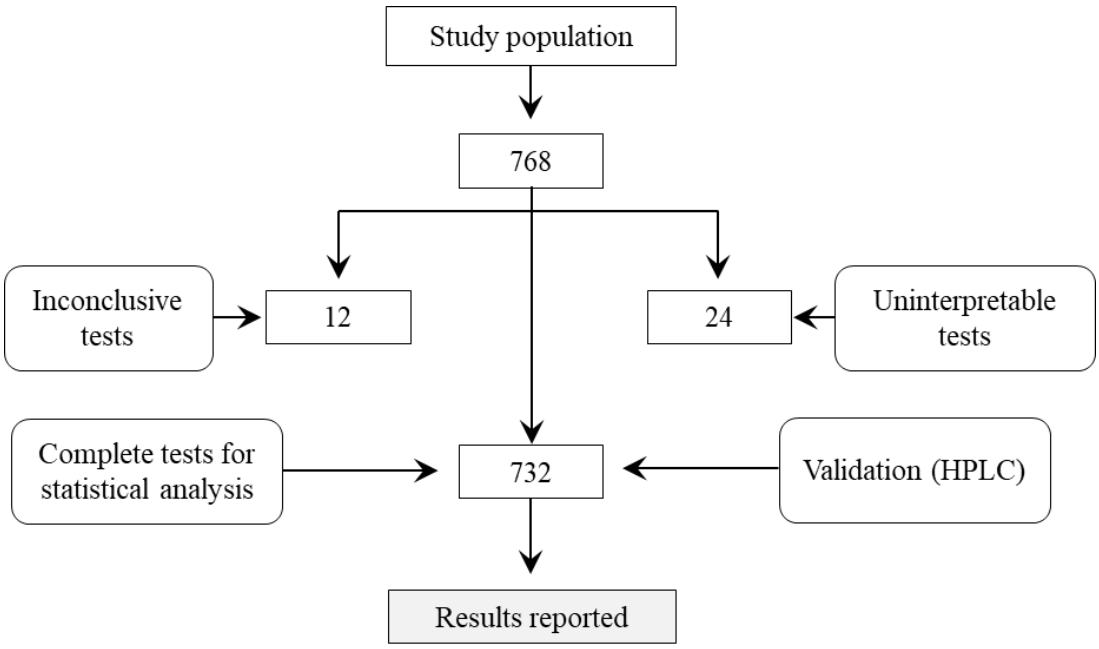

Figure 5.1. Flowchart illustrating the clinical study data collection, test rejection, and reported result. A total of 768 children and adults were tested for hemoglobin disorders, in the US, sub-Saharan Africa, South and Southeast Asia. In Nigeria, 315 subjects (6 weeks to 5 years of age), in Thailand, 124 subjects (7 weeks to 63 years old), in India, 298 subjects (8 months to 65 years old), and in the US 31 subjects (20 to 59 years old) were tested, after obtaining Institutional Review Board approval at each site. Tests were performed by local healthcare workers and clinical laboratory personnel. Blood samples were tested with both HemeChip and with the locally applicable reference standard method, high-performance liquid chromatography or cellulose acetate Hb electrophoresis. Study design, methods, and results are presented according to the Standards for Reporting Diagnostic Accuracy (STARD).

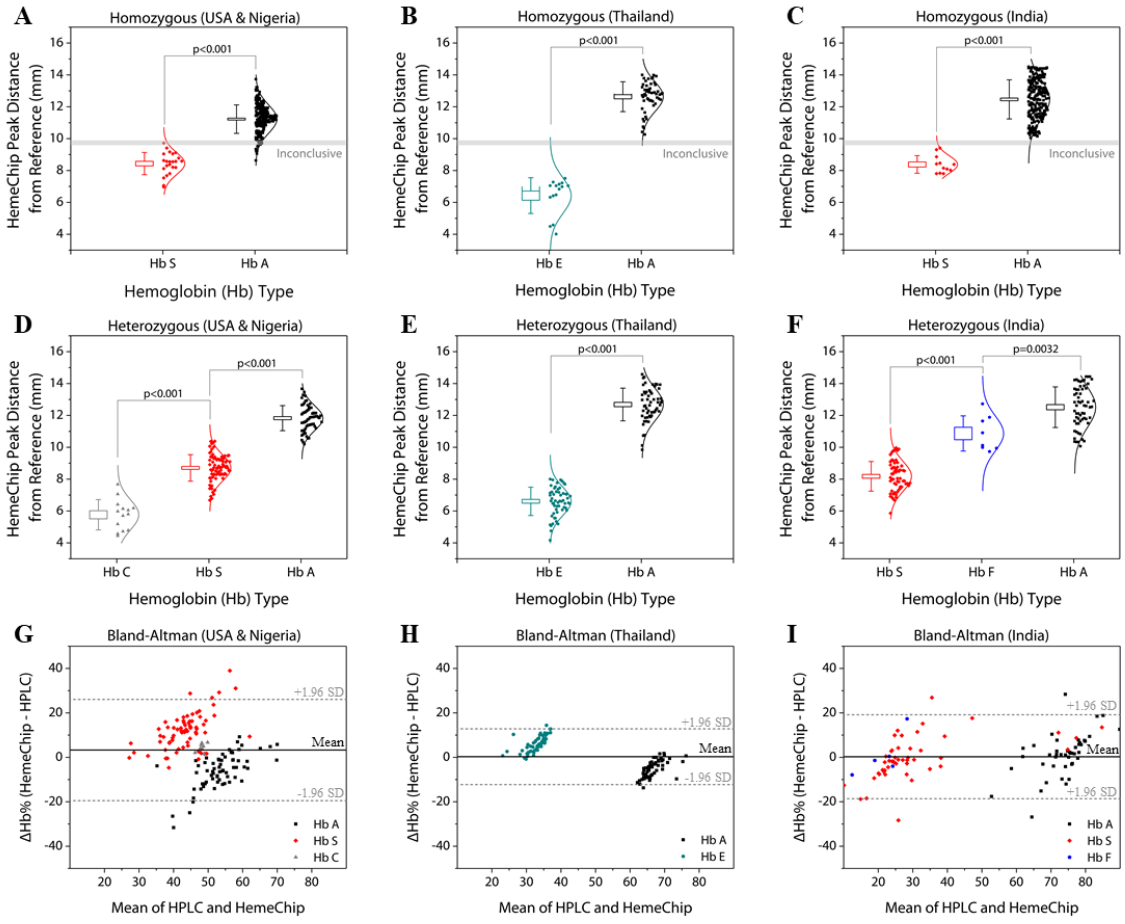

Figure 5.2. HemeChip hemoglobin band separation and quantification. The top row are data distribution plots that show the hemoglobin band separation for homozygous subjects tested in: **(A)** the USA (9 HbSS) and Nigeria (13 Hb SS, 212 Hb AA), **(B)** Thailand (15 Hb EE, 50 Hb AA), and **(C)** India (11 Hb SS, 219 Hb AA). The middle row are data distribution plots for heterozygous subjects tested in: **(D)** the USA (7 Hb AS, 14 Hb SC) and Nigeria (60 Hb AS), **(E)** Thailand (57 Hb AE), and **(F)** India (60 Hb AS, 7 Hb SF, 1 Hb AF). The horizontal lines between hemoglobin positions represent statistically significant differences based on one-way Analysis of Variance (ANOVA) with Tukey post-hoc test for multiple comparisons, where applicable. In whisker plots, brackets represent the standard deviation of the mean, and boxes represent standard error of the mean. The lower row is Bland-Altman analysis plots comparing HemeChip with reference standard method (HPLC) for hemoglobin percentage quantification for the heterozygous subjects tested in the USA and in Nigeria **(G)**, Thailand **(H)**, and India **(I).** In Bland-Altman plots, the solid line indicated the mean difference and dashed lines indicate 95% limits of the agreement defined as mean difference ± 1.96 times standard deviation (SD).

Table 5.1: Sample size calculation for clinical studies

		Nigeria	**India**	**Thailand**
Prevalence estimate	**P**	**0.030** [210]	**0.027** [211]	**0.087** [212]
Width of the 95% CI: 10%	W	0.10	0.10	0.10
Sensitivity expected: 98%	SN	0.98	0.98	0.98
Specificity expected: 98%	SP	0.98	0.98	0.98
Statistical constant, 1.96 for 95% CI	Z_{alpha}	1.96	1.96	1.96
Number with disease, True Positive + False Negative	TP+FN	8	8	8
Sample size required for sensitivity [213]	N1	251	279	87
Number without disease, False Positive + True Negative	FP+TN	8	8	8
Sample size required for specificity [213]	N2	8	8	8
Minimum sample size (greater of N1 and N2):		**251**	**279**	**87**
Minimum sample size total:		**616**		

approved by the institutional ethical committee of ICMR (Indian Council of Medical Research) National Institute of Research in Tribal Health, Jabalpur, Madhya Pradesh, India (Letter vide no. NIRTH/IEC/1153/2017). The study protocol in Thailand was approved by the Siriraj Institutional Review Board (SiRB Protocol no. 906/2561(EC1)).

Clinical sample size estimation was based on published methods by incorporating disease prevalence into sample size calculation [214] with 95% confidence interval and with estimated sensitivity and specificity of 98% (**Table 5.4**). The estimated SCD-SS (homozygous S) disease prevalence in the study population in Nigeria was 3% [210], which resulted in a minimum sample size of 251. SCD-SS prevalence was estimated at 2.7% in Central India [211], which resulted in a minimum sample size of 279 in India. In Bangkok,

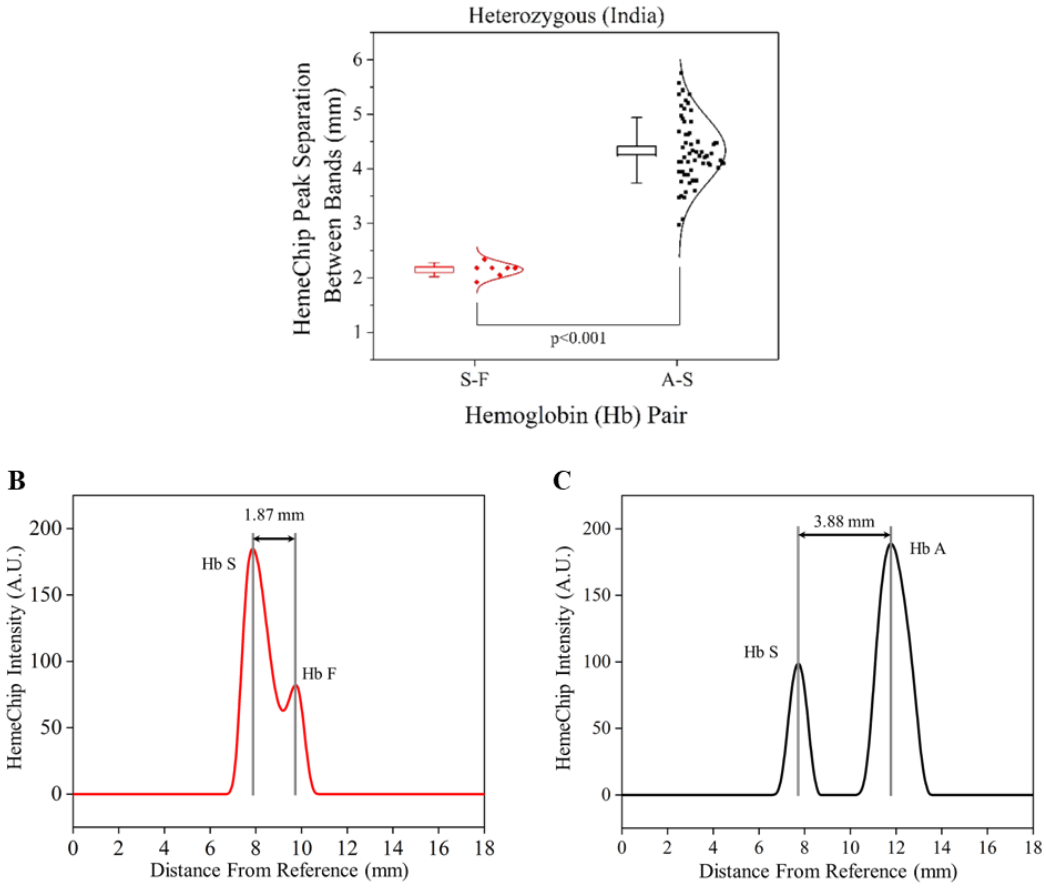

Figure 5.3. Hemoglobin F separation and identification in HemeChip. (A) The separation between hemoglobins A, F, and S can be used to distinguish Hb AS and Hb SF samples. The separation between Hb S and Hb F is significantly less than the separation between Hb A and Hb S. **(B)** A typical Hb SF result with 1.87 mm separation between S and F hemoglobin bands. **(C)** A typical Hb AS result with a 3.88 mm separation between A and S hemoglobin bands.

Thailand, since homozygous Hb E disease prevalence is low (1.8%), A combined homozygous and heterozygous Hb E (with or without α-thalassemia) prevalence estimated was 8.7% [212], which resulted in a minimum sample size of 87.

Table 5.2: Overview of clinical studies with HemeChip

	Total	**Valid tests**	**Uninterpretable tests**	**Inconclusive tests**
Subjects and tests	768	732	24	12
Percentage	100%	95.3%	3.1%	1.6%

768 subjects were tested in clinical studies with HemeChip and the reference standard method.

315 subjects (6 weeks to 5 years old) were tested in Kano, Nigeria, by local users.

124 subjects (7 weeks to 63 years old) were tested in Bangkok, Thailand, by local users.

298 subjects (8 months to 65 years old) were tested in Jagdalpur, Chhattisgarh, India, by local users.

31 subjects (20 to 59 years old) were tested in Cleveland, Ohio, United States, by the research team.

In the first clinical study, 315 children (6 weeks to 5 years of age) were tested in Kano, Nigeria. Study participants were enrolled as part of the existing Community-Acquired Pneumonia, and Invasive Bacteremia Disease study at three government hospitals, Amino Kano Teaching Hospital, Murtala Muhammad Specialist Hospital, and Hasiya Bayero Pediatric Hospital. Inclusion criteria for the Nigeria study included: 6 weeks to 5 years of age, fever or hypothermia and one of the following conditions: prostration, excessive crying, poor feeding, altered consciousness, convulsion, difficulty breathing, profuse vomiting, diarrhea, and a provision of signed and dated informed consent by the

parent or guardian. Exclusion criteria for the Nigeria study included parent or child choosing to opt-out of the study after initial consent and blood transfusion within 3 months of the study enrollment. In Cleveland, Ohio, 32 adult participants were recruited to the study as part of an ongoing clinical trial (ClinicalTrials.gov Identifier: NCT02824471). The main purpose of the clinical study in Cleveland was to test SCD-SC blood samples, which are rare in Nigeria and India.

Table 5.3: HemeChip diagnostic accuracy in comparison to reference standard method.

Category	Hemoglobin type	Correct	Incorrect	Accuracy
SCD-SS	Hb SS	33	0	100%
SCD-SC	Hb SC	14	0	100%
SCD Trait	Hb AS	129	0	100%
Hb E Disease	Hb EE	15	0	100%
Hb E Trait	Hb AE	57	0	100%
Normal (no abnormal Hb)	Hb AA	472	9*	98.1%
SCD-Sβ^+, SCD-Sβ^0	Hb SAA_2, Hb SFA_2	0	3†	-
All categories	-	720	12	98.4%

*Nine subjects with normal hemoglobin (Hb AA) were identified as SCD by HemeChip.

†Three subjects with compound heterozygous Sβ-thalassemia$^{+/0}$ were identified as SCD by HemeChip.

In the second clinical study, 124 subjects (7 weeks to 63 years old) were tested in Bangkok, Thailand, by local laboratory personnel. Surplus blood samples were obtained from patients undergoing clinical laboratory testing at Siriraj Hospital in Bangkok. Hb AA, Hb AE, and Hb EE (with or without alpha-thalassemia) samples were identified by laboratory

personnel using a combination of complete blood count, low-pressure liquid chromatography (LPLC) or HPLC, and clinical history of hemoglobin disorders. Inclusion criteria for the Thailand study included: any age or gender, residual blood sample available with a known date of collection within 1 month, and predicted hemoglobin types of Hb AA, Hb AE, or Hb EE. Exclusion criteria for the Thailand study included: unknown date of sample collection, blood sample older than 1 month at the time of use, any findings on complete blood count, LPLC or HPLC, or clinical history to suggest the presence of a beta-globin variant other than Hb E, such as a high quantitative Hb A_2 in the range suggestive of beta-thalassemia.

Table 5.4: HemeChip diagnostic sensitivity, specificity, positive predictive value (PPV), and negative predictive value (NPV) in comparison to reference standard method.

	SCD-SS vs. others	**SCD-SC vs. others**	**SCD Trait vs. others**	**Hb E Disease vs. others**	**Hb E Trait vs. others**
True positive, TP	33	14	129	15	57
True negative, TN	687	706	591	705	663
False Positive, FP	9	0	0	0	0
False negative, FN	0	0	0	0	0
Sensitivity, TP/(TP + FN)	100.0%	100.0%	100.0%	100.0%	100.0%
Specificity, TN/(TN + FP)	98.7%	100.0%	100.0%	100.0%	100.0%
PPV, TP/(TP + FP)	78.6%	100.0%	100.0%	100.0%	100.0%
NPV, TN/(TN + FN)	100.0%	100.0%	100.0%	100.0%	100.0%

In the third clinical study, 298 subjects (8 months to 65 years old) were tested at a referral testing facility of ICMR-National Institute of Research in Tribal Health located at Late Baliram Kashayap Memorial Medical College, Jagdalpur, Chhattisgarh, India. Inclusion criteria included: subjects of 6 weeks or older, with or without the signs and symptoms of pallor, jaundice, abdominal pain, joint pain, and provision of a signed informed consent (either by the subject or by the parent as appropriate if the subject is a minor). Subjects who withdrew their consent after enrolling were excluded from the study.

5.3.2 Blood Sample Acquisition and Testing

In all clinical studies, blood samples were collected as part of the standard clinical care, and only surplus de-identified blood samples were utilized for testing. The whole blood samples were tested with both HemeChip and the reference standard HPLC (VARIANT™ II, Bio-Rad Laboratories, Inc., Hercules, California) in Cleveland, Ohio, Nigeria, and Thailand. In India, blood samples were tested with both HemeChip and the standard laboratory-based reference standard cellulose acetate electrophoresis, followed by HPLC testing for discordant results. HPLC and cellulose acetate electrophoresis procedures were performed according to manufacturer's guidelines. HPLC was considered to be the reference standard for our comparisons. In any disagreement between HemeChip, cellulose acetate electrophoresis and HPLC, HPLC result was considered to be correct. HPLC %Hb results were normalized to a total of 100% for the cases in which the summation of reported Hb% values were less than 100%. In India, hemoglobin percentage values were reported for only Hb S, A_2, F by the standard reference laboratory, hence the balance percentage was assumed to be Hb A. The HemeChip reader guides the user step-

by-step through the test procedure (**Fig. S6**) with animated on-screen instructions to minimize user errors. Local users were trained to use a custom-designed micro-applicator (**Fig. S7**), which is included in a kit (**Fig. S8**) with graphical instructions for use (**Fig. S9**). Hemoglobin identification and quantification is automatically performed with custom software on the reader and results are reported to the user in a clear and objective way (**Fig. S10-S14**).

Clinical information and reference test results were not available to the performers of the test or the study team at the time of testing. Similarly, HemeChip test results were not available to the performers of the standard reference tests. In Nigeria, HemeChip tests were performed on eHealth Africa campus in Kano, Nigeria, by local healthcare workers using blood samples collected at the nearby Hasiya Bayero Pediatric Hospital, Murtala Muhammad Specialist Hospital, and Aminu Kano Teaching Hospital. Clinical standard (HPLC) testing was done independently by the International Foundation Against Infectious Disease in Nigeria (IFAIN, Abuja, Nigeria) for the blood samples obtained in Kano. In Cleveland, Ohio, HemeChip tests were performed at Case Biomanufacturing and Microfabrication laboratory by the research team members. HPLC testing was done independently by the University Hospitals Cleveland Medical Center Clinical Laboratories (Cleveland, Ohio) for the blood samples obtained in Cleveland. In Thailand, HemeChip tests were performed at Siriraj Thalassemia Center by local laboratory personnel. Reference standard testing (HPLC) was independently performed at ATGenes Co. Ltd. (Bangkok, Thailand). In India, HemeChip tests and standard reference cellulose acetate electrophoresis tests were performed by local laboratory personnel at the testing facility of ICMR-National Institute of Research in Tribal Health located at Late Baliram Kashyap

Memorial Medical College located at Jagdalpur, Chhattisgarh, and HPLC testing was performed at the central laboratory of ICMR-National Institute of Research in Tribal Health, Jabalpur, Madhya Pradesh, India.

5.3.3 Statistical Methods

Hemoglobin band separation data were analyzed statistically using a one-way Analysis of Variance (ANOVA) test with p-value set at 0.001 for statistically significant difference (**Fig. 6A-F**). Tukey post-hoc test was used for multiple comparisons, where applicable. Hemoglobin percent quantification agreement between HemeChip and the reference standard method (HPLC) was assessed by Bland-Altman analysis for heterozygous samples tested (**Fig. 6G-I**). For homozygous samples tested, Bland-Altman analysis was not performed, since for such samples, both HemeChip and the reference standard method display only one Hb%, which is greater than 90%. The Bland-Altman method was used to determine the repeatability of HemeChip quantification using residual analysis by comparison to the standard method. The coefficient of repeatability was set as 1.96 times the standard deviations of the differences between the two measurements. Diagnostic accuracy of the HemeChip test in comparison to HPLC was determined as the percent ratio of correct test results and summation of correct test results and incorrect test results for a hemoglobin variant category (**Table 5.3**). Sensitivity was determined as the ratio of true positive results divided by the summation of true positive results and false negative results. Specificity was determined as the ratio of true negative results divided by the summation of true negative results and false positive results (**Table 5.4**). Sensitivity, specificity, positive predictive value (PPV), and negative predictive value (NPV) were

analyzed and reported for binary pairs of SCD-SS vs. others, SCD-SC vs. others, SCD Trait vs. others, Hb E Disease vs. others, Hb E Trait vs. others (**Table 5.3**).

5.4 Results

5.4.1 International Multi-Site Clinical testing of HemeChip

The clinical study results and HemeChip diagnostic accuracy, performed in the US, Nigeria, Thailand, and India has been reported in this chapter (**Table 5.3**) [209]. A detailed description of the study design, participants, test methods, in these studies, the HemeChip test results included the following: Hb SS, Hb SC, SCT (Hb AS), homozygous Hb E (Hb EE), Hb E Trait (Hb AE), and Normal adult Hb (Hb AA). HemeChip identified these Hb variants with 100% accuracy (**Table 5.3**). Nine subjects with no abnormal Hb (Hb AA) were misidentified as Hb SS. Three subjects with compound heterozygous Sβ-thalassemias (2 subjects with Hb $S\beta^+$, 1 subject with Hb $S\beta^0$) were identified as Hb SS by HemeChip. Sensitivity and negative predictive value (NPV) was 100% for all hemoglobin types tested (**Table 5.4**). Specificity was 98.7% for Hb SS vs. others, and 100% for all other types. The positive predictive value was 78.6% for Hb SS vs. others, and 100% for all other types.

'Valid', 'Uninterpretable', and 'Inconclusive' tests were defined according to published recommendations in literature [215] and STARD guidelines [209]. A 'Valid' test was defined as a test that performed as expected according to objective standards, such as the normal movement of the blue control marker (**Figure 2.2&2.4**). An 'Uninterpretable' test was defined as a test that failed to produce any results, and that did not meet the minimum set of objective criteria that constitute a valid or adequate test, e.g., poor migration of the blue control marker, electrical connectivity issues, or faulty cartridges. An 'Inconclusive'

test was defined as a test that performed adequately according to an objective set of standards, such as the satisfactory movement of the blue control marker and appearance of Hb bands, but the test algorithm could not make an identification of Hb types present. Reasons for 'Inconclusive' tests include the appearance of a band or bands at or close to the borderline region between two adjacent detection windows (**Figure 5.2A-C**). An 'Uninterpretable' or 'Inconclusive' test can be recognized by the image analysis algorithm. In addition to the 'Valid', 'Uninterpretable', and 'Inconclusive' tests reported here, a number of tests were not included in the data analysis due to missing reference standard results, sample labeling errors, and the use of samples for training or algorithm development.

Among the total 768 test results reported here, 732 tests were 'Valid' (95.3%), 24 tests were 'Uninterpretable' (3.1%), and 12 were 'Inconclusive' (1.6%) (**Table 5.2**). An 'Uninterpretable' or 'Inconclusive' test does not result in a diagnostic decision [215]. As such, when an 'Uninterpretable' or 'Inconclusive' test is encountered, the test can be repeated, or other methods of testing can be utilized, which are common practices in diagnostics [215], as well as in hemoglobin testing [111,112]. Therefore, based on recommended practices in the literature [215] and the STARD guidelines [209], the uninterpretable and inconclusive test results were reported separately in this study (**Table 5.2**).

For studies reporting diagnostic accuracy, one of the recommendations in the published guidelines is that inconclusive results are excluded from binary statistics (i.e., sensitivity and specificity analyses), but an additional summary statistic is reported that accounts for them [215]. Based on these recommendations, if the twelve inconclusive results

are considered as incorrect, then the overall diagnostic accuracy of HemeChip is 96.8%. When the inconclusive results are reported separately according to the published guidelines [209,215], the overall diagnostic accuracy of HemeChip is 98.4% in identifying Hb SS, Hb SC, Hb AS (SCT), Hb EE, Hb AE, and Hb AA (**Table 5.3**).

5.5 Discussion and Conclusion

Hemoglobinopathy screening after birth is mandated by all 50 states in the United States and in the District of Columbia, as well as in many other developed states, including The United Kingdom and France [96,98-101]. Newborn screening programs in the United States and other developed countries typically utilize blood spots collected on special filter paper cards for screening. Once the samples are collected, they are shipped to centralized laboratories, where eluates from the dried blood spots are used for testing [98,102,103]. While decentralized blood sample collection and centralized testing work in developed countries, this approach is not practical in resource-limited regions due to the logistical and infrastructural challenges. Hemoglobinopathy screening studies conducted in low-resource settings, using centralized laboratories, have reported up to 50% lost to follow-up [104-106].

Screening for Hb disorders is not currently feasible in many low-income countries with high disease burden [82]. In sub-Saharan African countries [83], and in tribal populations of central India [84], where hemoglobinopathies have the highest prevalence [82], hundreds of thousands of undiagnosed afflicted babies are born each year [89-91]. For example, in Nigeria, where the occurrence of SCD is the highest in the world, approximately 24% of the population carry β^S (i.e., SCT, Hb AS) and the prevalence of Hb SS is up to 20-30 per 1000 births, or at least 150,000 children born with the disease every year [92]. An estimated 50-

90% of these babies die before age 5, in part because they are not diagnosed and hence not treated [89,93-96]. It is projected that by 2050, about 400,000 babies will be born with SCD annually worldwide [82,97].

In SCD, the WHO estimates that more than 70% of SCD related deaths are preventable with early diagnosis and widely available cost-efficient interventions (e.g., pneumococcal vaccinations, daily penicillin, hydroxyurea) [82,91,96,198,199,216-220]. For example, hydroxyurea use has been shown to reduce the vaso-occlusive crises, stroke, infections, malaria, transfusions, and death in children with SCD, warranting the need for wider access to this treatment [82,217-220]. Hydroxyurea treatment has been shown to be feasible, safe, and effective in children with SCD living in India [221] and in sub-Saharan Africa [82,217,222,223]. However, the realities of resource-limited environments demand a fundamentally different approach to diagnosis: one that is affordable, portable, and easily administered by entry-level healthcare workers in local health service settings or in rural areas at the point-of-need [94,95,109]. Importantly, test results must be available while the patient is still present so that the diagnosis can be given to the patient or legal guardian(s) immediately, and the treatment and education can begin without losing the patient to follow-up. Standard clinical methods for hemoglobin testing, such as HPLC and bench-top electrophoresis, are usually run in batches, which delays the results to patients and requires a central laboratory with highly trained personnel. In addition, these tests require infrastructure to handle remote patients, which involves collection and transportation of blood samples [224] and resources to locate patients, maybe weeks later, to report results [94,95,109,225]. Since a HemeChip test is completed within ten minutes and can be run at the point-of-care, the results would be available during a patient's visit. Furthermore, the

compact design of the HemeChip allows portability for decentralized testing and use at the point-of-need, which eliminates blood sample transfer to central laboratories.

HemeChip combines the benefits of standard hemoglobin electrophoresis with the benefits of a point-of-care test. HemeChip technology has a number of fundamental differences and unique features when compared to standard hemoglobin electrophoresis techniques. For example, HemeChip replaces the benchtop laboratory setup [111,112] with a portable reader and replaces the hemoglobin controls [111,112] with a blue control marker (**Figure 2.2&2.4**). HemeChip provides hemoglobin type identification and quantitative results of relative hemoglobin percentages (**Figure 2.5**). The overall simplicity of the HemeChip enables any user to quickly and accurately screen for SCD and other hemoglobin disorders. The user is guided through the step-by-step process with on-screen animated instructions, which minimizes errors (**Figure 3.6**). HemeChip does not require a dedicated lab environment and battery operation allows use in remote places lacking electrical power. These critical features distinguish HemeChip from currently available laboratory methods (**Table 3.1**) and other emerging point-of-care technologies for hemoglobin testing (**Table 3.2**).

Clinical studies with HemeChip in the US, sub-Saharan Africa, Central India, and Southeast Asia demonstrated high sensitivity and specificity hemoglobin variants S, C, and E. Current practice in resource-constrained settings is that all positive Hb variant test results (e.g., Hb SS) are confirmed with a secondary method prior to final diagnosis and treatment [226]. Therefore, all Hb SS tests would undergo secondary confirmation to rule out false positive tests. Further, with lessons learned in the first clinical studies in the US and

Nigeria, we significantly improved the test accuracy, specificity, and reduced the ratio of inconclusive and uninterpretable tests in Thailand and India. In Thailand and India, we minimized the fraction of faulty cartridges with better quality control and improved the image analysis algorithm utilizing normalization procedures on band migration. These improvements eliminated the inconclusive test results and false positives with better band separation (**Fig. 5.2B&C**) and increased the test specificity to 100% for Hb SS in India (**Tables 5&6**).

Hemoglobin electrophoresis techniques share a common limitation. Some hemoglobin types appear in the same electrophoretic window, as they exhibit the same or similar electrophoretic mobility in a given condition. For example, in capillary zone electrophoresis, it can be challenging to quantify hemoglobin A_2 in the presence of hemoglobin C, due to partial overlap between the two zones for these two hemoglobin types [121,122], which may be improved using curve fitting methods. Hemoglobin G and hemoglobin D are difficult to separate because they have identical migration in gel electrophoresis, in capillary electrophoresis, and they have overlapping elution times in HPLC. This sharing of detection window or peak overlapping is also a challenge for the reference standard method, HPLC, as well as its alternatives [121,123,124]. For example, in HPLC, hemoglobin S elutes in the S window with 28 other hemoglobin variants, including 10 other β-chain variants [125]. A similar issue occurs in the A_2 window for HPLC, where hemoglobin E and 18 other hemoglobin variants elude in the same window, and 13 of these 18 variants are β-chain variants [125]. A limitation of cellulose acetate paper-based electrophoresis is that hemoglobins C, E, and A_2, co-migrate [111,112]. With HemeChip, hemoglobins C, A_2, and E are all detectable, but it is not possible to differentiate them

[111,112]. Therefore, instead of reporting Hb C or E or A_2 individually, HemeChip reports hemoglobin C/E/A_2. Since HemeChip provides quantitative results, the relative percentages of these hemoglobins can be used to make a distinction. For example, hemoglobin A_2 is typically found at lower percentages (3-10%) in most subjects [112,227,228], whereas hemoglobin C is typically much higher (greater than 40% for Hb SC, greater than 90% for Hb CC) [229]. When hemoglobin C and hemoglobin A_2 are both present in the same blood sample, the HemeChip shows the hemoglobin C percentage plus hemoglobin A_2 percentage [230]. Clinical decision-making is not affected by this overlap, for Hb SC, Hb AC, or Hb CC results, but it is a limitation for detecting Hb Sβ-thalassemia and Hb Eβ-thalassemia. The algorithm has not yet been trained to identify Sickle β-thalassemia variants; however, it categorizes them as SCD (**Table 5.3**). Furthermore, some hemoglobin variants display a distinct geographical prevalence and distribution. For example, hemoglobin C is highly prevalent in West Africa [231], while hemoglobin E is the most prevalent in Southeast Asia [86-89,203]. The clinician can use the test location, the ethnicity of the subject, the hemoglobin percentage, and clinical history, to help differentiate between co-migrating Hb types.

Hb F represents 50-95% of total Hb in newborn babies but declines significantly over the course of the first 6 months of life [232,233]. At high levels, Hb F might mask Hb variants in the newborn [234]. However, screening for hemoglobin variants can be integrated into established, highly effective immunization programs in low-income countries [82], which are typically initiated at 6-8 weeks of age [82,97]. By this time, Hb F levels decrease sufficiently to allow identification of adult Hb variants. Non-β chain hemoglobinopathies, such as α-thalassemia, are also major world-wide health problems in children, especially

in Asia. This technology is expected to detect additional hemoglobins, such as hemoglobin Bart's or hemoglobin H, which are elevated in alpha thalassemia.

HemeChip is the first accurate, cost-effective, quantitative assay for hemoglobin variant identification and analysis at the point-of-care. The HemeChip reader guides the user step-by-step through the test procedure with animated on-screen instructions to minimize user errors. Hb identification and quantification is automatically performed, and Hb types and percentages are displayed in an easily understandable, objective, and quantitative way. The HemeChip reader records the results of the test, and can wirelessly transmit the test results to a central electronic database if needed. HemeChip has been developed based on a versatile, mass-producible microchip electrophoresis platform technology that may address other unmet needs in biology and medicine that require rapid, decentralized hemoglobin or protein analysis, identification, and/or quantification.

Despite SCD's historical recognition of being the first discovered molecular disease, the technological advances for this disease have been slow [235]. The promise of the development of accurate, low-cost, point-of-care diagnostics, especially for low-income countries, has come closer than ever before to being met with new technologies, such as HemeChip. HemeChip and its diagnostic promise will address the global health burden, help close the gap of information in our current state of science and healthcare delivery around hemoglobin diseases, and build space for further innovation and advancement for SCD and other hemoglobinopathies. Through multi-lateral partnerships with local governments, pharmaceutical companies, the technological industry, and university systems, the translation, implementation, and dissemination of affordable screening and

diagnostic technologies throughout countries with limited resources and infrastructure have the potential to change the paradigm of SCD, hemoglobin disorders, and global health.

Chapter 6: Summary and Future Direction

Rapid, reliable, accurate, and cost-effective miniaturization of electrophoretic separation technology can facilitate a plethora of novel applications, especially for medical and clinical. Instant detection, early-stage diagnosis, portable and remote testing capability can revolutionize the healthcare as it is perceived today.

HemeChip technology offers an original and innovative solution to POC diagnosis of hemoglobin variants (Hb A, F, S, C, and E). HemeChip is a low-cost, microchip electrophoresis device that can identify and quantify Hb types in a finger-prick volume of blood on a CA strip housed in a cartridge that has been designed for mass production. The test is rapid (<10 minutes), which includes sample preparation, Hb separation process, real-time data collection, and analysis of the result, which is displayed to the user. Electrophoretic separations between different Hb types are visible to the naked eye through the optically clear HemeChip body, providing a visual interpretation of the results. Furthermore, the results of the quantitative analysis showed that the HemeChip hemoglobin percentages were comparable to HPLC, which is the gold standard in clinical practice.

HemeChip is intended for use as a POC technology. To accomplish this objective, a fully portable, durable test platform with an easy-to-use interface (custom-built application) was developed, so that the HemeChip test may be performed in remote and low-resourced regions. The CASE-BML team, in collaboration with Hemex Health Inc., worked with a global team of engineers, physicians, and clinical experts to develop the

technology, identify global test sites, and conduct international multi-site clinical validation of the technology as a POC microchip electrophoresis platform.

The standard clinical approaches for detecting hemoglobin disorders, such as HPLC and bench-top electrophoresis, are often run in batches, which delays the results to patients and also requires a laboratory with highly trained personnel. This delay is especially inopportune in areas that lack the infrastructure for tracking and contacting patients after they have left the healthcare facility. The relatively high resourced environments, where clinical standards, such as capillary electrophoresis and HPLC are available, the turnaround time for hemoglobin quantification for SCD patients can vary from a few days to a week or more. This is due to reasons that these processes are highly technical, require the processing of samples by highly trained personnel. When patients are undergoing treatment, such as blood transfusions, the immediate result is highly desired to have a quick turnout of a quantitative assessment for hemoglobin percentages of the patient. This quick assessment can facilitate the optimum level of transfusion. Since HemeChip has a rapid test time, patients can receive their results as soon as the test is completed. Furthermore, the compact design of the HemeChip allows portability and application at the POC, which can eliminate sample transfer to central laboratories and improves time to diagnose.

The fundamental science of electrophoretic separation is the induction of charge of proteins due to the chemical environment (i.e., the pH) of the difference of the mobility of protein variants in a mixture. So, the understanding of the dynamic change of the runtime pH can provide a better understanding of the system and provide insights for system

development and process optimization. The runtime heat generation and dissipation also influence the system performance, as the increased temperature can assist quicker separation with elevated electrophoretic mobility, it can also damage sensitive analyte and electrophoretic support medium. The dynamic tracking of runtime pH and temperature change reveals the spatial and temporal pH distribution over the cellulose acetate paper and their relation to the test parameters. The dynamic assessment of the internal heat generation and thermal distribution of the HemeChip system also showed characteristic thermal distribution and their temporal evolution during the process.

One noticeable consequence of the dynamic tracking of the runtime pH change is the development of the pre-treatment of the cellulose acetate paper, which proved to be effective for minimizing runtime pH variation across the separation medium. The pre-treatment also seems to influence the thermal distribution and characteristic run-time behavior. The mechanism of minimizing the pH change and improving the thermal distribution and characteristic runtime behavior warrants further research.

Future effort to understand the mechanism of minimizing runtime pH variation and the effect of paper pre-treatment on characteristic runtime thermal behavior can lead to improved system design, application-specific paper material development and application-specific treatment and/or process development for existing paper which would result in improved separation resolution and limit of detection. The understanding of the spatial and temporal thermal distribution also holds the key to implement effective in-chip cooling for microchip electrophoresis. Future work to investigate these phenomena and their implementation would, in effect, provide improved microchip electrophoresis systems.

Bibliography

1 P. D. Patel & Weber, G. Electrophoresis in free fluid: A review of technology and agrifood applications. *Journal of Biological Physics and Chemistry* **3**, 60-73 (2003).

2 H. Lodish, Berk, A., Kaiser, C. A., Krieger, M., Scott, M. P., Bretscher, A., Ploegh, H. & Matsudaira, P. Molecular Cell Biology. *Molecular Cell Biology, sixth ed. WH Freeman* (2007).

3 A. L. Lehninger, Nelson, D. L., Cox, M. M. & Cox, M. M. *Principles of Biochemistry*. (Macmillan, 2005).

4 R. Westermeier. *Electrophoresis in practice: a guide to methods and applications of DNA and protein separations*. (John Wiley & Sons, 2016).

5 J. Kohn. A cellulose acetate supporting medium for zone electrophoresis. *Clinica Chimica Acta* **2**, 297-303 (1957).

6 J. Kohn. Separation of haemoglobins on cellulose acetate. *Journal of Clinical Pathology* **22**, 109-111 (1969).

7 A. Kaplan, Savory, J., Faulkner, W. R., Rudolph, G. G., Ford, W. J. & Deutsch, M. E. in *Standard Methods of Clinical Chemistry* Vol. 6 (ed Roderick P. MacDonald) 13-30 (Elsevier, 1970).

8 J. E. Kim, Kim, B. R., Woo, K. S., Kim, J. M., Park, J. I. & Han, J. Y. Comparison of Capillary Electrophoresis with Cellulose Acetate Electrophoresis for the Screening of Hemoglobinopathies. *Korean Journal of Laboratory Medicine* **31**, 238-243 (2011).

9 M. N. Hasan, Fraiwan, A., Little, J. A. & Gurkan, U. A. in *2017 IEEE Healthcare Innovations and Point of Care Technologies (HI-POCT).* 164-167.

10 R. Ung, Alapan, Y., Hasan, M. N., Romelfanger, M., He, P., Tam, A., Rosanwo, T., Akkus, A., Cakar, M. A., Icoz, K., Piccone, C. M., Little, J. A. & Curkan, U. A. Point-of-Care Screening for Sickle Cell Disease By a Mobile Micro-Electrophoresis Platform. *Blood* **126** (2015).

11 C. N. Ou & Rognerud, C. L. Diagnosis of hemoglobinopathies: electrophoresis vs. HPLC. *Clinica Chimica Acta* **313**, 187-194 (2001).

12 S. M. Khosa, Usman, M., Moinuddin, M., Mehmood, H. O. & Qamar, K. Comparative analysis of cellulose acetate hemoglobin electrophoresis and high performance liquid chromatography for quantitative determination of hemoglobin A_2. *Blood Research* **50**, 46-50 (2015).

13 F. C. Goodland & Thompson, E. J. A comparison of cellulose acetate immunofixation with polyacrylamide gel electrophoresis for the detection of oligoclonal bands in unconcentrated cerebrospinal fluid. *Journal of Clinical Pathology* **36**, 1309-1311 (1983).

14 L. Koontz. in *Methods in Enzymology* Vol. 529 (ed Jon Lorsch) 35-45 (Academic Press, 2013).

15 D. Janasek, Franzke, J. & Manz, A. Scaling and the design of miniaturized chemical-analysis systems. *Nature* **442**, 374-380 (2006).

16 E. Buyuktuncel. Microchip Electrophoresis and Bioanalytical Applications. *Current Pharmaceutical Analysis* **15**, 109-120 (2019).

17 J. Sádecká & Masár, M. FORENSIC SCIENCES| Capillary Electrophoresis. (2014).

18 A. Manz, Graber, N. & Widmer, H. M. Miniaturized Total Chemical-Analysis Systems - a Novel Concept for Chemical Sensing. *Sensors and Actuators B-Chemical* **1**, 244-248 (1990).

19 D. J. Harrison, Manz, A., Fan, Z. H., Ludi, H. & Widmer, H. M. Capillary Electrophoresis and Sample Injection Systems Integrated on a Planar Glass Chip. *Analytical Chemistry* **64**, 1926-1932 (1992).

20 C. S. Effenhauser, Manz, A. & Widmer, H. M. Glass Chips for High-Speed Capillary Electrophoresis Separations with Submicrometer Plate Heights. *Analytical Chemistry* **65**, 2637-2642 (1993).

21 S. C. Jacobson, Hergenroder, R., Koutny, L. B. & Ramsey, J. M. High-Speed Separations on a Microchip. *Analytical Chemistry* **66**, 1114-1118 (1994).

22 G. J. M. Bruin. Recent developments in electrokinetically driven analysis on microfabricated devices. *Electrophoresis* **21**, 3931-3951 (2000).

23 H. Becker & Gartner, C. Polymer microfabrication methods for microfluidic analytical applications. *Electrophoresis* **21**, 12-26 (2000).

24 V. Dolnik, Liu, S. R. & Jovanovich, S. Capillary electrophoresis on microchip. *Electrophoresis* **21**, 41-54 (2000).

25 N. A. Lacher, Garrison, K. E., Martin, R. S. & Lunte, S. M. Microchip capillary electrophoresis/electrochemistry. *Electrophoresis* **22**, 2526-2536 (2001).

26 A. T. Woolley, Lao, K. Q., Glazer, A. N. & Mathies, R. A. Capillary electrophoresis chips with integrated electrochemical detection. *Analytical Chemistry* **70**, 684-688 (1998).

27 H. G. Kunkel & Tiselius, A. Electrophoresis of Proteins on Filter Paper. *Journal of General Physiology* **35** (1951).

28 W. P. Jencks, Jetton, M. R. & Durrum, E. L. Paper electrophoresis as a quantitative method. Serum proteins. *Biochemical Journal* **60**, 205 (1955).

29 W. Mejbaumkatzenellenbogen & Dobryszycka, W. M. New Method for Quantitative Determination of Serum Proteins Separated by Paper Electrophoresis. *Clinica Chimica Acta* **4**, 515-522 (1959).

30 P. G. Righetti. Electrophoresis: The march of pennies, the march of dimes. *Journal of Chromatography A* **1079**, 24-40 (2005).

31 J. R. L. Ehrenkranz. Home and point-of-care pregnancy tests: A review of the technology. *Epidemiology* **13**, S15-S18 (2002).

32 A. W. Martinez, Phillips, S. T., Butte, M. J. & Whitesides, G. M. Patterned paper as a platform for inexpensive, low-volume, portable bioassays. *Angewandte Chemie-International Edition* **46**, 1318-1320 (2007).

33 P. Nanthasurasak, Cabot, J. M., See, H. H., Guijt, R. M. & Breadmore, M. C. Electrophoretic separations on paper: Past, present, and future-A review. *Analytica Chimica Acta* **985**, 7-23 (2017).

34 W. K. Tomazelli Coltro, Cheng, C. M., Carrilho, E. & de Jesus, D. P. Recent advances in low-cost microfluidic platforms for diagnostic applications. *Electrophoresis* **35**, 2309-2324 (2014).

35 D. M. Cate, Adkins, J. A., Mettakoonpitak, J. & Henry, C. S. Recent developments in paper-based microfluidic devices. *Analytical Chemistry* **87**, 19-41 (2015).

36 M. Santhiago, Nery, E. W., Santos, G. P. & Kubota, L. T. Microfluidic paper-based devices for bioanalytical applications. *Bioanalysis* **6**, 89-106 (2014).

37 Z. Y. Wu, Ma, B., Xie, S. F., Liu, K. & Fang, F. Simultaneous electrokinetic concentration and separation of proteins on a paper-based analytical device. *RSC Advances* **7**, 4011-4016 (2017).

38 L. Ge, Wang, S. W., Ge, S. G., Yu, J. H., Yan, M., Li, N. Q. & Huang, J. D. Electrophoretic separation in a microfluidic paper-based analytical device with an on-column wireless electrogenerated chemiluminescence detector. *Chemical Communications* **50**, 5699-5702 (2014).

39 L. Luo, Li, X. & Crooks, R. M. Low-Voltage Origami-Paper-Based Electrophoretic Device for Rapid Protein Separation. *Analytical Chemistry* **86**, 12390-12397 (2014).

40 C. Xu, Zhong, M., Cai, L., Zheng, Q. & Zhang, X. Sample injection and electrophoretic separation on a simple laminated paper based analytical device. *Electrophoresis* **37**, 476-481 (2016).

41 R. F. Carvalhal, Kfouri, M. S., Piazetta, M. H. D., Gobbi, A. L. & Kubota, L. T. Electrochemical Detection in a Paper-Based Separation Device. *Analytical Chemistry* **82**, 1162-1165 (2010).

42 L. Y. Shiroma, Santhiago, M., Gobbi, A. L. & Kubota, L. T. Separation and electrochemical detection of paracetamol and 4-aminophenol in a paper-based microfluidic device. *Analytica Chimica Acta* **725**, 44-50 (2012).

43 N. Dossi, Toniolo, R., Piccin, E., Susmel, S., Pizzariello, A. & Bontempelli, G. Pencil-Drawn Dual Electrode Detectors to Discriminate Between Analytes Comigrating on Paper-Based Fluidic Devices but Undergoing Electrochemical Processes with Different Reversibility. *Electroanalysis* **25**, 2515-2522 (2013).

44 M. Pumera. Contactless conductivity detection for microfluidics: Designs and applications. *Talanta* **74**, 358-364 (2007).

45 W. K. T. Coltro, Lima, R. S., Segato, T. P., Carrilho, E., de Jesus, D. P., do Lago, C. L. & da Silva, J. A. F. Capacitively coupled contactless conductivity detection on microfluidic systems-ten years of development. *Analytical Methods* **4**, 25-33 (2012).

46 J. A. F. da Silva & do Lago, C. L. An oscillometric detector for capillary electrophoresis. *Analytical Chemistry* **70**, 4339-4343 (1998).

47 A. J. Zemann, Mayrhofer, K., Schnell, E. & Bonn, G. K. Contactless conductivity detection for capillary electrophoresis. *Abstracts of Papers of the American Chemical Society* **216**, U162-U162 (1998).

48 J. Wang, Pumera, M., Collins, G., Opekar, F. & Jelinek, I. A chip-based capillary electrophoresis-contactless conductivity microsystem for fast measurements of low-explosive ionic components. *Analyst* **127**, 719-723 (2002).

49 P. Yager, Edwards, T., Fu, E., Helton, K., Nelson, K., Tam, M. R. & Weigl, B. H. Microfluidic diagnostic technologies for global public health. *Nature* **442**, 412-418 (2006).

50 A. M. Foudeh, Didar, T. F., Veres, T. & Tabrizian, M. Microfluidic designs and techniques using lab-on-a-chip devices for pathogen detection for point-of-care diagnostics. *Lab on a Chip* **12**, 3249-3266 (2012).

51 A. W. Martinez, Phillips, S. T., Whitesides, G. M. & Carrilho, E. Diagnostics for the Developing World: Microfluidic Paper-Based Analytical Devices. *Analytical Chemistry* **82**, 3-10 (2010).

52 C. D. Chin, Linder, V. & Sia, S. K. Commercialization of microfluidic point-of-care diagnostic devices. *Lab on a Chip* **12**, 2118-2134 (2012).

53 W. K. T. Coltro, de Jesus, D. P., da Silva, J. A. F., do Lago, C. L. & Carrilho, E. Toner and paper-based fabrication techniques for microfluidic applications. *Electrophoresis* **31**, 2487-2498 (2010).

54 A. K. Yetisen, Akram, M. S. & Lowe, C. R. Paper-based microfluidic point-of-care diagnostic devices. *Lab on a Chip* **13**, 2210-2251 (2013).

55 X. Li, Ballerini, D. R. & Shen, W. A perspective on paper-based microfluidics: Current status and future trends. *Biomicrofluidics* **6** (2012).

56 E. W. Nery & Kubota, L. T. Sensing approaches on paper-based devices: a review. *Analytical and Bioanalytical Chemistry* **405**, 7573-7595 (2013).

57 Z. Nie, Deiss, F., Liu, X., Akbulut, O. & Whitesides, G. M. Integration of paper-based microfluidic devices with commercial electrochemical readers. *Lab on a Chip* **10**, 3163-3169 (2010).

58 R. J. Block, Durrum, E. L. & Zweig, G. *A manual of paper chromatography and paper electrophoresis*. (Elsevier, 2016).

59 P. Lisowski & Zarzycki, P. K. Microfluidic paper-based analytical devices (μPADs) and micro total analysis systems (μTAS): development, applications and future trends. *Chromatographia* **76**, 1201-1214 (2013).

60 L. S. Ettre. The predawn of paper chromatography. *Chromatographia* **54**, 409-414 (2001).

61 H. Weil & Williams, T. I. Early History of Chromatography. *Nature* **167**, 906-907 (1951).

62 K. L. Sakodynskii & Chmutov, K. MS Tswett and Chromatography. *Chromatographia* **5**, 471-476 (1972).

63 R. Consden, Gordon, A. H. & Martin, A. J. P. Qualitative analysis of proteins: a partition chromatographic method using paper. *Biochemical Journal* **38**, 224-232 (1944).

64 R. Consden, Gordon, A. H. & Martin, A. J. Ionophoresis in silica jelly: A method for the separation of animo-acids and peptides. *Biochemical Journal* **40**, 33-41 (1946).

65 H. B. Bull, Hahn, J. W. & Baptist, V. H. Filter paper chromatography. *Journal of the American Chemical Society* **71**, 550-553 (1949).

66 R. J. Block. Quantitative Estimation of Amino Acids on Paper Chromatograms. *Science* **108**, 608-609 (1948).

67 A. Polson, Mosley, V. M. & Wyckoff, R. W. The Quantitative Chromatography of Silk Hydrolysate. *Science* **105**, 603-604 (1947).

68 L. B. Rockland, Blatt, J. L. & Dunn, M. S. Small Scale Filter Paper Chromatography - Filter Papers and Solvents. *Analytical Chemistry* **23**, 1142-1146 (1951).

69 O. Smithies. Starch-Gel Electrophoresis. *Metabolism-Clinical and Experimental* **13**, 974 (1964).

70 O. Vesterberg. History of Electrophoretic Methods. *Journal of Chromatography* **480**, 3-19 (1989).

71 D. Perrett. From 'protein' to the beginnings of clinical proteomics. *Proteomics Clinical Applications* **1**, 720-738 (2007).

72 S. J. Vella, Beattie, P., Cademartiri, R., Laromaine, A., Martinez, A. W., Phillips, S. T., Mirica, K. A. & Whitesides, G. M. Measuring Markers of Liver Function Using a Micropatterned Paper Device Designed for Blood from a Fingerstick. *Analytical Chemistry* **84**, 2883-2891 (2012).

73 T. Rosenfeld & Bercovici, M. 1000-fold sample focusing on paper-based microfluidic devices. *Lab on a Chip* **14**, 4465-4474 (2014).

74 B. Y. Moghadam, Connelly, K. T. & Posner, J. D. Isotachophoretic Preconcenetration on Paper-Based Microfluidic Devices. *Analytical Chemistry* **86**, 5829-5837 (2014).

75 C. L. Cassano & Fan, Z. H. Laminated paper-based analytical devices (LPAD): fabrication, characterization, and assays. *Microfluidics and Nanofluidics* **15**, 173-181 (2013).

76 M. P. Sousa & Mano, J. F. Superhydrophobic Paper in the Development of Disposable Labware and Lab-on-Paper Devices. *ACS Applied Materials & Interfaces* **5**, 3731-3737 (2013).

77 D. D. Liana, Raguse, B., Gooding, J. J. & Chow, E. Recent Advances in Paper-Based Sensors. *Sensors* **12**, 11505-11526 (2012).

78 H. Juvonen, Maattanen, A., Lauren, P., Ihalainen, P., Urtti, A., Yliperttula, M. & Peltonen, J. Biocompatibility of printed paper-based arrays for 2-D cell cultures. *Acta Biomaterialia* **9**, 6704-6710 (2013).

79 J. Wang. Printing and Characterization of Inks for Paper-based Biosensors. (2014).

80 R. Pelton. Bioactive paper provides a low-cost platform for diagnostics. *Trends in Analytical Chemistry* **28**, 925-942 (2009).

81 C. B. Laurell, Laurell, S. & Skoog, N. Buffer Composition in Paper Electrophoresis - Considerations on Its Influence, with Special Reference to the Interaction between Small Ions and Proteins. *Clinical Chemistry* **2**, 99-& (1956).

82 J. Mburu & Odame, I. Sickle cell disease: Reducing the global disease burden. *International Journal of Laboratory Hematology* **41**, 82-88 (2019).

83 T. N. Williams. Sickle Cell Disease in Sub-Saharan Africa. *Hematology/Oncology Clinics of North America* **30**, 343-358 (2016).

84 R. Colah, Mukherjee, M. & Ghosh, K. Sickle cell disease in India. *Current Opinion in Hematology* **21**, 215-223 (2014).

85 F. B. Piel, Howes, R. E., Patil, A. P., Nyangiri, O. A., Gething, P. W., Bhatt, S., Williams, T. N., Weatherall, D. J. & Hay, S. I. The distribution of haemoglobin C and its prevalence in newborns in Africa. *Scientific reports* **3**, 1671-1671 (2013).

86 S. Fucharoen & Weatherall, D. J. The hemoglobin E thalassemias. *Cold Spring Harbor perspectives in medicine* **2**, a011734.

87 D. Masiello, Heeney, M. M., Adewoye, A. H., Eung, S. H., Luo, H. Y., Steinberg, M. H. & Chui, D. H. Hemoglobin SE disease: a concise review. *American Journal of Hematology* **82**, 643-649 (2007).

88 J. Z. Xu, Riolueang, S., Glomglao, W., Tachavanich, K., Suksangpleng, T., Ekwattanakit, S. & Viprakasit, V. The origin of sickle cell disease in Thailand. *International Journal of Laboratory Hematology* **41**, e13-e16 (2019).

89 R. Colah, Gorakshakar, A. & Nadkarni, A. Global burden, distribution and prevention of beta-thalassemias and hemoglobin E disorders. *Expert Review of Hematology* **3**, 103-117 (2010).

90 L. L. Mulumba & Wilson, L. Sickle cell disease among children in Africa: An integrative literature review and global recommendations. *International Journal of Africa Nursing Sciences* **3**, 56-64 (2015).

91 S. Obaro. Preventable deaths in sickle-cell anaemia in African children. *Lancet* **375**, 460; author reply 461 (2010).

92 Sickle Cell Anemia, Report by the Secreteriat. A59/59 (World Health Organization Fifty-Ninth World Health Assembly, 2006).

93 S. D. Grosse, Odame, I., Atrash, H. K., Amendah, D. D., Piel, F. B. & Williams, T. N. Sickle cell disease in Africa: a neglected cause of early childhood mortality. *American Journal of Preventive Medicine* **41**, S398-405 (2011).

94 I. Odame. Perspective: We need a global solution. *Nature* **515**, S10 (2014).

95 Y. Alapan, Matsuyama, Y., Little, J. A. & Gurkan, U. A. Dynamic deformability of sickle red blood cells in microphysiological flow. *Technology (Singap World Sci)* **4**, 71-79 (2016).

96 F. B. Piel, Hay, S. I., Gupta, S., Weatherall, D. J. & Williams, T. N. Global burden of sickle cell anaemia in children under five, 2010-2050: modelling based on demographics, excess mortality, and interventions. *PLoS Med* **10**, e1001484 (2013).

97 B. Aygun & Odame, I. A global perspective on sickle cell disease. *Pediatric Blood & Cancer* **59**, 386-390 (2012).

98 J. M. Benson & Therrell, B. L. History and Current Status of Newborn Screening for Hemoglobinopathies. *Seminars in Perinatology* **34**, 134-144 (2010).

99 B. J. Bain. Neonatal/newborn haemoglobinopathy screening in Europe and Africa. *Journal of Clinical Pathology* **62**, 53 (2009).

100 A. Streetly, Latinovic, R., Hall, K. & Henthorn, J. Implementation of universal newborn bloodspot screening for sickle cell disease and other clinically significant haemoglobinopathies in England: screening results for 2005–7. *Journal of Clinical Pathology* **62**, 26 (2009).

101 J. Bardakdjian-Michau, Bahuau, M., Hurtrel, D., Godart, C., Riou, J., Mathis, M., Goossens, M., Badens, C., Ducrocq, R., Elion, J. & Perini, J. M. Neonatal screening for sickle cell disease in France. *Journal of Clinical Pathology* **62**, 31-33 (2009).

102 B. L. Therrell, Padilla, C. D., Loeber, J. G., Kneisser, I., Saadallah, A., Borrajo, G. J. C. & Adams, J. Current status of newborn screening worldwide: 2015. *Seminars in Perinatology* **39**, 171-187 (2015).

103 A. Streetly, Sisodia, R., Dick, M., Latinovic, R., Hounsell, K. & Dormandy, E. Evaluation of newborn sickle cell screening programme in England: 2010–2016. *Archives of Disease in Childhood* **103**, 648 (2018).

104 C. M. Wanjiku, Njuguna, F., Asirwa, F. C., Njuguna, C., Roberson, C. & Greist, A. Validation and Feasibility of a Point of Care Screening Test for Sickle Cell Disease in a Resource Constrained Setting — a New Frontier. *Blood* **132**, 2229 (2018).

105 F. Tluway & Makani, J. Sickle cell disease in Africa: an overview of the integrated approach to health, research, education and advocacy in Tanzania, 2004-2016. *British Journal of Haematology* **177**, 919-929 (2017).

106 P. T. McGann, Ferris, M. G., Macosso, P., de Oliveira, V., Ramamurthy, U., Luis, A. R., Bernardino, L. & Ware, R. E. A Prospective Pilot Newborn Screening and Treatment Program for Sickle Cell Anemia in the Republic of Angola. *Blood* **120**, 480 (2012).

107 R. L. Nagel, Fabry, M. E. & Steinberg, M. H. The paradox of hemoglobin SC disease. *Blood Rev* **17**, 167-178 (2003).

108 B. E. Clark & Thein, S. L. Molecular diagnosis of haemoglobin disorders. *Clinical & Laboratory Haematology* **26**, 159-176 (2004).

109 P. T. McGann & Hoppe, C. The pressing need for point-of-care diagnostics for sickle cell disease: A review of current and future technologies. *Blood Cells, Molecules, and Diseases* **67**, 104-113 (2017).

110 Y. Alapan, Fraiwan, A., Kucukal, E., Hasan, M. N., Ung, R., Kim, M., Odame, I., Little, J. A. & Gurkan, U. A. Emerging point-of-care technologies for sickle cell

disease screening and monitoring. *Expert Review of Medical Devices* **13**, 1073-1093 (2016).

111 B. J. Bain. *Haemoglobinopathy Diagnosis*. (Wiley, 2005).

112 B. J. Bain, Wild, B., Stephens, A. & Phelan, L. *Variant Haemoglobins: A Guide to Identification*. (Wiley, 2011).

113 J. M. Reilly, Rochester Institute of, T. & Image Permanence, I. *IPI storage guide for acetate film : instructions for using the wheel, graphs, and table : basic strategy for film preservation*. (Image Permanence Institute, Rochester Institute of Technology, 1993).

114 O. Desanctis, Gomez, L., Pellegri, N., Parodi, C., Marajofsky, A. & Duran, A. Protective Glass Coatings on Metallic Substrates. *Journal of Non-Crystalline Solids* **121**, 338-343 (1990).

115 T. Hanawa. in *Metals for Biomedical Devices* (ed Mitsuo Niinomi) 3-24 (Woodhead Publishing, 2010).

116 A. St John & Price, C. P. Existing and Emerging Technologies for Point-of-Care Testing. *Clinical Biochemist Reviews* **35**, 155-167 (2014).

117 S. Sharma, Zapatero-Rodriguez, J., Estrela, P. & O'Kennedy, R. Point-of-Care Diagnostics in Low Resource Settings: Present Status and Future Role of Microfluidics. *Biosensors (Basel)* **5**, 577-601 (2015).

118 M. Biehl & Velten, T. Gaps and challenges of Point-of-Care technology. *IEEE Sensors Journal* **8**, 593-600 (2008).

119 E. Prichard. - Practical Laboratory Skills Training Guides (Complete Set).

120 S. I. Goldberg, Niemierko, A. & Turchin, A. Analysis of data errors in clinical research databases. *AMIA Annual Symposium Proceedings*, 242-246 (2008).

121 D. F. Keren, Hedstrom, D., Gulbranson, R., Ou, C. N. & Bak, R. Comparison of Sebia Capillarys Capillary Electrophoresis With the Primus High-Pressure Liquid Chromatography in the Evaluation of Hemoglobinopathies. *American Journal of Clinical Pathology* **130**, 824-831 (2008).

122 N. Borbely, Phelan, L., Szydlo, R. & Bain, B. Capillary zone electrophoresis for haemoglobinopathy diagnosis. *Journal of Clinical Pathology* **66**, 29-39 (2013).

123 M. Nusrat, Moiz, B., Nasir, A. & Rasool Hashmi, M. An insight into the suspected HbA_2' cases detected by high performance liquid chromatography in Pakistan. *BMC Research Notes* **4**, 103-103 (2011).

124 P. Sharma & Das, R. Cation-exchange high-performance liquid chromatography for variant hemoglobins and HbF/A_2: What must hematopathologists know about methodology? *World Journal of Methodology* **6**, 20-24 (2016).

125 J. D. Hoyer & Scheidt, R. M. Identification of hemoglobin variants by HPLC. *Clinical Chemistry* **51**, 1303-1304; author reply 1305 (2005).

126 M. Guerra-Balcazar, Morales-Acosta, D., Castaneda, F., Ledesma-Garcia, J. & Arriaga, L. G. Synthesis of Au/C and Au/Pani for anode electrodes in glucose microfluidic fuel cell. *Electrochemistry Communications* **12**, 864-867 (2010).

127 W. Schrott, Svoboda, M., Slouka, Z. & Snita, D. Metal electrodes in plastic microfluidic systems. *Microelectronic Engineering* **86**, 1340-1342 (2009).

128 L. L. Qiang, Vaddiraju, S., Rusling, J. F. & Papadimitrakopoulos, F. Highly sensitive and reusable Pt-black microfluidic electrodes for long-term electrochemical sensing. *Biosensors and Bioelectronics* **26**, 682-688 (2010).

129 M. M. Maharbiz, Holtz, W. J., Howe, R. T. & Keasling, J. D. Microbioreactor arrays with parametric control for high-throughput experimentation. *Biotechnology and Bioengineering* **85**, 376-381 (2004).

130 M. B. Fox, Esveld, D. C., Valero, A., Luttge, R., Mastwijk, H. C., Bartels, P. V., van den Berg, A. & Boom, R. M. Electroporation of cells in microfluidic devices: a review. *Analytical and Bioanalytical Chemistry* **385**, 474-485 (2006).

131 S. W. Lee & Tai, Y. C. A micro cell lysis device. *Sensors and Actuators A-Physical* **73**, 74-79 (1999).

132 M. Fox, Esveld, E., Luttge, R. & Boom, R. A new pulsed electric field microreactor: comparison between the laboratory and microtechnology scale. *Lab on a Chip* **5**, 943-948 (2005).

133 S. M. Knowlton, Sencan, I., Aytar, Y., Khoory, J., Heeney, M. M., Ghiran, I. C. & Tasoglu, S. Sickle cell detection using a smartphone. *Scientific Reports* **5**, 15022 (2015).

134 M. Baday, Calamak, S., Durmus, N. G., Davis, R. W., Steinmetz, L. M. & Demirci, U. Integrating Cell Phone Imaging with Magnetic Levitation (i-LEV) for Label-Free Blood Analysis at the Point-of-Living. *Small* **12**, 1222-1229 (2015).

135 L. F. Ross. Mandatory versus voluntary consent for newborn screening? *Kennedy Institute of Ethics Journal* **20**, 299-328 (2010).

136 X. Yang, Kanter, J., Piety, N. Z., Benton, M. S., Vignes, S. M. & Shevkoplyas, S. S. A simple, rapid, low-cost diagnostic test for sickle cell disease. *Lab on a Chip* **13**, 1464-1467 (2013).

137 N. Z. Piety, Yang, X., Kanter, J., Vignes, S. M., George, A. & Shevkoplyas, S. S. Validation of a Low-Cost Paper-Based Screening Test for Sickle Cell Anemia. *PLoS One* **11**, e0144901 (2016).

138 N. Z. Piety, George, A., Serrano, S., Lanzi, M. R., Patel, P. R., Noli, M. P., Kahan, S., Nirenberg, D., Camanda, J. F., Airewele, G. & Shevkoplyas, S. S. A Paper-Based Test for Screening Newborns for Sickle Cell Disease. *Scientific Reports* **7**, 45488 (2017).

139 A. A. Kumar, Patton, M. R., Hennek, J. W., Lee, S. Y., D'Alesio-Spina, G., Yang, X., Kanter, J., Shevkoplyas, S. S., Brugnara, C. & Whitesides, G. M. Density-based separation in multiphase systems provides a simple method to identify sickle cell disease. *Proceedings of the National Academy of Sciences of the United States of America* **111**, 14864-14869 (2014).

140 T. N. Williams. An accurate and affordable test for the rapid diagnosis of sickle cell disease could revolutionize the outlook for affected children born in resource-limited settings. *BMC Medicine* **13** (2015).

141 L. Mine, Nguyen-Khoa, T., Allaf, B., Ribeil, J.-A., Remus, C., Gauthereau, V., Enouz, S., Kim, J. S., Yang, X., Gluckman, E., Munnich, A., Cavazzana, M. & Girot, R. Hemoglobin S Screening Using the « Sickle Scan » - Biomedomics System. the Necker-Enfants Malades Hospital Experience. *Blood* **128**, 1308 (2016).

142 A. Y. Segbena, Guindo, A., Buono, R., Kueviakoe, I., Diallo, D. A., Guernec, G., Yerima, M., Guindo, P., Lauressergues, E., Mondeilh, A., Picot, V. & Leroy, V. Diagnostic accuracy in field conditions of the sickle SCAN® rapid test for sickle cell disease among children and adults in two West African settings: the DREPATEST study. *BMC Hematology* **18**, 26 (2018).

143 P. T. McGann, Schaefer, B. A., Paniagua, M., Howard, T. A. & Ware, R. E. Characteristics of a rapid, point-of-care lateral flow immunoassay for the diagnosis of sickle cell disease. *American Journal of Hematology* **91**, 205-210 (2016).

144 J. Kanter, Telen, M. J., Hoppe, C., Roberts, C. L., Kim, J. S. & Yang, X. Validation of a novel point of care testing device for sickle cell disease. *BMC Medicine* **13**, 225 (2015).

145 C. T. Quinn, Paniagua, M. C., DiNello, R. K., Panchal, A. & Geisberg, M. A rapid, inexpensive and disposable point-of-care blood test for sickle cell disease using novel, highly specific monoclonal antibodies. *British Journal of Haematology* **175**, 724-732 (2016).

146 C. Steele, Sinski, A., Asibey, J., Hardy-Dessources, M. D., Elana, G., Brennan, C., Odame, I., Hoppe, C., Geisberg, M., Serrao, E. & Quinn, C. T. Point-of-care screening for sickle cell disease in low-resource settings: A multi-center evaluation of HemoTypeSC, a novel rapid test. *American Journal of Hematology* (2018).

147 O. Nnodu, Isa, H., Nwegbu, M., Ohiaeri, C., Adegoke, S., Chianumba, R., Ugwu, N., Brown, B., Olaniyi, J., Okocha, E., Lawson, J., Hassan, A. A., Diaku-Akinwumi, I., Madu, A., Ezenwosu, O., Tanko, Y., Kangiwa, U., Girei, A., Israel-Aina, Y., Ladu, A., Egbuzu, P., Abjah, U., Okolo, A., Akbulut-Jeradi, N.,

Fernandez, M., Piel, F. B. & Adekile, A. HemoTypeSC, a low-cost point-of-care testing device for sickle cell disease: Promises and challenges. *Blood Cells, Molecules and Diseases* (2019).

148 R. Nankanja, Kadhumbula, S., Tagoola, A., Geisberg, M., Serrao, E. & Balyegyusa, S. HemoTypeSC Demonstrates >99% Field Accuracy in a Sickle Cell Disease Screening Initiative in Children of Southeastern Uganda. *American Journal of Hematology* (2019).

149 A. Wuethrich & Quirino, J. P. A decade of microchip electrophoresis for clinical diagnostics - A review of 2008-2017. *Analytica Chimica Acta* **1045**, 42-66 (2019).

150 L. P. Bressan, de Jesus, D. P., Gunasekara, D. B., Lunte, S. M. & da Silva, J. A. F. Microchip Electrophoresis Containing Electrodes for Integrated Electrochemical Detection. *Methods in Molecular Biology* **1906**, 79-85 (2019).

151 X. Li, Tian, J., Nguyen, T. & Shen, W. Paper-based microfluidic devices by plasma treatment. *Analytical Chemistry* **80**, 9131-9134 (2008).

152 X. Li, Tian, J., Garnier, G. & Shen, W. Fabrication of paper-based microfluidic sensors by printing. *Colloids and Surfaces B: Biointerfaces* **76**, 564-570 (2010).

153 C. Heller, Stem, C., Wamwayi, H. & Grieve, A. Development of a filter paper-based ELISA for rinderpest antibodies. *Veterinary Record* **142**, 729 (1998).

154 G. Chitnis, Ding, Z., Chang, C. L., Savran, C. A. & Ziaie, B. Laser-treated hydrophobic paper: an inexpensive microfluidic platform. *Lab on a Chip* **11**, 1161-1165 (2011).

155 J. Yu, Ge, L., Huang, J., Wang, S. & Ge, S. Microfluidic paper-based chemiluminescence biosensor for simultaneous determination of glucose and uric acid. *Lab on a Chip* **11**, 1286-1291 (2011).

156 M. S. Sotoudegan, Mohd, O., Ligler, F. S. & Walker, G. M. Paper-based passive pumps to generate controllable whole blood flow through microfluidic devices. *Lab on a Chip* **19** (2019).

157 T. Akyazi, Gil-Gonzalez, N., Basabe-Desmonts, L., Castano, E., Morant-Minana, M. C. & Benito-Lopez, F. Manipulation of fluid flow direction in microfluidic paper-based analytical devices with an ionogel negative passive pump. *Sensors and Actuators B-Chemical* **247**, 114-123 (2017).

158 C. L. S. Chagas, Cardoso, T. M. G. & Coltro, W. K. T. in *Microfluidic Electrophoresis* 133-142 (Springer, 2019).

159 M. N. Hasan, Fraiwan, A., Little, J. A. & Gurkan, U. A. Hemechip: An Automated Portable Microchip Electrophoresis Platform for Point-of-Care Sickle Cell Disease Screening. *Blood* **130**, 3519 (2017).

160 M. N. Hasan, Fraiwan, A., Thota, P., Oginni, T., Olanipekun, G. M., Hassan-Hanga, F., Little, J., Obaro, S. K. & Gurkan, U. A. Clinical Testing of Hemechip in Nigeria for Point-of-Care Screening of Sickle Cell Disease. *Blood* **132**, 1095 (2018).

161 D. Wencel, Abel, T. & McDonagh, C. Optical Chemical pH Sensors. *Analytical Chemistry* **86**, 15-29 (2014).

162 V. Dolnik & Liu, S. R. Applications of capillary electrophoresis on microchip. *Journal of Separation Science* **28**, 1994-2009 (2005).

163 B. A. Fogarty, Lacher, N. A. & Lunte, S. M. in *Microchip Capillary Electrophoresis: Methods and Protocols* (ed Charles S. Henry) 159-186 (Humana Press, 2006).

164 S. A. Mousavi Shaegh, De Ferrari, F., Zhang, Y. S., Nabavinia, M., Binth Mohammad, N., Ryan, J., Pourmand, A., Laukaitis, E., Banan Sadeghian, R., Nadhman, A., Shin, S. R., Nezhad, A. S., Khademhosseini, A. & Dokmeci, M. R. A microfluidic optical platform for real-time monitoring of pH and oxygen in microfluidic bioreactors and organ-on-chip devices. *Biomicrofluidics* **10**, 044111 (2016).

165 N. Klauke, Monaghan, P., Sinclair, G., Padgett, M. & Cooper, J. Characterisation of spatial and temporal changes in pH gradients in microfluidic channels using optically trapped fluorescent sensors. *Lab on a Chip* **6**, 788-793 (2006).

166 L. Florea, Fay, C., Lahiff, E., Phelan, T., O'Connor, N. E., Corcoran, B., Diamond, D. & Benito-Lopez, F. Dynamic pH mapping in microfluidic devices by integrating adaptive coatings based on polyaniline with colorimetric imaging techniques dagger. *Lab on a Chip* **13**, 1079-1085 (2013).

167 A. Rogacs & Santiago, J. G. Temperature Effects on Electrophoresis. *Analytical Chemistry* **85**, 5103-5113 (2013).

168 D. Liang & Chu, B. High speed separation of DNA fragments by capillary electrophoresis in poly(ethylene oxide)-poly(propylene oxide)-poly(ethylene oxide) triblock polymer. *Electrophoresis* **19**, 2447-2453 (1998).

169 S. R. Liu, Shi, Y. N., Ja, W. W. & Mathies, R. A. Optimization of high-speed DNA sequencing on microfabricated capillary electrophoresis channels. *Analytical Chemistry* **71**, 566-573 (1999).

170 J. Zhang, Fang, Y., Hou, J. Y., Ren, H. J., Jiang, R., Roos, P. & Dovichi, N. J. Use of Non-Cross-Linked Polyacrylamide for Four-Color DNA Sequencing by Capillary Electrophoresis Separation of Fragments up to 640 Bases in Length in Two Hours. *Analytical Chemistry* **67**, 4589-4593 (1995).

171 N. J. Petersen, Nikolajsen, R. P., Mogensen, K. B. & Kutter, J. P. Effect of Joule heating on efficiency and performance for microchip-based and capillary-based electrophoretic separation systems: a closer look. *Electrophoresis* **25**, 253-269 (2004).

172 E. Grushka, Mccormick, R. M. & Kirkland, J. J. Effect of Temperature-Gradients on the Efficiency of Capillary Zone Electrophoresis Separations. *Analytical Chemistry* **61**, 241-246 (1989).

173 C. J. Evenhuis, Guijt, R. M., Macka, M., Marriott, P. J. & Haddad, P. R. Temperature profiles and heat dissipation in capillary electrophoresis. *Analytical Chemistry* **78**, 2684-2693 (2006).

174 B. Gas & Kenndler, E. Dispersive phenomena in electromigration separation methods. *Electrophoresis* **21**, 3888-3897 (2000).

175 S. Ghosal & Chen, Z. Nonlinear waves in capillary electrophoresis. *Bulletin of Mathematical Biology* **72**, 2047-2066 (2010).

176 Z. Chen & Ghosal, S. Strongly nonlinear waves in capillary electrophoresis. *Physical review E: Statistical, nonlinear, and soft matter physics* **85**, 051918 (2012).

177 R. J. Fritsch & Krause, I. in *Encyclopedia of Food Sciences and Nutrition (Second Edition)* (ed Benjamin Caballero) 2055-2062 (Academic Press, 2003).

178 B. Modell & Darlison, M. Global epidemiology of haemoglobin disorders and derived service indicators. *Bulletin of the World Health Organization* **86**, 480-487 (2008).

179 D. T. Jamison, Bank, W. & Project, D. C. P. *Disease Control Priorities in Developing Countries*. (Oxford University Press, 2006).

180 D. J. Weatherall & Clegg, J. B. Inherited haemoglobin disorders: an increasing global health problem. *Bulletin of the World Health Organization* **79**, 704-712 (2001).

181 D. C. Rees, Williams, T. N. & Gladwin, M. T. Sickle-cell disease. *Lancet* **376**, 2018-2031 (2010).

182 H. F. Bunn. Pathogenesis and treatment of sickle cell disease. *The New England Journal of Medicine* **337**, 762-769 (1997).

183 M. J. Stuart & Nagel, R. L. Sickle-cell disease. *Lancet* **364**, 1343-1360 (2004).

184 J. Makani, Ofori-Acquah, S. F., Nnodu, O., Wonkam, A. & Ohene-Frempong, K. Sickle cell disease: new opportunities and challenges in Africa. *The Scientific World Journal* **2013**, 193252 (2013).

185 G. M. Brittenham, Schechter, A. N. & Noguchi, C. T. Hemoglobin S polymerization: primary determinant of the hemolytic and clinical severity of the sickling syndromes. *Blood* **65**, 183-189 (1985).

186 C. Dong, Chadwick, R. S. & Schechter, A. N. Influence of sickle hemoglobin polymerization and membrane properties on deformability of sickle erythrocytes in the microcirculation. *Biophysical Journal* **63**, 774-783 (1992).

187 D. Manwani & Frenette, P. S. Vaso-occlusion in sickle cell disease: pathophysiology and novel targeted therapies. *Blood* **122**, 3892-3898 (2013).

188 Y. Alapan, Little, J. A. & Gurkan, U. A. Heterogeneous red blood cell adhesion and deformability in sickle cell disease. *Scientific Reports* **4**, 7173 (2014).

189 M. Kim, Alapan, Y., Adhikari, A., Little, J. A. & Gurkan, U. A. Hypoxia-enhanced adhesion of red blood cells in microscale flow. *Microcirculation* **24** (2017).

190 G. A. Barabino, Platt, M. O. & Kaul, D. K. Sickle cell biomechanics. *Annual Review of Biomedical Engineering* **12**, 345-367 (2010).

191 Y. Alapan, Kim, C., Adhikari, A., Gray, K. E., Gurkan-Cavusoglu, E., Little, J. A. & Gurkan, U. A. Sickle cell disease biochip: a functional red blood cell adhesion assay for monitoring sickle cell disease. *Translational Research* **173**, 74-91 e78 (2016).

192 R. P. Hebbel. Beyond hemoglobin polymerization: the red blood cell membrane and sickle disease pathophysiology. *Blood* **77**, 214-237 (1991).

193 D. J. Schaer, Buehler, P. W., Alayash, A. I., Belcher, J. D. & Vercellotti, G. M. Hemolysis and free hemoglobin revisited: exploring hemoglobin and hemin scavengers as a novel class of therapeutic proteins. *Blood* **121**, 1276-1284 (2013).

194 L. A. Verduzco & Nathan, D. G. Sickle cell disease and stroke. *Blood* **114**, 5117-5125 (2009).

195 J. B. Caboot & Allen, J. L. Hypoxemia in Sickle Cell Disease: Significance And Management. *Paediatric Respiratory Reviews* **15**, 17-23 (2014).

196 D. R. Hargrave, Wade, A., Evans, J. P. M., Hewes, D. K. M. & Kirkham, F. J. Nocturnal oxygen saturation and painful sickle cell crises in children. *Blood* **101**, 846 (2003).

197 M. H. Steinberg. Management of Sickle Cell Disease. *The New England Journal of Medicine* **340**, 1021-1030 (1999).

198 C. Booth, Inusa, B. & Obaro, S. K. Infection in sickle cell disease: a review. *International Journal of Infectious Diseases* **14**, e2-e12 (2010).

199 S. K. Obaro & Iroh Tam, P. Y. Preventing Infections in Sickle Cell Disease: The Unfinished Business. *Pediatric Blood & Cancer* **63**, 781-785 (2016).

200 S. Kapoor, Little, J. A. & Pecker, L. H. Advances in the Treatment of Sickle Cell Disease. *Mayo Clinic Proceedings* **93**, 1810-1824 (2018).

201 E. Vichinsky, Hurst, D., Earles, A., Kleman, K. & Lubin, B. Newborn screening for sickle cell disease: effect on mortality. *Pediatrics* **81**, 749-755 (1988).

202 T. Frempong & Pearson, H. A. Newborn screening coupled with comprehensive follow-up reduced early mortality of sickle cell disease in Connecticut. *Connecticut Medicine* **71**, 9-12 (2007).

203 S. Warghade, Britto, J., Haryan, R., Dalvi, T., Bendre, R., Chheda, P., Matkar, S., Salunkhe, Y., Chanekar, M. & Shah, N. Prevalence of hemoglobin variants and hemoglobinopathies using cation-exchange high-performance liquid

chromatography in central reference laboratory of India: A report of 65779 cases. *Journal of laboratory physicians* **10**, 73-79 (2018).

204 E. Wastnedge, Waters, D., Patel, S., Morrison, K., Goh, M. Y., Adeloye, D. & Rudan, I. The global burden of sickle cell disease in children under five years of age: a systematic review and meta-analysis. *Journal of Global Health* **8** (2018).

205 T. N. Williams. Sickle Cell Disease in Sub-Saharan Africa. *Hematology/Oncology Clinics of North America* **30**, 343 (2016).

206 F. B. Piel. The Present and Future Global Burden of the Inherited Disorders of Hemoglobin. *Hematology/Oncology Clinics of North America* **30**, 327 (2016).

207 S. K. Obaro, Daniel, Y., Lawson, J. O., Hsu, W. W., Dada, J., Essen, U., Ibrahim, K., Akindele, A., Brooks, K., Olanipekun, G., Ajose, T., Stewart, C. E. & Inusa, B. P. Sickle-Cell Disease in Nigerian Children: Parental Knowledge and Laboratory Results. *Public Health Genomics* **19**, 102-107 (2016).

208 N. Galadanci, Wudil, B. J., Balogun, T. M., Ogunrinde, G. O., Akinsulie, A., Hasan-Hanga, F., Mohammed, A. S., Kehinde, M. O., Olaniyi, J. A., Diaku-Akinwumi, I. N., Brown, B. J., Adeleke, S., Nnodu, O. E., Emodi, I., Ahmed, S., Osegbue, A. O., Akinola, N., Opara, H. I., Adegoke, S. A., Aneke, J. & Adekile, A. D. Current sickle cell disease management practices in Nigeria. *International Health* **6**, 23-28 (2014).

209 P. M. Bossuyt, Reitsma, J. B., Bruns, D. E., Gatsonis, C. A., Glasziou, P. P., Irwig, L., Lijmer, J. G., Moher, D., Rennie, D., de Vet, H. C. W., Kressel, H. Y., Rifai, N., Golub, R. M., Altman, D. G., Hooft, L., Korevaar, D. A. & Cohen, J. F. STARD

2015: an updated list of essential items for reporting diagnostic accuracy studies. *BMJ : British Medical Journal* **351**, h5527 (2015).

210 A. S. Adewoyin. Management of sickle cell disease: a review for physician education in Nigeria (sub-saharan Africa). *Anemia* **2015**, 791498 (2015).

211 D. L. Jain, Sarathi, V., Upadhye, D., Gulhane, R., Nadkarni, A. H., Ghosh, K. & Colah, R. B. Newborn screening shows a high incidence of sickle cell anemia in Central India. *Hemoglobin* **36**, 316-322 (2012).

212 M. Nuinoon, Kruachan, K., Sengking, W., Horpet, D. & Sungyuan, U. Thalassemia and hemoglobin e in southern thai blood donors. *Advances in Hematology* **2014**, 932306-932306 (2014).

213 N. M. F. Buderer. Statistical methodology: I. Incorporating the prevalence of disease into the sample size calculation for sensitivity and specificity. *Academic Emergency Medicine* **3**, 895-900 (1996).

214 N. M. Buderer. Statistical methodology: I. Incorporating the prevalence of disease into the sample size calculation for sensitivity and specificity. *Academic Emergency Medicine* **3**, 895-900 (1996).

215 B. Shinkins, Thompson, M., Mallett, S. & Perera, R. Diagnostic accuracy studies: how to report and analyse inconclusive test results. *BMJ : British Medical Journal* **346**, f2778 (2013).

216 J. Makani, Cox, S. E., Soka, D., Komba, A. N., Oruo, J., Mwamtemi, H., Magesa, P., Rwezaula, S., Meda, E., Mgaya, J., Lowe, B., Muturi, D., Roberts, D. J., Williams, T. N., Pallangyo, K., Kitundu, J., Fegan, G., Kirkham, F. J., Marsh, K. &

Newton, C. R. Mortality in sickle cell anemia in Africa: a prospective cohort study in Tanzania. *PLoS One* **6**, e14699 (2011).

217 L. Tshilolo, Tomlinson, G., Williams, T. N., Santos, B., Olupot-Olupot, P., Lane, A., Aygun, B., Stuber, S. E., Latham, T. S., McGann, P. T. & Ware, R. E. Hydroxyurea for Children with Sickle Cell Anemia in Sub-Saharan Africa. *The New England Journal of Medicine* **380**, 121-131 (2019).

218 E. Voskaridou, Christoulas, D., Bilalis, A., Plata, E., Varvagiannis, K., Stamatopoulos, G., Sinopoulou, K., Balassopoulou, A., Loukopoulos, D. & Terpos, E. The effect of prolonged administration of hydroxyurea on morbidity and mortality in adult patients with sickle cell syndromes: results of a 17-year, single-center trial (LaSHS). *Blood* **115**, 2354-2363 (2010).

219 M. H. Steinberg, McCarthy, W. F., Castro, O., Ballas, S. K., Armstrong, F. D., Smith, W., Ataga, K., Swerdlow, P., Kutlar, A., DeCastro, L. & Waclawiw, M. A. The risks and benefits of long-term use of hydroxyurea in sickle cell anemia: A 17.5 year follow-up. *American Journal of Hematology* **85**, 403-408 (2010).

220 W. C. Wang, Ware, R. E., Miller, S. T., Iyer, R. V., Casella, J. F., Minniti, C. P., Rana, S., Thornburg, C. D., Rogers, Z. R., Kalpatthi, R. V., Barredo, J. C., Brown, R. C., Sarnaik, S. A., Howard, T. H., Wynn, L. W., Kutlar, A., Armstrong, F. D., Files, B. A., Goldsmith, J. C., Waclawiw, M. A., Huang, X. & Thompson, B. W. Hydroxycarbamide in very young children with sickle-cell anaemia: a multicentre, randomised, controlled trial (BABY HUG). *Lancet* **377**, 1663-1672 (2011).

221 S. V. Deshpande, Bhatwadekar, S. S., Desai, P., Bhavsar, T., Patel, A., Koranne, A., Mehta, A. & Khadse, S. Hydroxyurea in Sickle Cell Disease: Our Experience

in Western India. *Indian Journal of Hematology and Blood Transfusion* **32**, 215-220 (2016).

222 I. Lagunju, Brown, B. J., Oyinlade, A. O., Asinobi, A., Ibeh, J., Esione, A. & Sodeinde, O. O. Annual stroke incidence in Nigerian children with sickle cell disease and elevated TCD velocities treated with hydroxyurea. *Pediatric Blood & Cancer* **66**, e27252 (2019).

223 R. O. Opoka, Ndugwa, C. M., Latham, T. S., Lane, A., Hume, H. A., Kasirye, P., Hodges, J. S., Ware, R. E. & John, C. C. Novel use Of Hydroxyurea in an African Region with Malaria (NOHARM): a trial for children with sickle cell anemia. *Blood* **130**, 2585-2593 (2017).

224 M. Mvundura, Kiyaga, C., Metzler, M., Kamya, C., Lim, J. M., Maiteki-Sebuguzi, C. & Coffey, P. S. Cost for sickle cell disease screening using isoelectric focusing with dried blood spot samples and estimation of price thresholds for a point-of-care test in Uganda. *Journal of Blood Medicine* **10**, 59-67 (2019).

225 X. Yang, Reavis, H. D., Roberts, C. L. & Kim, J. S. Quantitative, Point-of-Care Immunoassay Platform to Guide and Monitor Sickle Cell Disease Therapy. *Analytical Chemistry* **88**, 7904-7909, (2016).

226 K. Ryan, Bain, B. J., Worthington, D., James, J., Plews, D., Mason, A., Roper, D., Rees, D. C., de la Salle, B. & Streetly, A. Significant haemoglobinopathies: guidelines for screening and diagnosis. *British Journal of Haematology* **149**, 35-49 (2010).

227 M. S. Figueiredo. The importance of hemoglobin A_2 determination. *Revista Brasileira de Hematologia e Hemoterapia* **37**, 287-289 (2015).

228 A. Giambona, Passarello, C., Renda, D. & Maggio, A. The significance of the hemoglobin A_2 value in screening for hemoglobinopathies. *Clinical Biochemistry* **42**, 1786-1796 (2009).

229 K. T. B. Tracy I. George, Sherrie L. Perkins. Hemoglobin SC Disease. (2010).

230 J. S. Krauss, Drew, P. A., Jonah, M. H., Trinh, M., Shell, S., Black, L. & Baisden, C. R. Densitometry and microchromatography compared for determination of the hemoglobin C and A_2 proportions in hemoglobin C and hemoglobin SC disease and in hemoglobin C trait. *Clinical Chemistry* **32**, 860-862 (1986).

231 B. Kreuels, Kreuzberg, C., Kobbe, R., Ayim-Akonor, M., Apiah-Thompson, P., Thompson, B., Ehmen, C., Adjei, S., Langefeld, I., Adjei, O. & May, J. Differing effects of HbS and HbC traits on uncomplicated falciparum malaria, anemia, and child growth. *Blood* **115** (2010).

232 C. Thomas & Lumb, A. B. Physiology of haemoglobin. *Continuing Education in Anaesthesia Critical Care & Pain* **12**, 251-256 (2012).

233 A. D. Metaxotou-Mavromati, Antonopoulou, H. K., Laskari, S. S., Tsiarta, H. K., Ladis, V. A. & Kattamis, C. A. Developmental changes in hemoglobin F levels during the first two years of life in normal and heterozygous beta-thalassemia infants. *Pediatrics* **69**, 734-738 (1982).

234 J. Watson. The significance of the paucity of sickle cells in newborn Negro infants. *The American Journal of the Medical Sciences* **215**, 419-423 (1948).

235 R. E. Ware. Technological Advances in Sickle Cell Disease. *Blood Cells, Molecules and Diseases* **67**, 102-103 (2017).